Identification and Functional Validation of Novel Ligands of PPAR gamma
– Therapeutic Implications for Breast Cancer

May 2014

Babita SHASHNI

Identification and Functional Validation of Novel Ligands of PPAR gamma
– Therapeutic Implications for Breast Cancer

A Dissertation Submitted to
the Graduate School of Life and Environmental Sciences,
the University of Tsukuba
in Partial Fulfillment of the Requirements
for the Degree of Doctor of Philosophy in Biotechnology
(Doctoral Program in Bioindustrial Sciences)

Babita SHASHNI

ABSTRACT

Breast cancer is the second most common cancer globally and accounts for the highest morbidity and mortality. Although anti-estrogens have provided an effective endocrine therapy, a significant proportion of patients have acquired resistance to these drugs. In addition, due to high levels of toxicity associated with nuclear hormone receptor, Peroxisome Proliferator-Activated Receptor gamma (PPARγ) agonists - Thiazolidinediones (TZDs) (e.g. - troglitazone (Rezulin), rosiglitazone (Avandia), and pioglitazone (Actos)), and their recent withdrawal in several countries, there is a requirement for alternative therapeutics, such development of new PPAR drugs to treat breast cancer that exhibit better efficacy but lesser toxicity. PPARγ agonist's role in inhibiting breast cancer is well known, however their role in cellular bioenergetics of cancer still needs to be explored. Taking into account, the PPARγ over-expression in breast cancer, this study focuses on the computational identification of PPARγ metabolic targets and validating their modulation by PPARγ natural and novel ligands as therapeutic targets of PPARγ involved in breast cancer pathophysiology.

Computational identification and validation of novel transcriptional targets of PPARγ involved in breast cancer pathophysiology

In this study, I carried out prediction of the PPARγ binding motifs - peroxisome proliferator response element (PPRE) and PPAR-associated conserved motif (PACM) in 2332 genes reported to be involved in breast cancer in literature. A total of 218 genes were found to have PPRE (DR1/DR2) and / or PACM motifs. I further constructed protein-protein interaction network, disease gene network and gene ontology (GO) analyses to identify novel key genes for experimental validation. I identified two novel PPARγ target genes in the glycolytic pathway (phosphoglycerate kinase 1 (PGK1) and pyruvate kinase M2 (PKM2)) at the ATP production steps and experimentally validated their repression by PPARγ activation in two breast cancer cell lines - MDA-MB-231 and MCF-7 by PPARγ natural ligand, 15-Deoxy-Delta12, 14-Prostaglandin J2 (15d-PGJ2). Further analysis suggested that this repression leads to decrease in ATP levels and apoptosis in breast cancer cell lines.

Identification and functional validation of the putative PPARγ ligands – Coffee component Hydroxyl Hydroquinone (HHQ) and Ibrutinib.

In this study, I prospectively investigated whether coffee component HHQ and Ibrutinib are a potential PPARγ ligands and their modulatory effects on glycolytic and pro-apoptotic genes via PPARγ dependent pathway in breast cancer cells. In this study, HHQ and Ibrutinib were confirmed as ligands for PPARγ by docking procedure. Further analysis suggested that HHQ and Ibrutinib also had significant apoptotic effect as well as down regulation of glycolytic genes phosphoglycerate kinase 1 (PGK1) and pyruvate kinase M2 (PKM2) expression on breast cancer cell lines - MDA-MB-231 and MCF-7 cells.

Understanding the molecular pathways that link tumor biology to the staggering array of pathologies and genes is of paramount scientific and medical importance. Our results have established previously unknown novel cross-link between HHQ, Ibrutinib, PPARγ, apoptosis and glycolysis; thereby adding a new dimension to therapeutic potential of PPARγ ligands. These investigations will help us in understanding the molecular mechanisms by which PPARγ regulates the cellular energy pathway and opens a new direction for development of its ligands- HHQ and Ibrutinib in human breast cancer therapeutics.

CONTENTS

CHAPTER 1

INTRODUCTION

CHAPTER 2

COMPUTATIONAL IDENTIFICATION AND VALIDATION OF NOVEL TRANSCRIPTIONAL TARGETS OF PPAR GAMMA IN BREAST CANCER PATHOPHYSIOLOGY

CHAPTER 3

COFFEE COMPONENT HYDROXYL HYDROQUINONE (HHQ) AS A PUTATIVE LIGAND FOR PPAR GAMMA AND IMPLICATIONS IN BREAST CANCER

CHAPTER 4

IBRUTINIB TARGETS GLYCOLYTIC ENZYMES THROUGH PPAR GAMMA DEPENDENT SIGNAL PATHWAY - THERAPEUTIC INTERVENTION IN HUMAN BREAST CANCER

CHAPTER 5

ABBREVIATIONS

15d-PGJ2 : 15-Deoxy-Delta12, 14-Prostaglandin
AIB1 : Amplified in breast cancer-1
ATP : Adenosine triphosphate
BSA : Bovine Serum Albumin
DMEM : Dulbecco's Modified Eagle's Medium
DMSO : Dimethyl Sulfoxide
DNA : Deoxyribonucleic Acid
DR1/DR2 : Direct Repeat 1/ Direct Repeat 2
ECL : Enhanced Chemiluminescence
EGFR : Epidermal growth factor receptor
ER : Estrogen receptor (alpha)
FBS : Fetal Bovine Serum
G6PD : Glucose-6-Phosphate Dehydrogenase
GFP : Green Fluorescent Protein
HER2 : Human epidermal growth factor receptor 2
HHQ : Hydroxy Hydro Quinone
HRP : Horseradish Peroxidase
PACM : PPAR- Associated Conserved Motif
PBS : Phosphate Buffered Saline
PGK1 : Phospho Glycerate Kinase 1
PKM2 : Pyruvate Kinase M2
PPARγ : Peroxisome Proliferator-Activated Receptor gamma
PPRE : Peroxisome Proliferator Response Element
PSN : Pencillin-Streptomycin-Neomycin
PVDF : Poly Vinylidene Fluoride
RNA : Ribonucleic Acid
ROS : Reactive Oxygen Species
SDS : Sodium Dodecyl Sulfate

CHAPTER 1

INTRODUCTION

1.1 BACKGROUND

Breast cancer is the second most common cancer globally and accounts for the highest morbidity and mortality. It is the second highest occurring cancer in women and one of the leading causes of death. Despite advances in early detection, effective endocrine therapy and understanding of the molecular bases of breast cancer pathophysiology, a significant proportion of patients have acquired resistance to the drugs, increased side effects of the therapies and about 30% of patients with early-stage breast cancer have recurrent disease. Hence, there is a requirement for alternative therapeutics with increased efficacy and low toxicity, based on the patient and the clinical and molecular characteristics of the tumor.

Currently, researchers are focusing on the target-based therapy involving modulation of transcription factors by ligands, which play critical roles in tumorigenesis such as tumor development and progression as well as metastasis. Transcription factors can be used as potential molecular therapeutic tools in cancer development and progression to regulate transcriptional levels of genes associated with disease, verify gene function and to validate target genes for drug design.

1.2 BREAST CANCER BURDEN

Breast cancer is the second most common cancer in the world and the most frequent cancer among women with an estimated 1.67 million new cancer cases diagnosed in 2012 representing about 12% of all new cancer cases and 25% of all cancers in women. It is the most common cancer in women both in the developed and less developed regions with more cases in less developed (883,000 cases) than in more developed (794,000) regions [1].

1.3 BREAST CANCER RISKS

Although several risk factors for breast cancer have been well documented but for the majority of women suffering with breast cancer it may not possible to identify specific risk factors. Lifestyle, genes and environment together contribute to the

probability of developing female breast cancer. Known risk factors for breast cancer includes, obesity, BRCA mutations, change in endogenous hormone levels, exogenous hormones etc. [2]. Lacey et al. [3], evaluated known risk factors for breast cancer among 70,575 women in a cancer screening trial. They calculated relative risks for lifestyle and reproductive factors for 5 years from date of randomization. They found that increasing age, positive family history of breast cancer, nulliparity, and use of menopausal hormone therapy were positively associated with breast cancer. Unexpectedly menarche and menopause were less strongly associated with breast cancer. Only severe was statistically significantly associated with breast cancer.

1.4 AVAILABLE THERAPIES FOR BREAST CANCER

Different types of treatment are available for patients with breast cancer. Treatment for breast cancer depends on the kind, severity and invasiveness of the breast cancer. People with breast cancer often get more than one kind of standard treatment depending upon the severity of the breast cancer. Available therapies for breast cancer are described below.

1.4.1 Surgery:

Many patients with breast cancer have surgery to remove the cancer from the breast. Surgeries include, lumpectomy (remove tumor or lump), partial mastectomy, (remove the tumor and breast tissues surrounding the tumor), total mastectomy (remove the whole breast that has cancer) and modified radical mastectomy (remove the whole breast that has cancer, lymph nodes and chest muscles). The patient may be given chemotherapy to remove the tumor or shrink the tumor size. Chemotherapy before the surgery is done to reduce the amount of tissues removed dire to surgeries. This kind of treatment is called neo adjuvant therapies. Some times after the surgeries patients may be given radiation therapy, hormone therapy or chemotherapy to kill the breast cancer cells left after surgery in order to lower the chances of reoccurrence. This kind of treatment is called adjuvant therapy.

1.4.2 Radiation therapy

Radiation therapy involves cancer treatment with high-energy x-rays or other types of radiation to kill cancer cells. There are two types of radiation therapies. In external radiation therapy the body is exposed to the radiation externally by a machine to treat the breast caner where as in case of internal radiation therapy involves direct

contact of radioactive substance into or near the cancer by needles or catheters. It depends on the stage and the type of cancer to be treated by radiation therapies.

1.4.3 Hormone therapy

Estrogens are female hormones that are primarily secreted by ovaries. Once the estrogen binds to the receptors, which can cause estrogen positive breast cancers to grow. Anti-estrogen therapy or hormone therapy involves manipulation of the endocrine system by blocking receptor binding with an antagonist or by depriving the tumor of estrogen. The Estrogen is the major driver in the majority of breast cancers and is expressed in 75% of breast cancers overall. Currently, aromatase inhibitors are used to block the enzyme aromatase, which synthesizes estrogen in the body. Some popular aromatase inhibitors are Arimidex (anastrozole), aromasin (exemestane) and femara (letrozole). Treatment to stop the ovaries from making estrogens is called ovarian ablation.

1.4.4 Chemotherapy

Chemotherapy uses drugs to stop the cancer cells from growing or dividing. The drugs when taken orally and intravenously enter the bloodstream and are able to reach the cancer cells throughout the body, this type of therapy is called systemic therapy. But when drugs are placed directly into the affected area such as organ or cerebrospinal, this is called regional chemotherapy. The type of chemoptheaputic treatment given to patient depends on the type and stage of the cancer being treated. There are many drugs for breast cancer approved by Food and Drug Administration (FDA). The individual drugs are approved by FDA, however now a days many combination of drugs are used by breast cancer patients which are not approved by FDA. The drugs for treatment of breast cancer are described below [4].

1.5 BREAST CANCER RESISTANCE

The effectiveness of breast cancer treatment is limited due to high de novo resistance and resistance acquired during treatment by the breast cancer cells. The potential mechanisms involved in intrinsic or acquired endocrine resistance are still poorly comprehended [5]. The important diagnostic and therapeutic challenges in current breast cancer research are therefore to identify the factors and pathway responsible for the resistance, and the ways to overcome it.

Tamoxifen, a nonsteroidal (selective estrogen receptor modulator) SERM, is FDA approved drug for the treatment of breast cancer [6]. It inhibits breast cancer growth through competitive blocking of the estrogens (ER), thereby inhibiting estrogen-induced growth. Tamoxifen has shown to inhibit more than half of patients with metastatic ER-positive tumors disease. Although the tamoxifen is initially effective in many patients, but due course the tumors develop resistance [7]. Despite the presence of ER almost 50% of breast cancers, fail to respond to tamoxifen. This acquired resistance to tamoxifen by breast caner is attributed by either *de novo* at the beginning of the treatment or acquired after prolonged treatment, to be stimulated rather than inhibited by the drug [8,9]. Osborne et al [10] studied an *in vivo* ER-positive MCF-7 human breast cancer cells xenograft model of tamoxifen-stimulated tamoxifen resistance, in nude mice. They observed that Tamoxifen treatment initially suppresses tumor growth for several months, but later tumor grew as the tumors become stimulated by the drug.

Evidences suggest that ER and GF (Growth factor) - receptor pathways (EGFR/HER2 family and IGF-I receptor) contributes to endocrine resistance [6]. Studies by Nickolsan [11], confirmed that the increased GF signaling pathways may account for loss of some estrogen dependence, resulting in anti estrogen-resistant tumors. They found out that the acquired resistance of MCF-7 cells *in vitro* is associated with increased levels of EGFR and MAPK activity after long-term treatment with tamoxifen. The key signaling kinases, including p42/44MAPK, the stress-related c-Jun NH_2-terminal kinase and p38 MAPKs, and protein kinase A, AKT, have all been reported to activate the ER pathway by direct phosphorylation of the ER, its coactivators, or both [12-14]. Schith et al [15,16] has shown in the preclinical studies, *de novo* and/or acquired tamoxifen resistance is associated with increased levels of these different kinases. Benz at al [17] demonstrated in human breast cancers overexpressing HER2 xenograft model are resistant to tamoxifen. Some studies too correlated High HER2 expression with tamoxifen resistance in patients in some studies [18]. Also high levels of activated ER coactivator AIB, reduce the antagonist effects of tamoxifen in tumors that also overexpress GF receptors, such as HER2. AIB1 is phosphorylated and activated by kinases p42/44 MAPK, which in turn can be activated by HER2 [19]. According to Osborne et al [5] tumors with high abundance of coactivators, such as AIB1, and enhanced HER2 signaling, which can activate AIB1, are less responsive to tamoxifen therapy due to increased estrogen agonistic activity of tamoxifen.

1.6 NEED OF ALTERNATIVE THERAPIES FOR BREAST CANCER

Extreme side effects of chemotherapy, radiation, reoccurrence of breast cancer after therapy, increased metastasis and increased resistance acquired de novo or during the course of treatment to drugs had led the focus to shift on new-targeted therapies. New targeted therapies such as target specific drugs may be a promising approach to improve present treatment strategies and overcome endocrine resistance.

1.7 NUCLEAR HORMONE RECEPTOR – PEROXISOME PROLIFERATOR ACTIVATED RECEPTOR (PPARγ)

Peroxisome proliferator-activated receptors (PPARs) belong to the nuclear hormone receptor superfamily of ligand-activated transcription factors. Upon ligand activation, PPAR translocates from cytoplasm to nucleus and heterodimerizes with retinoid X receptor (RXR) to regulate gene expression. Three isoforms (α, β, and γ) for PPAR have been identified so far in Xenopus, mouse, human, rats, and hamsters. The PPAR subtypes share a highly conserved DNA-binding domain that matches with specific DNA sequences known as peroxisome proliferator response elements (PPREs). These PPAR isoforms are encoded by different genes, perform different functions and exhibit different tissue localizations [20, 21].

The PPAR isoforms exhibit a tissue specific expression pattern. The first isoform PPAR α is expressed in tissues of liver, kidney, heart, and intestine. This isoform regulates the genes encoding lipid-metabolizing enzymes [22]. The second isoform, PPAR β also called as FAAR (fatty acid activated receptor) expressed mainly in the brain, skin, skeletal muscle, gut, placenta, adipose tissues [23]. The expression profile of this isoform varies based on the cell proliferation and differentiation. PPAR γ has seven alternatively spliced isoforms. Differential promoter usage and alternate splicing of the gene generates seven mRNA isoforms: PPARγ1, PPARγ2, PPARγ3, PPARγ4, PPARγ5, PPARγ6 and PPARγ7 (Figure 1-1). PPARγ1 and PPARγ3 encode the same protein product; the PPARγ2 isoform contains an additional 28 amino acids at its N-terminus. PPARγ1 exhibits widespread expression, although at low levels, while PPARγ2 and PPARγ3 are highly expressed in adipose tissue. The 28 additional N-terminal amino acids in PPARγ2 confer a 5- to 6-fold increase in transcription-stimulating activity of the ligand-independent activation function-1 domain [24].

It is of interest to mention that DNA-binding activity of PPARγ is modulated by the isotype of the RXR heterodimeric partner [24]. Chandra et al [25] reported structures of

intact PPARγ and RXRα as a heterodimer bound to DNA, ligands and coactivator peptides. It was observed that PPARγ and RXRα form a non-symmetric complex, allowing the ligand-binding domain of PPARγ to contact multiple domains in both proteins (Figure 1-2). PPREs are described to consist of juxtaposed degenerate hexamer AGGTCA separated by one nucleotide, direct repeat 1 (DR1) or two nucleotides (DR2), suggesting that both DR1 and DR2 sites could be bound by PPARγ-RXRα nuclear receptor complex [26, 27] Recently, a 15 bp novel PPARγ motif PACM (PPAR-associated conserved motif) with the consensus sequence TTCATTTGGACATTG was reported (Figure 1-3). The PACM motifs were reported to be more common than PPREs [28].

1.8 NATURAL AND SYNTHETIC LIGANDS OF PPARγ

PPARγ receptor can be activated by endogenous ligands, for example, prostaglandin D2 (PGD2), 15-deoxy prostaglandin J2 (15d-PGJ2), or 15-hydroxyeicosatetraenoic acid (15-HETE) [29-30]. Recently, an oxidized phosphatidylcholine has also been identified as a potent alternative (patho) physiological natural ligand of PPARgamma. Synthetic ligands for PPARγ include insulin sensitizing antidiabetic thiazolidinediones (TZD); troglitazone (TGZ), rosiglitazone (RGZ), ciglitazone (CGZ), or pioglitazone (PGZ) [31-33], and nonsteroidal anti-inflammatory compounds indomethacin, ibuprofen, flufenamic acid, or fenoprofen [34] are commonly known as PPARγ ligands (Table 2-2). Due to high levels of toxicity associated with the first generation TZDs, troglitazone (Rezulin), rosiglitazone (Avandia), and pioglitazone (Actos), there is a renewed search for newer PPAR drugs that exhibit better efficacy but lesser toxicity.

Towards this end, developing known dietary components (nutraceuticals) that bind and activate PPARγ with more efficacy and safety, while promoting health benefits has become an absolute necessity [35]. The majority of nutraceuticals are of plant origin and hence these compounds are considered safe and are popular among consumers. Dietary components that act as ligands of PPARγ include dietary lipids such as n-3 and n-6 fatty acids and their derivatives, isoflavones and flavonoids. Though a plethora of ligands are known to activate PPARγ, what is lacking, however, is the delineation of the metabolic effects that are specific to this PPAR gamma activation.

These investigations will provide a cause and effect relationship between ligand activation of PPAR gamma and its physiological function and will help in effective therapeutic options in several pathophysiological conditions.

1.9 PPARγ AND CANCER

It is prudent to note that the expression of PPARγ in tumor breast tissue is significantly higher than in normal breast epithelium [36]. Toward this end, development of a new class of anticancer drugs through a new approach employing PPARγ activators to inhibit proliferation and increased cell death in breast cancer cell lines is hypothesized. PPARγ on activation by specific ligands exerts antitumor activity through growth inhibition and cellular differentiation [37, 38] and is also reported to negatively regulate the cell cycle [39]. PPARγ activation is reported to inhibit the proliferation of malignant cells, including those derived from liposarcoma, breast adenocarcinoma, prostate carcinoma, colorectal carcinoma, non small-cell lung carcinoma, pancreatic carcinoma, bladder cancer, gastric carcinoma, and glial tumors of the brain [40, 41]. Ligand activated PPARγ is also reported to inhibit invasion and metastasis of breast cancer cells and induce G1/S arrest by up regulation of p21WAF1/Cip1 or p27Kip1, and down regulation of cyclin D1 [42, 43]. Despite these promising results, the target genes involved in the anticancer activity of PPARγ ligands and their pathways still remain elusive.

1.9.1 PPAR gamma transcriptional targets in cancer pathophysiology

PPARγ once ligand activated has found to modulate many genes involved in apoptosis, glycolysis, lipid metabolism, angiogenesis, differentiation, cell proliferation, inflammation, redox regulation etc. (Figure 1-4) [44]. Recently, Venkatachalam et al [25] showed that activation of PPARγ inhibits the expression of pH Regulator NHE1 (Na+/H+ exchanger 1) and MnSOD, that was associated with the sensitization of breast cancer cells to chemotherapeutic treatment. They computationally identified presence of 2 PPRE motifs in NHE1 and 3 PPRE motifs in MnSOD and further validated the true motifs and their regulation by PPAR in vitro.

Cancer cells thrive in an acidic environment and do not survive in normal or more alkaline environment. NHE1 is a ubiquitously expressed membrane phospho glycoprotein comprising of 10-12 transmembrane segments (N-terminal) and a large cytoplasmic tail. NHE1 regulates intracellular pH (pHi) homeostasis and cell volume

regulation [45,46]. Under physiological conditions, the Na+/H+ exchanger NHE1 extrudes one H+ ion in exchange for one extracellular Na+ ion. An alkaline pHi together with an acidic extracellular environment is associated with more tumorigenic phenotype. The alkaline pHi favours metabolic processes associated with cellular proliferation, whereas the acidic extracellular environment enhances the invasive capacity of transformed cells [47]. NHE1 also plays a role in cellular proliferation [48] and is activated upon growth factor stimulation. Tumor cells deficient in NHE1 activity either show severely arrested growth in immunodeficient mice [49]. Interestingly, a recent report implicated the pH regulator, NHE1 in tumor cell growth is arrested by activated PPARγ [50]. Also, it was recently reported that decrease in NHE1 expression led to tumor cell growth arrest, intracellular acidification, and sensitization to death stimuli [51].

Cancer cells have high reactive oxygen species (ROS) levels than normal cells. The increased endogeneous oxidative stress is due to increased metabolic activity, oncogenic stimulation, and mitochondrial malfunction [52]. The ROS in cancer cells may stimulate cellular proliferation, and genetic instability, and alterations in cellular sensitivity to anticancer agents and promotion of mutations. Cells have intracellular ROS-scavenging system that includes superoxide dismutases (SOD), glutathione peroxi- dase (GPx), peroxiredoxins (PRDXs), glutaredoxins, and catalases. Enzymes copper-zinc superoxide dis-mutase (CuZnSOD) and manganese superoxide dismutase (MnSOD), are present in the mitochondrial matrix and in the intermembrane space, respectively dismutate superoxide anion (O^-) to hydrogen peroxide 2 (H_2O_2). GPx then quenches H_2O_2 generated in mitochondria, or by catalase in the cytosol [53]. The increased ROS stress in cancer cells will tend to increase expression of SOD and other antiox- idant enzymes. Many reports confirmed that CuZnSOD (SOD1) and MnSOD (SOD2) expression levels are significantly higher in primary tissues of adenocarcinomas of the stomach, squamous cell carcinomas of the oesophagus, chronic lymphocytic leukemia cells and ovarian cancer cells compared to normal tissues [54]. Increased SOD levels were also observed in breast cancer tissue from 23 patients [55]. Venkatachalam et al [25] reported that human MnSOD expression is downregulated by PPARγ agonists in vitro in prostate cancer cell lines.

1.9.2 PPARγ, Glycolysis and Cancer

The general principles of metabolic control analysis can be effective for cancer management as abnormal energy metabolism and biological disorder are characteristics of tumors [56]. Coordinated upregulation of glycolysis pathway proteins has been detected in several different tumor types including breast cancer tumors [57,58]. Amon et al. [59] identified increased levels of glycolysis proteins in plasmas of women with breast cancer. Warburg [91] determined that there is a tenfold increase of glucose consumption in cancer cells as compared to normal cells, and a twofold production of lactic acid as compared to that produced by normal tissue. Cancer cells are provided with several growth advantages like growth of cells in adverse microenvironment, generation of substrates for glycosylation reactions, and supply of precursors for biosynthetic reactions by aerobic glycolysis/enhanced glucose uptake [60,61]. Conflicting evidence suggests that hydrogen ions production by glycolysis create the acidic environment responsible for degradation of the extracellular matrix, critical for facilitating tumor invasion into normal host tissue [62]. Adaptive advantages are also conferred by increased glycolysis (or pentose phosphate metabolism) if it allows excess pyruvate to be available for lipid synthesis or providing essential anabolic substrates, such as ribose for nucleic acid synthesis [63].

Glucose consumption through the pentose pathway may also provide essential reducing equivalents (NADPH) to reduce the toxicity of reactive oxygen species conferring resistance to senescence and anabolic substrates such as ribose for nucleic acid synthesis [64]. These evolutionary advantages can explain the remarkable prevalence of the glycolytic phenotype in human cancers. This is important since aerobic glycolysis is an existing metabolic function in all eukaryotic cells and using normal isoforms as target for cancer therapeutics may lead to cytotoxicity issues. Interestingly, hypoxia-mediated HIF-1 has been suggested to lead to the expression of specific isoforms of glycolytic enzymes and transporters through alternative splicing [65].

Concurrently, PPARγ activates a number of genes in tissues increasing glucose and lipid uptake and glucose oxidation, simultaneously decreasing free fatty acid concentration and insulin resistance. Hence, targeted therapies may be eventually led by understanding the molecular and physiological causes and consequences of upregulated glycolysis and modulation of these. In line with the above, cancer treatment strategies through the target of energy metabolism of cancer could include glucose deprivation,

inhibition of the glycolytic pathway (3-bromopyruvate (3-BrPA)), glucose analogues (2-deoxyglucose (2DG)), inhibition of glucose transport (Imatinib), and exploitation of HIF (PX-478) [44].

Glycolytic inhibitors in combination with other therapies have proven to be more promising than being alone as tumor cells and tumor microenvironment are very heterogeneous and cells within an invasive cancer may use a range of metabolic pathways including some in which oxidative metabolism of glucose or fatty acids contributes significantly to ATP production [66].

1.9.3 Isoforms of Glycolytic Genes and PPARγ

Cancer cells are found to upregulate glucose transport and switch their main energy supply pathway from oxidative phosphorylation to glycolysis depending heavily on glucose as both energy and biosynthesis sources. Thus, cancer cells are more sensitive than normal cells to changes in glucose concentration [67] and it is easier than normal cells to induce death in limited glucose supply and disruption of glycolysis [68]. These molecular and metabolic changes also provide targets for cancer treatment. Inhibiting either various steps of glycolysis or glucose transport, the first rate-limiting step leading to glycolysis, is likely to severely disrupt both energy supply and biosynthesis processes inside cancer cells, resulting in reduction of proliferation rate and induction of apoptosis of cancer cells. Imbalances in expression of target genes that have a pivotal role in regulating metabolic syndrome and cancer through atherogenic metabolic triad/lipid triad metabolism has recently been noted to be modulated by PPARs [69]. Several glycolytic enzymes are predicted by us to have the PPRE site, suggesting their regulation by PPARγ (Figure 1-5). The enzymes in glycolytic pathway and their isoforms are discussed below.

Hexokinases: They catalyze the first irreversible step of the glycolytic pathway for the phosphorylation of glucose to glucose-6-phosphate with consumption of ATP. Four important mammalian hexokinase isozymes that vary in subcellular locations and kinetics with respect to different substrates and conditions and physiological functions are known and designated as HK1-4 [70]. HK2, the predominant isoform overexpressed in malignant tumors, strategically binds to the outer mitochondrial membrane coupling ATP formation in mitochondria to the phosphorylation of glucose, thus confer- ring cancer cells with a highly glycolytic phenotype and ample biosynthetic precursor [71,72]. In addition to its critical metabolic role, HK2 can also promote cancer by

repressing mitochondrial function on cell death, immortalizing cancer cells.

Fructose-2, 6-Bisphosphatase: 6-phosphofructo-2-kinas- e/fructose-2, 6-bisphosphatase 3 (PFKFB3), is a bifunctional enzyme and is central to glycolytic flux. It is downstream to the metabolic stress sensor AMP-activated protein kinase (AMPK) that modulates glycolysis and possibly activates isoforms of PFKFB, specifically PFKFB3 expressed in tumor cells. It has been demonstrated that long-term low pH exposure induces AMPK activation, which results in the upregulation of PFKFB3 and an increase in its serine residue phosphorylation. Pharmacologic activation of AMPK is responsible for increase in PFKFB3 as well as an increase in glucose consumption, whereas inhibition of AMPK results in the down regulation of PFKFB3 and decreased glycolysis [73].

Pyruvate Kinase (PKM): It converts phosphoenolpyruvate to pyruvate and regulates the rate-limiting step of glycolysis. It has two specific isoforms: the adult isoform, PKM1, promotes oxidative phosphorylation and the PKM2 isoform, which promotes aerobic glycolysis and is expressed in embryonic and cancerous cells. The above isoforms are produced as a result of mutually exclusive alternative splicing of the PKM pre-mRNA that corresponds to inclusion of either exon 9 (PKM1) or exon 10 (PKM2) [74].

Development of selective anticancer agents based on the biological differences between normal and cancer cells is essential to improve therapeutic selectivity, sensitivity, and specificity. The modulation of PPARγ receptor action in cancer may be of therapeutic value.

1.10 COMPOSITION OF THESIS

This thesis involves mainly two objectives based on target therapy for breast cancer:

1. To identify computationally novel transcriptional factors of nuclear hormone receptor - peroxisome proliferator activated receptor gamma (PPARγ) involved in breast cancer pathophysiology and validate the identified PPARγ novel targets by its natural ligand 15-Deoxy-Δ12, 14-prostaglandin J (15d-PGJ2).
2. Identification and functional validation of novel PPARγ ligands on the above identified novel transcriptional targets of PPARγ.

Chapter 1 gives a brief introduction of breast cancer burden in the world, available therapies for breast cancer and reasons for need of alternatives for breast cancer therapy. In addition, the details of resistance acquired by breast cancer is also discussed in detail. Furthermore, PPAR gamma mechanism of action, its role in cancer and its transcriptional targets are also discussed in detail.

Chapter 2 focuses on computational identification of PPARγ binding motifs, PPRE and PACMs in the whole human genome by PPRE search tool and *in vitro* validation of the putative PPARγ targets in human breast adenocarcinoma, MDA-MB-231 and MCF-7.

Chapter 3 focuses on the *in vitro* validation of proposed PPARγ ligand - coffee component, Hydroxyl Hydro Quinone on identified novel transcriptional targets of PPARγ in human breast adenocarcinoma, MDA-MB-231 and MCF-7. In addition effect of HHQ on the cytotoxicity and mechanism of death in MDA-MB-231 and MCF-7 is also investigated.

Chapter 4 focuses on the cytotoxic effect of FDA approved drug Ibrutinib on human breast adenocarcinoma, MDA-MB-231 and MCF-7. The effect of Ibrutinib on glycolytic transcriptional targets of PPARγ is also investigated. In addition, mechanism of cell death induced by Ibrutinib is also investigated in MDA-MB-231 and MCF-7.

Chapter 5, conclusion is drawn based upon my research and summarized it. I addition the potential and future direction of my research is discussed briefly.

Table 1-1: FDA approved drugs for breast cancer therapy

ANTI-CANCER DRUG	IUPAC NAME	DRUG TARGET
Abitrexate	Methotrexate	Acts on dihydrofolate reductase a major enzyme for formation of adenine guanine
Abraxane	Paclitaxel albumin-stabilized nanoparticle	Acts on active G_2/M phase of cell cycle.
Adriamycin RDF	Doxorubicin Hydrochloride	Acts on active S and G_2 phase.
Adrucil	Fluorouracil	Acts on dTMP that is needed for DNA synthesis and cell growth.
Afinitor Disperz®	Everolimus	Acts on extracellular domain of the HER2 growth receptor.
Aredia	Pamidronate Disodium	Inhibition of the osteolactic proton pump necessary for dissolution of hydroxyapatite.
Arimidex	Anastrozole	Helps in acting on aromatase inhibitors which helps in formation of androgens and estrogens
Cytoxan	Cyclophosphamide	Acts on P_{450} enzymes which helps in formation of alkylated DNA
Ellence	Epirubicin Hydrochloride	Acts on active S and G_2 phase of cell cycle
Fareston	Toremifene	Act on selective estrogen receptor modulators also known to modulate SERM's in breast
Gemzar	Gemcitabine Hydrochloride	Acts on 2'2'-difluorodeoxycytidine and thus inhibits DNA synthesis
Herceptin	Trastuzumab	Acts on extracellular domain of the HER2 growth receptor
Kadcyla	Trastuzumab Emtansine	Acts on extracellular domain of the HER2 growth receptor.
Perjeta	Pertuzumab	Acts on extracellular domain of the HER2 growth receptor
Taxol	Paclitaxel	Acts on active G_2/M phase of cell cycle
Taxotere	Docetaxel	Acts on active G_2/M phase of cell cycle

Table 1-2: List of natural and synthetic ligands of PPARγ.

Natural Ligands	**Abietic acid** [PMID: 12935909] **Biochanin A** [PMID: 16549448] **Bixin** [PMID: 21307572] **Capsaicin** [PMID: 15383218] **Citronellol** [PMID: 21597168] **Daidzein** [PMID: 19775880] **Dehydroabietic acid (DAA)** [PMID: 18267111] **Equol** [PMID: 19775880] **Farnesol** [PMID: 21307572]	**Genistein** [PMID: 12421816] **Geraniol** [PMID: 21597168] **Geranylgeraniol** [PMID: 18608213] **Glycyrrhizic acid** [PMID: 20011054] **Hesperidin** [PMID: 18086153] **Hydroxy Hydroquinone [Ref:]**	**Lipoxygenase (LOX)** [PMID: 15698583] **Phytol** [PMID: 21629877] **Psi-baptigenin** [PMID: 18086153] **Quercetin** [PMID: 22226987] **Resveratrol** [PMID: 22792089] **Rosmarinic acid** [PMID: 22226987] **2′-Hydroxy chalcone** [PMID: 22226987]
Synthetic Ligands	**Azelaoyl phosphatidylcholine (in oxidized LDL)** [PMID: 11279149] **Arachidonic acid (20:4, n-3)** [PMID: 11422732] **Balsalazide** [PMID: 18077625] **Bezafibrate** [PMID: 12676649] **CAY10599** [PMID: 19301897] **Ciglitazone** [PMID: 8576907] **Conjugated linoleic acid isomers (CLA)** [PMID: 15986437] **Docosahexaenoic acid (DHA)** [PMID: 18193404] **DRF 2519** [PMID: 15140637] **Gliquidone** [PMID: 17082235] **Glipizide** [PMID: 16168052] **GW 1929** [PMID: 23100239] **Icosapent** [PMID: 11552681] **Indomethacin** [PMID: 20665425] **Linoleic acid** [PMID: 15701701]	**Methyl-8-hydroxy-8-(2-pentyl-oxyphenyl)-oct-5-ynoate** [PMID: 20518620]**Mitiglinide** [PMID: 17082235] **Muraglitazar** [PMID: 23594962] **Nateglinide** [PMID: 17082235] **Nitroalkenes (NO2-FA)** [PMID: 20097754] **nTZDpa** [PMID: 12554792] **Omega-3 (or n-3) polyunsaturated fatty acids (PUFAs)** [PMID: 18769551] **PAz-PC** [PMID: 11279149] **PGD_2** [PMID: 11422732] **PGJ_2** [PMID: 11422732] **Pioglitazone** [PMID: 11422732] **Ripaglinide** [PMID: 17082235] **Rosiglitazone (BRL49653)** [PMID: 11422732]	**Telmisartan** [PMID: 23829789] **Tesaglitazar** [PMID: 17166340] **Troglitazone** [PMID: 11422732] **WY-14643** [PMID: 11422732] **4-Hydroxy docosahexaenoic acid (4-HDHA)** [PMID: 18193404] **4-Oxodocosahexaenoic acid (4-oxo-DHA) [PMID: 18193404]** **9-HODE** [PMID: 11422732] **9/10-NO_2-linoleic acid** [PMID: 19105608] **12-NO_2-linoleic acid** [PMID: 19105608] **13-NO_2-linoleic acid** [PMID: 19105608] **13-HODE** [PMID: 11422732] **15-Deoxy-^{12,14}-prostaglandin J_2** [PMID: 11422732]

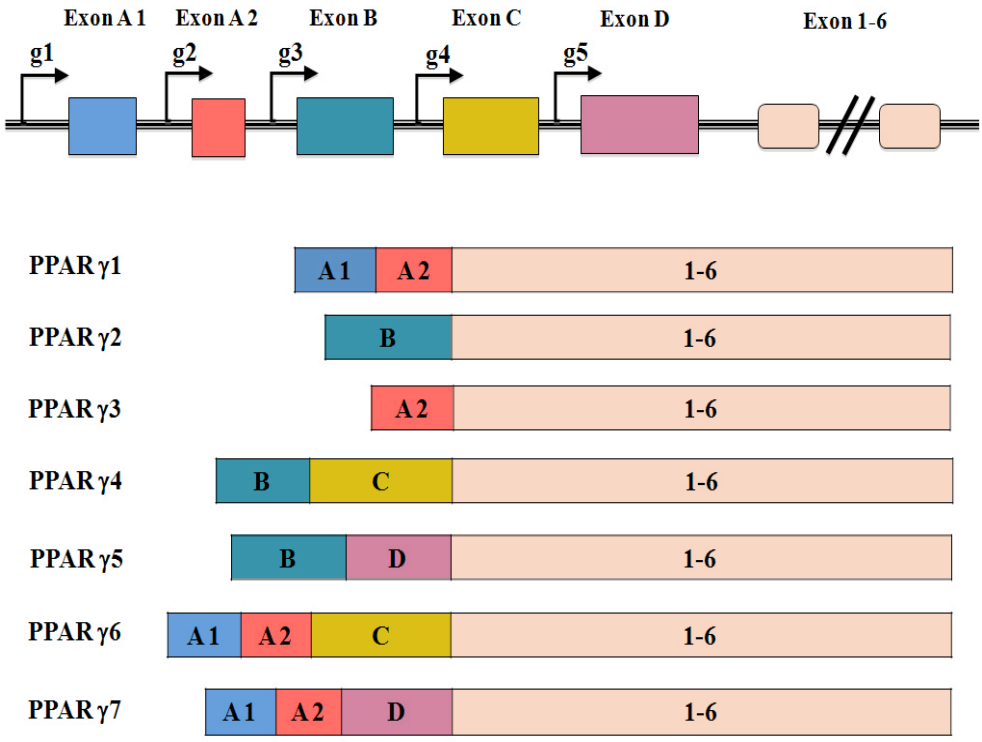

Figure 1-1: Genomic structure of the human PPAR gamma gene (5' end) and PPARγ mRNA splicing forms and protein variants. There are seven isoforms of PPARγ with common exons 1-6.

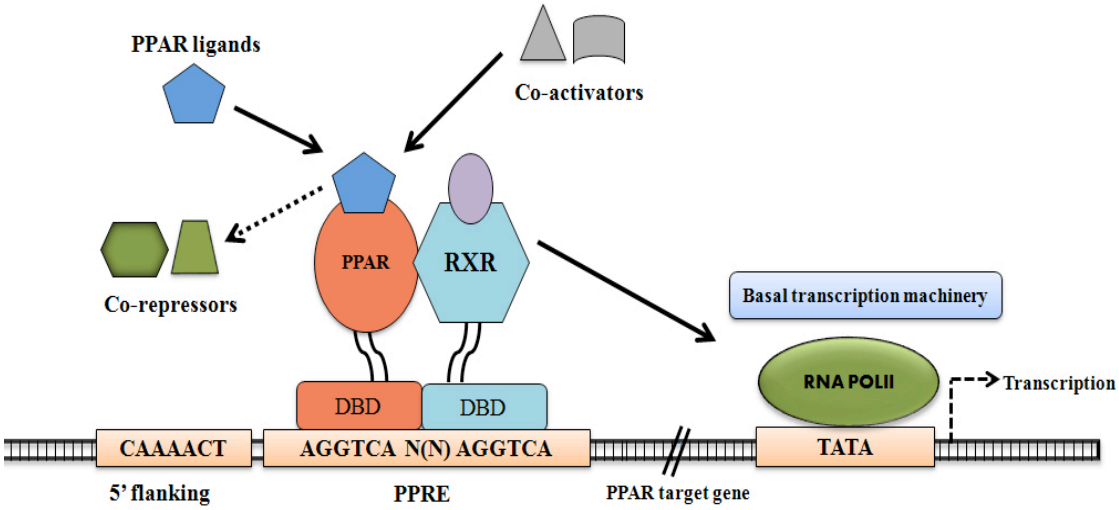

Figure 1-2: PPAR gamma activation mechanism. Upon ligand activation PPARγ hetero dimerizes with Retinoid X Receptor (RXR) in nucleus and binds to PPRE and/or PACM motifs in the promoter region and modulates the expression of genes downstream. The consensus PPRE site consists of a direct repeat of the sequence AGGTCA separated by a single/double nucleotide, which is designated as DR-1 site/DR-2 site and PACM site consist of 15 bp consensus sequence, TTCATTTGGACATTG. The PACM motifs are reported to be more common than PPREs.

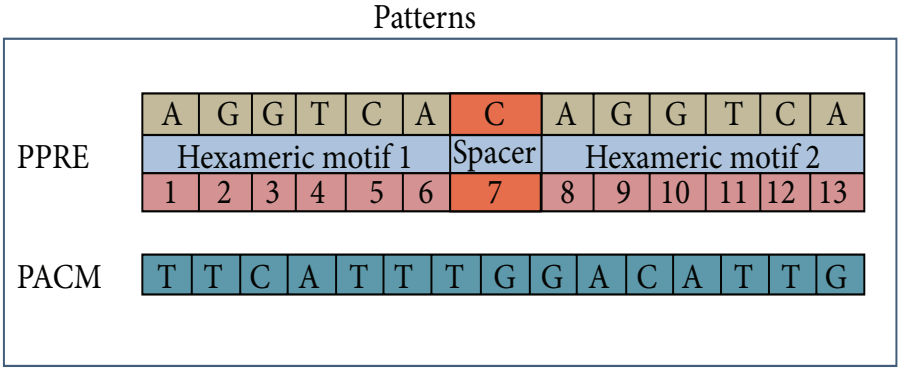

Figure 1-3: PPAR gamma binding patterns - PPRE and PACM motifs.

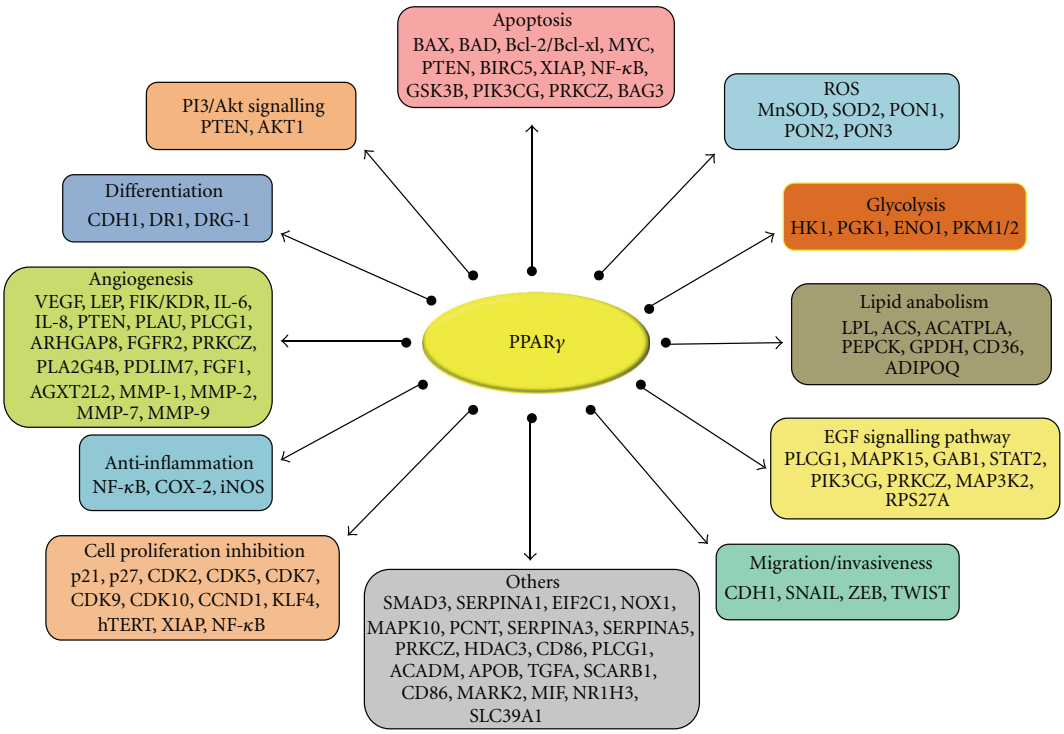

Figure 1-4: Molecular targets of PPARγ and pathways associated.

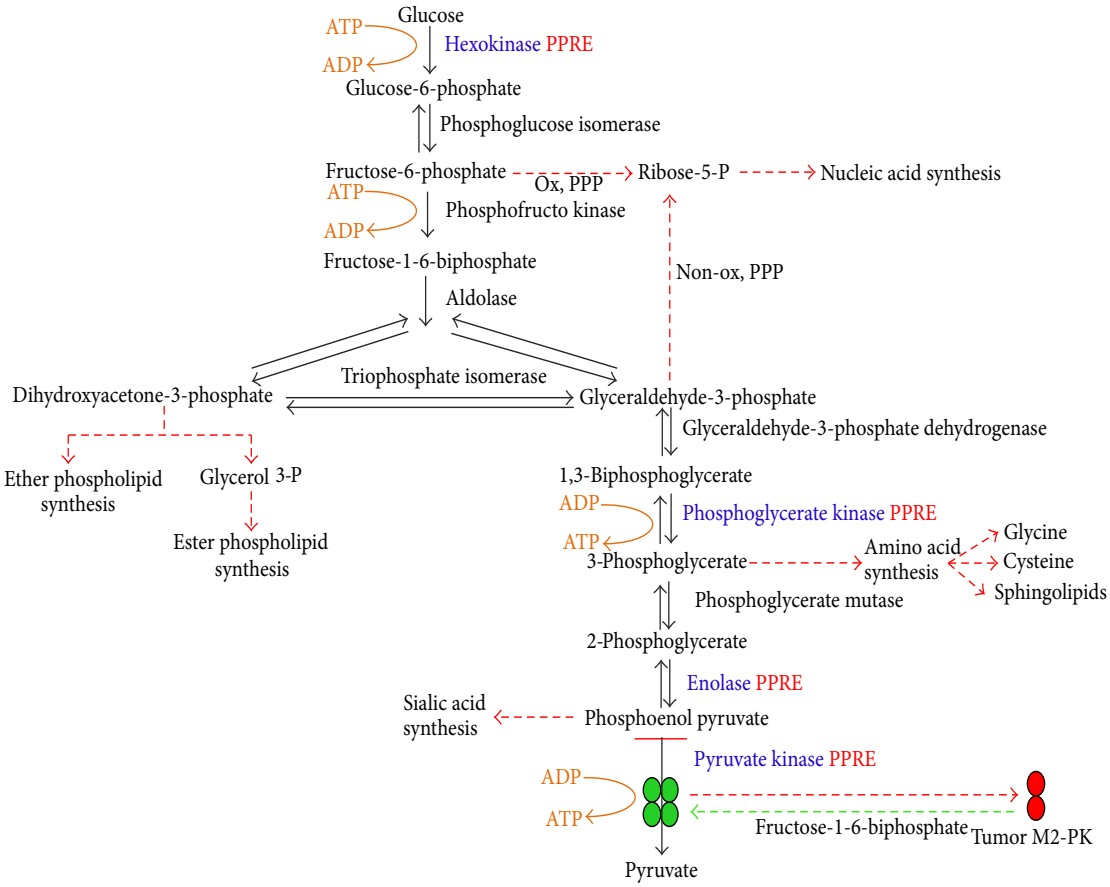

Figure 1-5: Metabolic targets of PPARγ. Many glycolytic enzymes are over expressed in cancers. Glycolytic enzyme pyruvate kinase-muscle 2 (PKM2) is a key regulator of tumor metabolism which promotes tumor growth and Warburg effect by switching between its dimeric form the active one, which has higher affinity for substrate Phosphoenol pyruvate (PEP) to tetrameric form the inactive form, with lower affinity for substrate PEP and vice-versa. This switching behavior of PKM2 keeps a balance of activation of many pathways including, glycerol, serine/ glycine, ether/ester phospholipid pyrimidine biosynthesis (in green) and oxidative metabolism for energy production, thereby promoting tumor growth and tumor cell proliferation.

CHAPTER 2

COMPUTATIONAL IDENTIFICATION AND VALIDATION OF NOVEL TRANSCRIPTIONAL TARGETS OF PPAR GAMMA IN BREAST CANCER PATHOPHYSIOLOGY

2.1 INTRODUCTION

Peroxisome proliferator-activated receptors (PPARs) belong to the nuclear hormone receptor superfamily of ligand-activated transcription factors. Upon ligand activation, PPAR translocates from cytoplasm to nucleus and heterodimerizes with retinoid X receptor (RXR) to regulate gene expression. Three isoforms (α, β, and γ) for PPAR have been identified so far in Xenopus, mouse, human, rats, and hamsters. The PPAR subtypes share a highly conserved DNA-binding domain that matches with specific DNA sequences known as peroxisome proliferator response elements (PPREs). These PPAR isoforms are encoded by different genes, perform different functions and exhibit different tissue localizations [75-80]. Imbalances in expression of target genes that have a pivotal role in regulating metabolic syndrome and cancer through atherogenic metabolic triad/lipid triad metabolism has recently been noted to be modulated by PPARs [81]. 15-Deoxy-Δ12, 14-prostaglandin J (15d-PGJ2) is a natural ligands [82]. It is prudent to note that the expression of PPARγ in tumor breast tissue is significantly higher than in normal breast epithelium.

Toward this end, development of a new class of anticancer drugs through a new approach employing PPARγ activators to inhibit proliferation and increased cell death in breast cancer cell lines is hypothesized. Concurrently, PPARγ is also reported to control the expression of genes involved in differentiation and is also reported to negatively regulate the cell cycle [83, 84]. PPARs are also involved in various independent and DNA-dependent molecular and enzymatic pathways in adipose tissue, liver and skeletal muscles. PPARγ activation is reported to inhibit the proliferation of malignant cells, including those derived from liposarcoma, breast adenocarcinoma, prostate carcinoma, colorectal carcinoma, non small-cell lung carcinoma, pancreatic carcinoma, bladder cancer, gastric carcinoma, and glial tumors of the brain [85-88]. Thus, PPARs can provide therapeutic targets for several diseases such as dyslipidemia, diabetes, obesity,

inflammation, neurodegenerative disorder, and cancer. Recently, it was showed that activation of PPARγ inhibits the expression of Na+/H+ exchanger 1 (NHE1) that was associated with the sensitization of breast cancer cells to chemotherapeutic treatment [89]. Hence, modulation of PPARγ receptor action in these diseases may be of therapeutic value. The effect of PPARγ ligands on breast cancer cell motility and the plasminogen activator system has also been investigated [90]. The metabolic phenotype of cancer is distinct from that of normal cells. In comparison to the normal aerobic glucose metabolism pathway, which uses mitochondrial oxidation, cancer cells develop Warburg's effect, in which aerobic glycolysis is increased and for which drug-driven disruption might lead to minimal side effects [91]. Altenberg and Greulich [92], found overexpression of glycolytic genes in 24 cancer cell lines Hypoxic tumors have generally been known to evolve into invasive and metastatic tumors as compared to those with normal oxygen levels due to increase glycolysis requirements in hypoxia. These results demonstrated the clinical importance of glucose metabolism in treatment of cancer. Hence, disruption of Warburg effect may help resolve the malignant process independently of tumor origin and is likely to have broad therapeutic implications.

It is of interest to mention that DNA-binding activity of PPARγ is modulated by the isotype of the RXR heterodimeric partner. Chandra et al [93] reported structures of intact PPARγ and RXRα as a heterodimer bound to DNA, ligands and coactivator peptides. It was observed that PPARγ and RXRα form a non-symmetric complex, allowing the ligand-binding domain of PPARγ to contact multiple domains in both proteins. PPREs are described to consist of juxtaposed degenerate hexamer AGGTCA separated by one nucleotide, direct repeat 1 (DR1) or two nucleotides (DR2), suggesting that both DR1 and DR2 sites could be bound by PPARγ-RXRα nuclear receptor complex [89, 94]. Apart from the effects of PPARγ on cell death, none of the studies on the effect of PPARγ on breast cancer demonstrates the molecular mechanisms, pathways, or genes that are modulated by PPARγ to cause cell death.

Breast cancer is the fifth most common cancer globally and accounts for the highest morbidity and mortality. It is the second highest occurring cancer in women and one of the leading causes of death [95]. Although anti-estrogens have provided an effective endocrine therapy, a significant proportion of patients have acquired resistance to these drugs. Hence, there is a requirement for alternative therapeutics to treat breast cancer. It is pertinent to screen drugs with a potential to target critical molecules involved in metabolic transformation because several drugs that inhibit metabolism of cancer cells by

targeting a variety of molecules (including enzymes) directly or indirectly, are currently under clinical trials [96].

The main objective in this chapter is to identify novel PPARγ target genes which are reported to be involved in breast cancer, followed by their functional classification, disease ontology (DO) and network construction. Further investigations on these could possibly help us in understanding the molecular mechanisms by which PPARγ regulates disease targets specifically in breast cancer and the use of its ligands in breast cancer therapeutics.

2.2 EXPERIMENTAL SECTION

2.2.1 COMPUTATIONAL METHODOLOGY

Computational identification of PPRE in genome data

The sequences 5 kb upstream of annotated transcription starts of human RefSeq genes were downloaded from UCSC genome browser (http://genome.ucsc.edu/) [97]. The sequences downloaded were from the February 2009 assembly of the human genome (hg19, GRCh37 Genome Reference Consortium Human Reference 37(GCA_000001405.1). The PPRE motifs were searched in the 5 kb promoter region of the genes using the PPRESearch tool in command line mode (http://the-systembiology.com/OVista/PPRE2/) [89]. PPRESearch is a database searching tool that contains a comprehensive collection of experimentally validated PPRE motifs reported in literature and allows the user to search for PPRE motifs in a gene of interest. Gene promoters whose PPREs match exactly with experimental PPREs were selected. Both DR1 and DR2 PPREs were searched. Recently, a 15 bp novel motif PACM (PPAR-associated conserved motif) was reported [98]. I also included this motif in our search. Since the gene sequences were represented by transcript ID, their corresponding gene symbols and gene names were retrieved using the gene ID conversion tool from DAVID http://david.abcc.ncifcrf.gov/ [99]. Genes that have more than one transcript ID (due to gene polymorphism) have same gene symbol and same PPRE sites and hence were grouped together under one gene name.

Collection of genes for breast cancer

The genes involved in breast cancer pathophysiology were collected from several sources such as literature, Gene cards database (http://www.genecards.org) [100] and the Breast Cancer Gene Database (BCGD) (http://mbcr.bcm.tmc.edu/ermb/bcgd/bcgd.

html) [101]. A total of 2332 non-duplicate genes were to be involved directly and indirectly in breast cancer pathophysiology.

Identification of genes that have PPRE and are reported to be involved in breast cancer

A total of 217 breast cancer genes were found to be having the PPRE motif and/or the PACM motif.

PPARγ target identification

Protein–protein interaction and molecular interaction network construction

The complex global network of protein interactions dictates cellular behavior. The putative PPARγ targeted breast cancer genes were mapped to the Biological General Repository for Interaction Datasets (BioGRID) version 3.1.91 a curated protein–protein and genetic interactions database to identify the interacting partners (http://www.thebiogrid.org). BioGRID is a public data- base with 48,831 human protein interactions compiled through comprehensive curation efforts (10,247 publications) [102].

Gene Ontology, protein and pathway

The PANTHER (Protein ANalysis THrough Evolutionary Relationships) classification System is a unique resource that classifies genes by their functions, using published scientific experimental evidence and evolutionary relationships to predict function even in the absence of direct experimental evidence (http://www.pantherdb.org/). The genes were classified according to GO classes: molecular function, biological process, cellular component, PANTHER protein classes and pathways [103].

Functional Disease Ontology

In order to find the enrichment of predicted PPARγ breast cancer target gene set in various disease profiles I mapped the gene set to Functional DO (FunDO) tool. DOLite has been used in the FunDO Web application. FunDO is an online tool from Northwestern University Feinberg School of Medicine's own Biomedical Informatics Core (NUBIC), to find out disease association with gene of interest (http://projects.bioinformatics. northwestern.edu/fundo/) [104].

Network construction

Disease gene network and protein interaction network were drawn using Cytoscape.

Cytoscape is an open source bioinformatics software platform for visualizing molecular interaction networks and also integrates these interactions with gene expression profiles and other state data [105]. It is available at http://www.cytoscape.org/. Though scale free networks do not have a well-defined threshold for a node to be a hub, several researchers have defined a degree threshold. Gaci [106] recently proposed that any node with a degree higher that 3/2 times of z (average degree), could be considered as a hub. I have used the above procedure for identification of hubs in our network. Network parameters such as the node degree, betweenness centrality and stress centrality were calculated using Cytoscape plug-in CentiScaPe [107]. Degree is an estimate on the regulatory relevance of the node. In biological networks, proteins with very high degree interact with several proteins, thus suggesting a central regulatory role that is they are likely to be hubs. The centrality value of a node can be interpreted as the probability of a protein to be functionally capable of organizing discrete protein clusters or modules. Thus, a protein with high centroid value, compared to the average centroid value of the network, will be possibly involved in coordinating the activity of other highly connected proteins. Stress of a node indicates the relevance of a protein as functionally capable of holding together communicating nodes. Thus, stress simply indicates a molecule heavily involved in cellular processes. Betweenness of a node in a network indicates the relevance of a protein as functionally capable of holding together communicating proteins. Proteins with high betweenness value are crucial in maintaining functionality and coherence in biological mechanisms [107]. All the centralities are calculated simultaneously in this special plug in.

Target selection

I further focused on energy generation pathways and selected two glycolytic genes phosphoglycerate kinase 1 (PGK1) and pyruvate kinase M2 (PKM2) for experimental validation on their regulation by PPARγ. These genes were selected because they were reported to be involved in breast cancer in literature [92], they had PPRE motif but were not earlier reported to be regulated by PPARγ. Also, they were at important steps in biological pathway and were hubs. Here, it must be mentioned that PGK1 has a node degree of 13 and PKM2 has a node degree of 10.

2.2.2 EXPERIMENTAL VALIDATION METHODOLOGY

Reagents

Dulbecco's modified Eagle's medium (1000 mg/L glucose, l-glutamine, and sodium bicarbonate), Fetal bovine serum, 15-deoxy-Δ12, 14-Prostaglandin J and crystal violet were purchased from Sigma-Aldrich, St Louis, MO, USA. Penicillin–Streptomycin–Neomycin antibiotic mixture and Hoechst 33,258 were procured from Hoechest; Invitrogen, Eugene, OR, USA and JC-1 dye from Biotium (Hayword, CA, USA). Sodium chloride, potassium chloride, Tris base, glycine, sodium phosphate di basic, sodium di hydrogen phosphate were purchased from Wako Pure Chemical Industries, Osaka, Japan.

Cell culture and treatment

The human breast adenocarcinoma cell lines MDA-MB-231 and MCF-7 were purchased from the American Type Culture Collection (ATCC; Manassas, VA, USA). The carcinoma cells were maintained in Dulbecco's modified eagle's medium supplemented with 10% fetal bovine serum and PNS antibiotic mixture 100 ng/mL at 37°C and 5% CO_2/95% O_2. Cells at about 50% confluency were treated with 5 and 10 μM of 15-deoxy-Δ12, 14-Prostaglandin J for 48 h and harvested for further use.

Cell viability analysis

Cell viability was assessed using MTT cell proliferation assay kit (Roche, Mannheim, Germany) following manufacturer's instructions. This assay is a nonradioactive cell proliferation assay that identifies living cells, and is based on the cellular conversion of a tetrazolium salt into a formazan product, a chromophore, which can be quantified by spectrophotometry. 10^4 cells/well were plated in 96-well plates. Cells were grown for 24 h followed by 48 h treatment of 5 and 10 μM of 15-deoxy-Δ12, 14-Prostaglandin J2. The intensity of the reduced dye which corresponds to the viable cells was measured at 570 nm wavelength by Thermo Scientific Varioskan Flash Multimode Reader.

Western blot analysis

The cells were lysed in RIPA lysis buffer (25 mM Tris–HCl (pH 7.6), 150 mM NaCl, 1% NP-40, 1% sodium deoxy cholate, 0.1% SDS) complemented with complete protease inhibitors (Roche) for 15 min on ice followed by centrifugation at 14,000 g for 15 min at 4°C. The protein concentration was determined using BCA reagents (Pierce,

Rockford, IL, USA). Twenty microgram of protein was resolved in 10% in SDS-polyacrylamide gel under standard denaturing conditions according to Laemmli's method (1970). The proteins were transferred onto polyvinylidene difluoride membranes using a Trans-Blot SD (Bio-Rad, Lewes, E. Sussex, UK.) semi-dry electroblotter for 30 min at 20 V. Subsequently, the membranes were blocked for 45 min at room temperature (RT) with 2% bovine serum albumin in 0.1% PBST. The membranes were then probed with anti-PGK1 (1:1000; Abcam, Cambridge, UK), anti-PKM2 (1:500, Abcam), anti-PPARγ (1:000; Cell Signaling), anti-caspase 8 (1:1000; Cell Signaling, Boston, MA, USA), anti-β-actin (1:20,000; Abcam) at 4°C overnight followed by three washes for 5 min each with 0.1% PBST. The membranes were then incubated with horseradish peroxidase conjugated secondary antibody (1:20,000; Abcam) for 45 min at RT and washed thrice for 5 min each with 0.1% PBST followed by chemiluminescent detection using luminescent image analyser equipped with charge-coupled device camera (LAS-4000 Ver. 2.1; Fuji Film, Tokyo, Japan).

ATP depletion studies

In order to examine the extent of ATP depletion due to PPARγ activation, I next examined ATP concentration in cytosol and mitochondria. ATP concentration was quantified using commercially available luciferin – luciferase bioluminescence assay kit (Molecular Probes, Inc., Eugene, OR, USA). The assay is based on luciferase's requirement for ATP in producing light (emission maximum ~560 nm at pH 7.8). Mitochondria from cultured cells were isolated using a mitochondria isolation kit according to manufacturer's instructions (Pierce Biotechnology, Inc., Rockford, IL, USA). ATP level was estimated in cytosolic and mitochondrial fraction according to manufacturer's instructions. The amount of ATP in the experimental samples was calculated from standard curve prepared with ATP (1–100 μM) and expressed as percentage of ATP in cells. Light emission was monitored using a luminometer (Wallac 1420 Victor 2 multiplate counter system; Perkin Elmer Life Science, Inc., Gaitherburg, MD, USA).

Hoechst staining

To determine the nuclear condensation and DNA fragmentation in cells undergoing apoptosis I stained the nucleus with nucleus specific stain Hoechst 33258, pentahydrate (bis-Benzimide) (Molecular Probes, Inc.). The cells were cultured on glass coverslips and treated according with 15d-PGJ2 concentrations. Cells were fixed with ice-cold

methanol: acetone (1:1) for 10 min at –20°C and later permeabilized with 0.32% PBST (PBS-Triton). Subsequently, coverslips were washed and exposed to Hoechst 33258 (0.5 μg/ml) in the dark at room temperature for 15 min. After washes, the ProLong+® Gold anti- fade reagent (Molecular Probes, Inc.) was dropped onto the coverslips and the fluorescent images were captured using Zeiss LSM 700 Zen 2009 confocal microscope.

Assessment of mitochondrial membrane potential (Δψ)

Mitochondrial transmembrane potential was investigated using a fluorochrome, JC-1 dye (Biotium). JC-1 has the unique property among ΔΨm-sensitive fluorophores of developing large shifts in its fluorescence signal at the levels of uptake induced by the high ΔΨm characteristic of energized mitochondria. This is due to the formation of red fluorescent (595 nm) J-aggregates of the molecule in the mitochondrial matrix. At the levels of JC-1 uptake seen during low ΔΨm, the fluorophore remains as a green fluorescent (535 nm) monomer [108,109]. The reciprocal behavior at the two emission wavelengths, which can easily be measured simultaneously, results in large changes in the 595/535 nm ratio [110]. Only the multimeric, red fluorescent form of JC-1 specifically measures ΔΨm-dependent mitochondrial uptake of the probe. The green fluorescence of the monomeric form may be highly sensitive to its distribution in non-mitochondrial cell membranes. This dye accumulates in intact mitochondria and forms aggregates under influence of difference in potential where as it remains monomer in cytosol with characteristic absorption and emission spectra. After 48 h of 15d-PGJ2 treatment, the cells were incubated with 1X JC-1 dye at 37°C for 15 min followed by washes with assay buffer. The JC-1 labeled cells were analyzed by fluorescence microscope (Zeiss LSM 700 Zen 2009) confocal microscope and photographed. JC-1 appeared to be particularly useful for following changes in ΔΨm during the model.

Statistical Analysis

All experiments were performed in triplicates. The quantitative data is presented as mean ± SEM. Statistical analysis was performed using analysis of variance (One way ANOVA) followed by Bonferroni's on test to determine differences in mean and $p < 0.05$ was considered as statistically significant.

2.3 RESULTS AND DISCUSSIONS

I identified 217 genes from human genome reported to be involved directly or

indirectly in breast cancer that contain the PPRE and/or PACM motifs and could possibly be regulated by PPARγ. Interestingly, majority of PPARγ target genes are involved in biological processes such as cell cycle, cell–cell signaling, and signal transduction. Other important molecular functions that PPARγ target genes are associated with include transcription factor activity, protein kinase activity, and transmembrane protein kinase activity. The functional DO shows their involvement in cancer, breast cancer, and diabetes mellitus among several other disorders. These data suggest the important role of these genes in the listed disorders and could possibly contribute toward understanding their molecular mechanism.

2.3.1 Computational identification of PPARγ-binding sites in genes involved in breast cancer pathophysiology

The steps involved in identification of potential targets of PPARγ involved in breast cancer and their associations with diseases are outlined in Figure 2-1. A total of 217 breast cancer genes were predicted as putative PPARγ targets (Table 2-1).

PPARγ target identification

Protein–protein interaction and molecular interaction network construction

I further undertook protein–protein interaction analysis to find the interacting partner of these 217 genes using BioGRID database. Further, to identify important hubs (targets) I constructed an interacting network (Figure 2-2) and calculated centrality parameters; node degree, closeness, betweenness, and stress using CentiScape plug-in. All nodes above the degree value of 5.55 were considered as hub for this analysis [106]. The highest value for node degree, betweenness, and stress was 238, 844494.11, and 5520696, respectively. The lowest calculated values for degree, betweenness, and stress was 1.0, 0, and 0, respectively. The average value of the node degree, betweenness and stress was 3.7, 6242.74, and 46561.29, respectively. BRCA1 scores the highest for all the three centrality parameters (Table 2-2). The node degree, betweenness, and stress for PGK1 was 13, 29554.82, and 191676, respectively whereas for PKM2 the node degree, betweenness, and stress was 10, 19079.22, and 110048, respectively.

Gene Ontology, protein class and pathways

I analyzed the GO terms for all the 217 PPARγ target genes that are associated with breast cancer pathophysiology (Figure 2-3). The analysis revealed that cell cycle (52), cell–cell signaling (30), and signal transduction (28) were the most common GO categories representing biological processes. A total of 855 classifications were

identified suggesting that several proteins are involved in more than one biological process. A total of 280 classifications were identified under the molecular function and the three most abundant were transcription factor activity, protein kinase activity, and transmembrane protein kinase activity. The non-receptor serine threonine protein kinase class of proteins was amongst the most represented, comprising 30 protein entries followed by nucleic acid binding proteins with 19 entries.

Functional Disease Ontology

Functional gene ontology is a tool to study the gene disease relationship. These studies greatly facilitate understanding of pathogenesis, which could lead to better diagnostics and treatments. DOLite is a simplified vocabulary list from the Disease Ontology (DO). It has been used in the FunDO (FunDO) Web application [104]. Here, I undertook functional enrichment test for 217 PPARγ target genes. All the genes were found to be associated with diseases. My disease gene network shows predominant role of PPARγ in cancer in general (18.5%), followed by breast cancer (10.1%), and prostate cancer (8.9%) (Figure 2-4). Notably, diabetes mellitus, atherosclerosis and rheumatoid arthritis are other important disorders, with 15, 12, and 13 PPARγ target genes, respectively. All nodes above the degree value of 6.68 were considered as a hub for this analysis [106]. The highest value for node degree, betweenness, and stress was 33, 4620.93, and 68152, respectively whereas the lowest calculated values for degree, betweenness, and stress was 1.0, 0, and 0, respectively. The average value of the node degree, betweenness, and stress was 4.55, 272.47, and 4616.38. Cancer had the highest centrality parameters in protein–protein interaction network (Table 2-3) whereas the gene associated with maximum number of diseases was SERPINE1 with centrality parameters as node degree (15), betweenness, (1818.93) and stress (33750) (Table 2-4). SERPINE1 is a serine protease inhibitor (serpin) protein and is recently reported to be over expressed in colorectal cancer associated with tumor invasiveness and aggressiveness [111]. It has been reported to be modulated by PPARγ [112].

Target selection for experimental validation on their regulation by PPARγ

Panasyuk et al. [113] recently reported that the PPARγ transcription factor and nuclear hormone receptor contributes to selective PKM2 and hexokinase 2 gene expression in PTEN-null fatty liver. However, there are no reports on the regulation of PGK1 and PKM2 by PPARγ in breast cancer and our understanding of molecular mechanisms selectively controlling specific glycolytic enzymes is limited. It was

interesting to note that several glycolytic genes had PPRE motif. Here, I report for the first time the down regulation of two key glycolytic genes—PGK1 and PKM2 by PPARγ upon ligand activation. PGK1 and PKM2 catalyze the sixth and ninth step, respectively, in the glycolysis pathway generating two ATPs each. Additionally M2 isoform of pyruvate kinase has been reported as the key regulator in maintaining metabolic budget system in tumor cells [114].

Glycolysis is the initial stage of glucose metabolism, the conversion of glucose into pyruvate and generation of energy in the form of ATP. Coordinated upregulation of glycolysis pathway proteins has been reported in several different tumor types [119-117] including breast cancer [118]. Recently, it was also suggested that women with breast cancer have increased levels of glycolytic proteins in plasmas [119]. Mechanisms such as gene amplification, increased gene expression, increased translation, posttranslational modification, and regulation by protein–protein interactions in the cytoplasm or even small RNA networks or RNA interference make possible enhancement of glycolysis [92]. Given this large number of different mechanisms, and the assumption that carcinogenesis is the result of a large number of stochastic events, one might expect that different cancers exploit different mechanisms to achieve increased glucose consumption owing to the variety of mechanisms and acceptance of the postulate that the underlay of carcinogenesis is a large number of stochastic events. The complexity of the underlying biochemical and molecular mechanisms of breast cancer make metabolic reprogramming in breast cancer unclear.

In this study, I carried out prediction of PPRE motifs in glycolytic genes to determine the possible role of PPARγ in altered regulation of glycolysis in tumor metabolism and explored PPARγ as the potential link between energy balance, cellular metabolism, and cancer pathogenesis.

2.3.2 Cytotoxic and anti-proliferative effect of micromolar concentration of 15d-PGJ2 for PPARγ activation in breast cancer cells

Breast cancer cells were exposed to 15d-PGJ2 concentrations of 3, 5, 10, 15, and 20 μM for 48 h. The cytotoxic and anti-proliferative effect of 15d-PGJ2 was assessed by MTT dye reduction assay. The IC-50 value for MDA-MB-231 and MCF-7 were found to be 10 and 15.9 μM, respectively. I preferred to proceed with 10 μM to see the comparable effects of same concentration on both the cell lines. As shown in Figure 2-5, cell numbers decreases in dose-dependent fashion.

2.3.3 Constitutive expression levels of PPARγ in breast cancer cells

To assess whether inhibition of cells' growth by PPARγ ligand, 15d-PGJ2 is a function of PPARγ expression, I first screened two representative breast cancer cell lines, MDA-MB231 and MCF-7 for expression of PPARγ protein. I observed MDA-MB-231 cells expressed higher level of PPARγ protein than MCF-7. MDA-MB-231 was found to have 2.4-folds higher level of PPARγ as compared to MCF-7, which accounted for its higher susceptibility toward PPARγ activation by 15d-PGJ2 (Figure 2-6). The results are comparable with studies of Huang et al. [120].

2.3.4 Repression of glycolytic enzymes upon activation of PPARγ by its natural ligand

PGK1 and PKM2 are reported to be over expressed in many cancers [92] accounting for their pivotal role in most fundamental metabolic alterations [91]. Down regulating these enzymes would not only starve the cells for ATP but also for building blocks like amino acid and nucleic acid precursors. Here, I hypothesized that PGK1 and PKM2 expressing PPRE motifs may be modulated upon activation of PPARγ. Therefore, I undertook expression analysis of these metabolic enzymes in order to examine the above hypothesis. I observed reduction in expression of PGK1 (Figure 2-7) and PKM2 (Figure 2-8) with increase in 15d-PGJ2 concentration. These results were comparable with results from anti-proliferative studies. Similar results for PGK1 were observed in prostate cancer cells by Venkatachalam et al. [89].

2.3.5 Decrease in energy currency level upon repression of glycolytic genes

ATP plays an important role in metabolism, irrespective of whether it is being produced or used. Since both the enzymes are involved in ATP synthesis I hypothesized that with repression in PGK1 and PKM2, the ATP level will be altered. Therefore, to test this hypothesis I undertook ATP depletion studies in cytosol and mitochondria in both the breast cancer cell lines. Significant depletion of the cytosolic ATP and mitochondrial ATP level was observed. However I observed higher level of ATP depletion in MDA-MB-231 as compared to that in MCF-7, which could possibly be related to higher basal expression of PPARγ in MDA-MB-231 (Figure 2-9).

2.3.6 PPARγ activation leads to apoptosis in breast cancer cells

Patel et al. [121] observed that the activation of PPAR by its selective ligand, rosiglitazone, upregulates PTEN expression in human macrophages, Caco2 colorectal cancer cells, and MCF-7 breast cancer cells possibly by binding to two putative PPREs

identified within the PTEN promoter. As a result of upregulated PTEN, Akt phosphorylation and concomitant cell proliferation was significantly reduced. It was also shown that PPARγ-dependent PTEN expression could be blocked by estrogen receptor binding to the PPRE site of the PTEN promoter [122]. This crosslink has to be carefully considered when new therapy approaches are developed.

Downregulation of PGK1 and PKM2 decreases ATP production in the cytoplasm and mitochondria, initiating apoptosis and suppressing cancer metabolism. ATP depletion, used in combination with chemotherapy and/or radiation, has a variety of effects on cancer cells including inducing apoptosis in multidrug resistant cells and decreasing tumor promotion. Cellular ATP level has been reported as an important determinant of cell death [123]. The exact mechanisms of these effects have not been fully elucidated.

Disruption of mitochondrial integrity and caspase-8 activation are one of the early events leading to apoptosis. It has earlier been elucidated that PPARγ synthetic ligands activate intrinsic and extrinsic apoptotic cascade [124,125]. To confirm the effects of down regulation of PGK1 and PKM2 on cell survival, I undertook analysis for caspase 8 expression, mitochondrial membrane potential and nuclear damage. It was observed that activation of PPARγ causes caspase-8 activation (decrease in caspase-8 proenzyme expression). This data demonstrates that the caspase-8 proenzyme is being cleaved to active caspase-8 fragments in dose dependent fashion of 15d-PGJ2 (Figure 2-10). Apoptosis leads to activation of series of biochemical events that alter cell characteristics. One of these important changes is chromatin condensation and nuclear frag- mentation. To further examine these changes, I stained the nucleus with nucleic acid specific stain Hoechst stain. Figure 2-11 clearly presents the increase in condensed nuclei (apoptotic cells) in dose-dependent fashion. Also the MDA-MB-231 apoptotic cells were greater in number as compared to that in MCF-7 accounting for its higher basal level of PPARγ expression.

I next examined whether PPARγ activation causes mitochondrial damage by analyzing mitochondrial membrane potential with mitochondria fluorescent dye JC-1. A cationic dye that exhibits potential-dependent accumulation in mitochondria, indicated by a fluorescence emission shift from green (525 nm) to red (590 nm), JC-1 is most widely employed in detection of mitochondrial depolarization during early apoptosis, hallmarked by loss of mitochondrial membrane potential, coinciding with caspase 8 activation. In non-apoptotic cells, JC-1 exists as a monomer in the cytosol (green) and

accumulates as aggregates in the mitochondria, which appear red. In apoptotic and necrotic cells, less dye accumulates in the mitochondria, and more is retained in the cytoplasm, hence more green and less red is visible. As shown in Figure 2-12, in the control cells with high mitochondrial membrane potential, the JC-1 dye formed J-aggregates with intense red fluorescence. On the other hand, on treatment with 10 μM 15d-PGJ2 there was progressive loss of red J-aggregate fluorescence and increased cytoplasmic diffusion of green monomer fluorescence, depicting disruption of mitochondrial potential. Together, these data demonstrate the activation of caspase-8, disruption in mitochondrial potential and chromatin condensation upon PPARγ activation leading to apoptotic cascade activation.

2.4 CONCLUSION

My results have established previously unknown novel crosslink between PPARγ and glycolysis via PGK1 and PKM2; thereby adding a new dimension to therapeutic potential of PPARγ ligands. Although the exact mechanism remains unclear and further studies are still needed to clarify the potential role and molecular basis of action of PPARγ in breast carcinogenesis, my investigation open a new direction for development of novel therapeutic method by targeting PGK1 and PKM2 in breast cancer treatment

Table 2-1: List of putative PPARγ targets involved in breast cancer pathophysiology (PGK1 and PKM2 are putative PPARγ targets)

ABCA1	COL18A1	HLA-B	MXD1	RAB6A
ABL1	COL1A2	HLA-C	MYCBP	RCAN1
ACADM	CREB1	HMGB1	MYCN	RET
ACE	CRX	HOXC9	MYOD1	RNPC3
ADAMDEC1	CSE1L	HPX	NAMPT	RPA1
ADSL	CXCL2	HRG	NES	RPS6KA1
AKAP12	CXCR3	HSPA4	NF1	S100A9
ALOX15	CXCR5	IFNGR2	NOS3	SCARB1
APC	CYCS	IGFBP5	NOX1	SCP2
APOC3	CYP21A2	IKBKB	NR0B2	SEMA5A
APOE	DAZAP1	IKBKE	NRG1	SERPINE1
ARHGEF6	DDIT3	IL10RA	NTRK1	SFRP4
ASS1	DDR1	IL11	OPRM1	SLC11A2
AVP	DDR1	IL13RA1	OXER1	SLC2A2
BACE2	DKK1	IL1RN	PARK7	SLC9A2
BBS2	DLG3	IL4	PARP4	SOD2
BCL10	DNMT3B	ILK	PARVB	SPAG5
BCL2L1	DPP4	INS	PCNT	SSBP3
BIRC3	DUSP13	INSL3	PDCD1LG2	ST6GAL1
BRCA1	DYSF	INSR	PDE5A	STAP1
CA9	EIF2AK2	IRF5	PER2	STC2
CALCR	EIF2C1	IRF7	PGK1	TAC1
CALM2	EPHB3	ITCH	PIK3C2B	TACC3
CALM3	EWSR1	ITGA3	PIK3CA	TAT
CAMK2D	EZR	ITGB4	PKM2	TBP
CAMP	F2R	JUB	PKP1	TERF2
CASP14	FBL	KCNN3	PLAU	TFRC
CBX5	FBXW7	KIF11	PLAUR	TGFA
CCL20	FCGR2A	KLRD1	PLCG1	TH
CCNB1	FGF8	KRIT1	POLD4	TIMP1
CD1C	FGFR2	LCK	POLR2L	TLR4
CD27	FKBP5	LGR6	PPA1	TMPO
CD3D	FLT1	LSM2	PPARA	TMSB10
CD80	FUT4	LTBR	PPP2R2B	TNC
CD86	GATA3	MAD1L1	PRG2	TNFRSF1A
CDC25C	GHRL	MAP1B	PRKCD	TNFRSF6B
CDC34	GJC1	MAP2K7	PRKCG	TNNI2
CDK7	GLS	MAP3K14	PRNP	TPO
CDK9	GNA15	MAPK1	PSMB5	UGT1A7
CDS1	GNB1	MAPK10	PTGER3	VAV3
CENPF	HDAC3	MDM4	PTN	WFDC2
CFTR	HEY1	MEN1	PTPN6	WNT3A
CHEK1	HIPK2	MET	PTPRA	XRCC6
CHKB	HK1	MIF	PXN	YWHAH

Table 2-2: Network parameters for top 20 PPARγ regulated genes involved in Breast cancer pathophysiology.

Gene Name	Node degree	Betweenness	Stress
BRCA1	238	844494.11	5520696
TERF2	191	688999.13	3567270
HDAC3	184	389054.34	3237646
YTHDC1	172	447848.96	0
SP1	171	346739.49	2519974
AKT1	125	344673.91	2539832
ERCC2	117	442363.28	132142
DEF1	116	312543.31	0
ABL1	106	221707.21	1373642
H2AFX	101	193243.75	181736
PLCG1	93	233214.41	1115962
ITCH	81	221022.57	1293228
CREB1	74	154538.71	1058272
MYOD1	73	132531.74	1030916
EZH2	71	118931.96	658402
RPA1	66	131552.69	799232
VCP	66	217296.63	1036336
BCL2L1	59	159560.98	1044134
PRKCZ	56	136275.83	870684
	Average: 3.7	Average: 6242.74	Average: 46561.29
	Max: 238	Max: 844494.11	Max: 5520696
	Min: 1	Min: 0	Min: 0

Table 2-3: List of diseases associated with the genes possibly regulated by PPARγ and involved in breast cancer pathophysiology, detected by connectively and centrality parameters (node degree, betweenness, and stress) using Disease-Ontology Lite (DoLite).

Disease name	Node Degree	Betweenness	Stress
Cancer	33	4620.93	68152
Breast cancer	18	1272.90	15444
Prostate cancer	16	1484.50	18790
Diabetes mellitus	15	1313.39	24032
Rheumatoid arthritis	13	1150.80	17250
Atherosclerosis	12	979.75	12622
Embryoma	12	905.12	16224
Colon cancer	11	998.42	19908
Alzheimer's disease	10	633.48	11036
Asthma	9	773.96	532
	Average: 4.55	Average: 272.47	Average: 4616.38
	Max: 33	Max: 4620.93	Max: 68152
	Min: 1	Min: 0	Min: 0

Table 2-4: List of highly connected genes associated with the genes that are possibly regulated by PPARγ and involved in breast cancer pathophysiology, detected by connectivity and centrality parameters (node degree, betweenness and stress) using Disease-Ontology Lite (DOLite).

Gene name	Node degree	Betweenness	Stress
SERPINE1	15	1818.93	33750
IL1A	10	833.54	16768
MIF	10	561.79	9760
APOE	9	646.21	11220
AKT1	8	825.62	15534
EGR1	7	925.69	16434
SOD2	7	601.33	9782
TNC	7	414.27	5494
BCL2L1	6	633.33	9746
SMAD3	6	316.71	4858
	Average: 4.55	Average: 272.47	Average: 4616.38
	Max: 33	Max: 4620.93	Max: 68152
	Min: 1	Min: 0	Min: 0

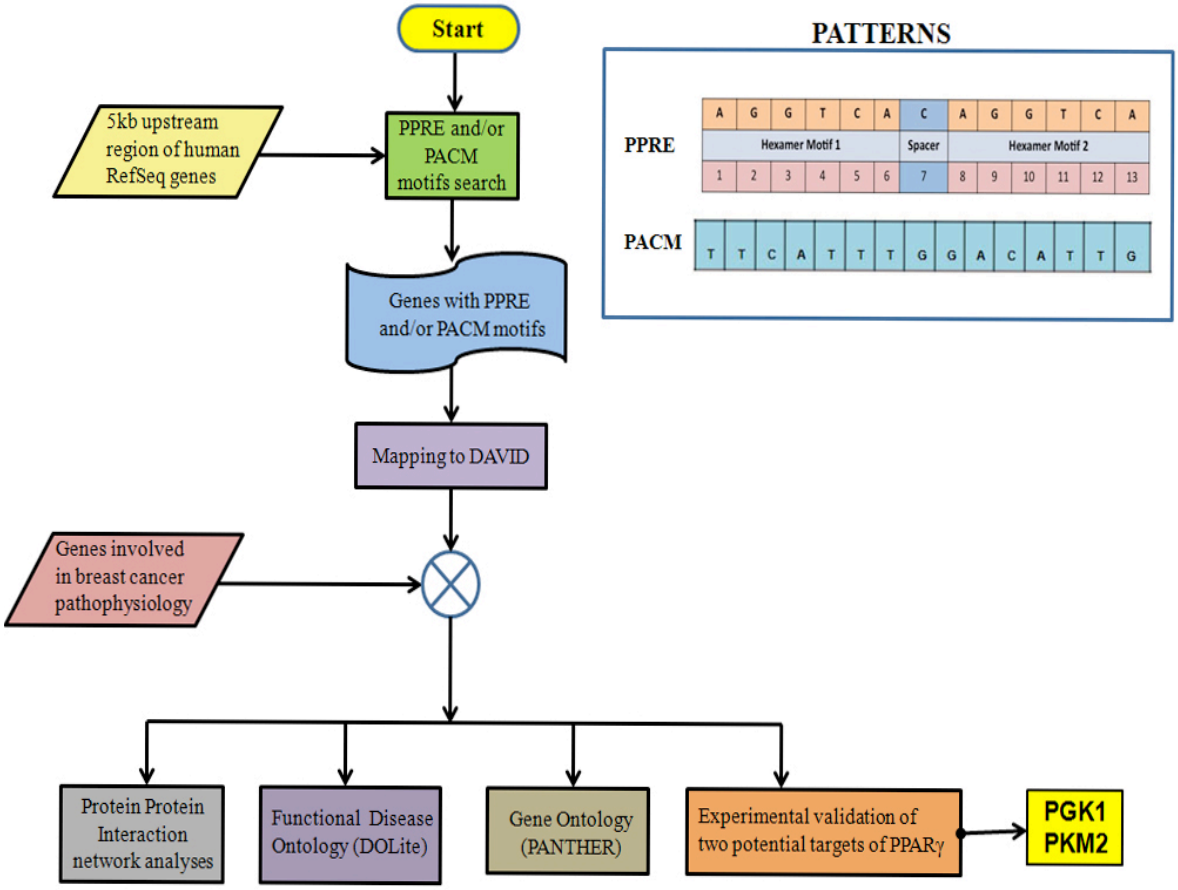

Figure 2-1: Flow chart depicting a simplified scheme of the methodology used for identification of PPARγ target genes that are associated with breast cancer. The effects of the glycolytic pathway genes PGK1 and PKM2 were studied using molecular and biochemical methods.

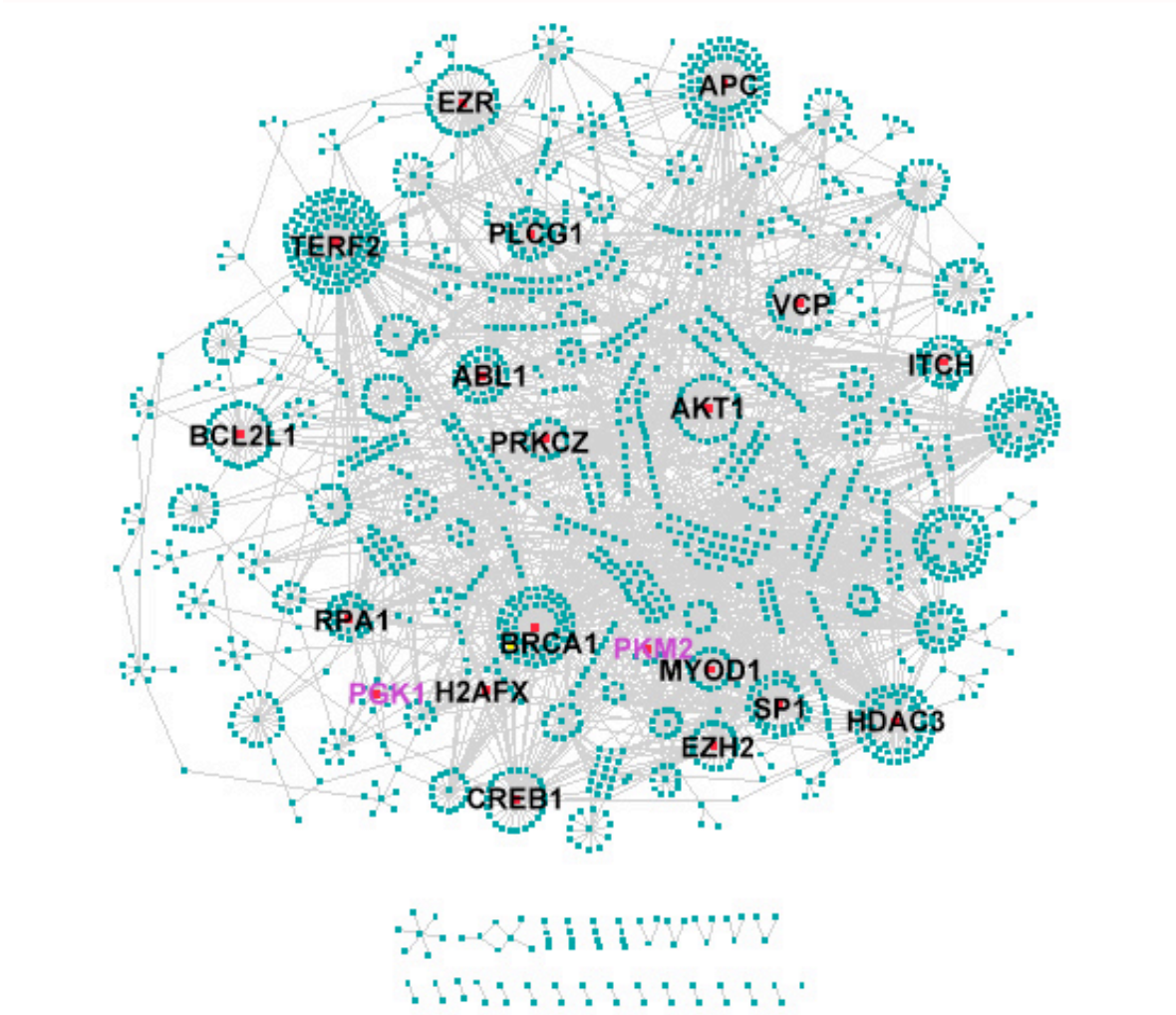

Figure 2-2: PPARγ disease gene network associated with breast cancer. Top 20 highly connected genes are shown in red and labeled. Genes chosen for experimental validation are labeled in pink.

[A]

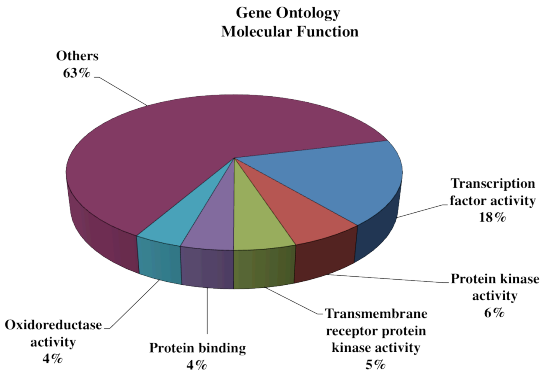

[B]

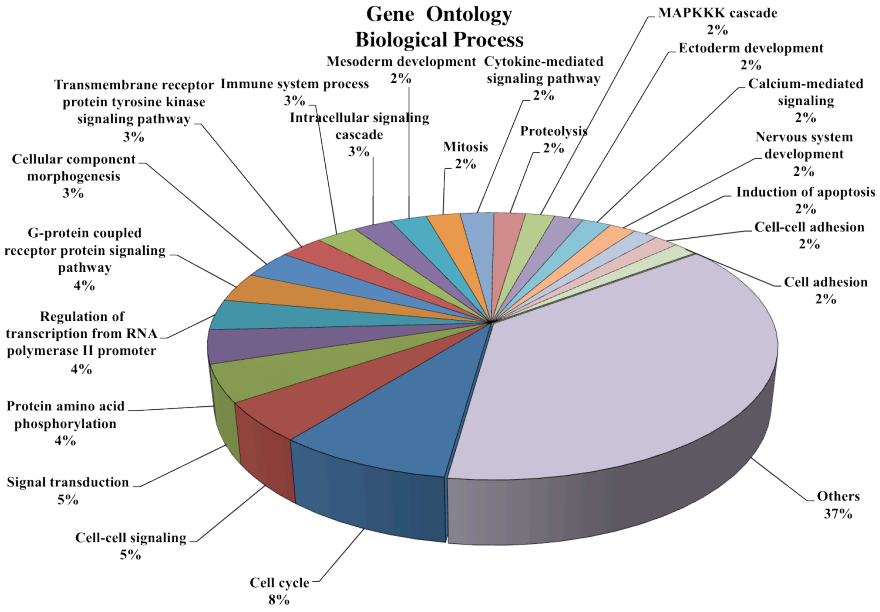

[C]

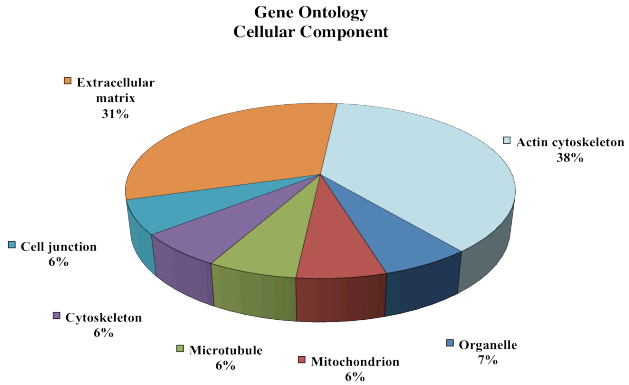

Figure 2-3: Classification of PPARγ target genes that are associated with breast cancer pathophysiology according to Gene ontology biological terms; Molecular function [A], Biological process [B] and Cellular component [C].

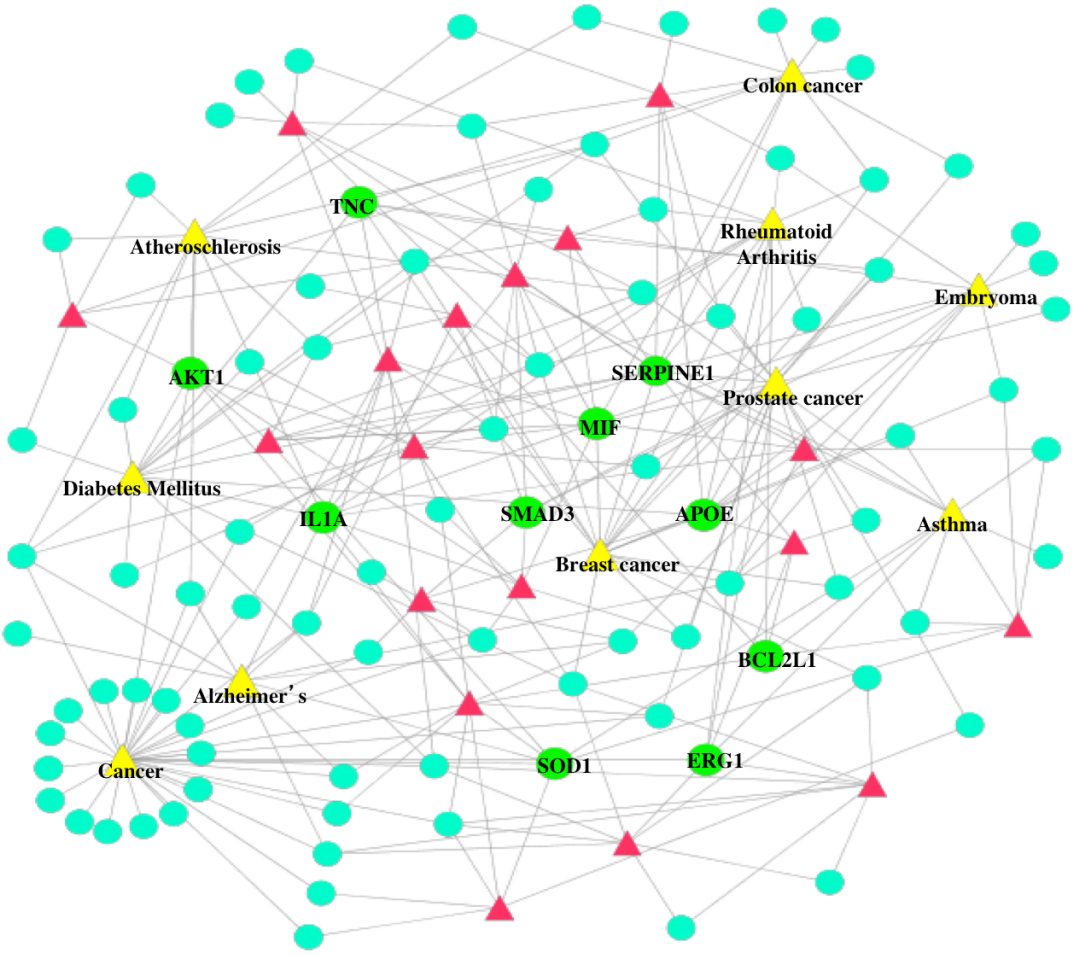

Figure 2-4: DOLite analyses for PPARγ target genes that are associated with breast cancer. Top 10 diseases are shown in yellow triangle and top 10 genes are shown in green circles.

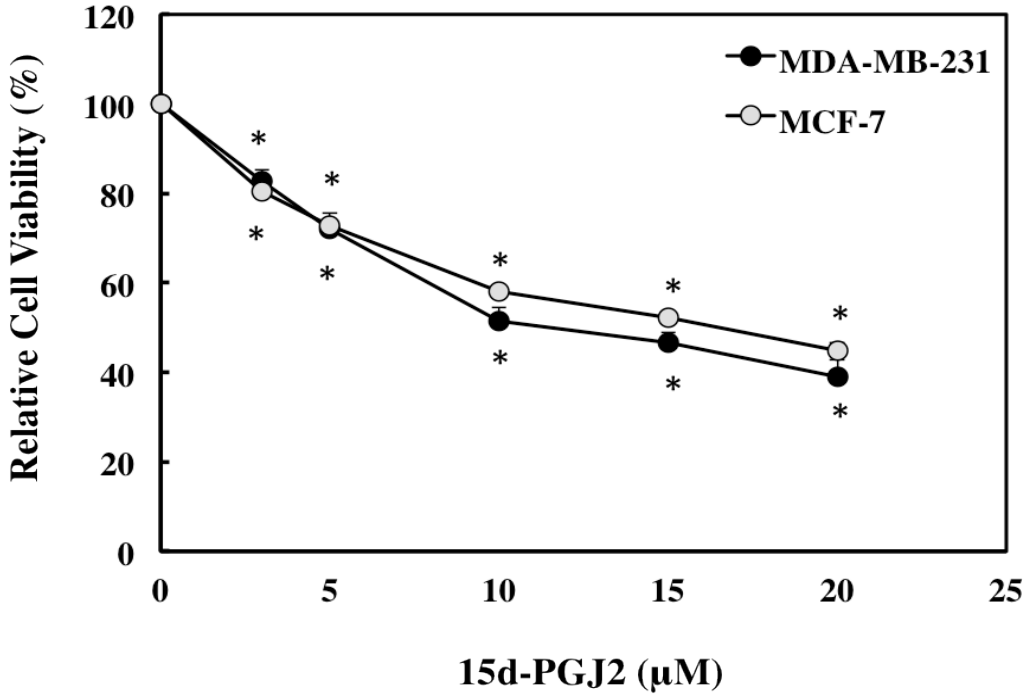

Figure 2-5: Cell viability in breast cancer cell lines, MDA-MB-231 and MCF-7 upon exposure to different doses of 15d-PGJ2 concentrations for 48 h. Data are presented as mean ± SEM of 3 independent experiments done in triplicates. '*' ($p<0.001$).

[A]

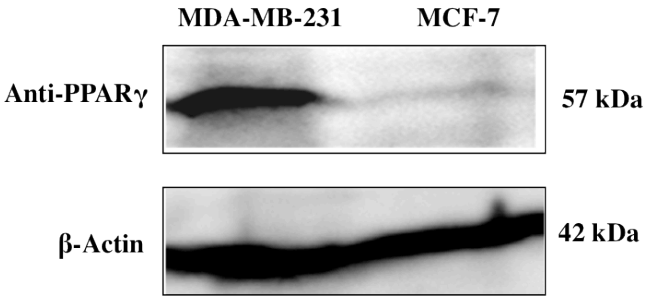

[B]

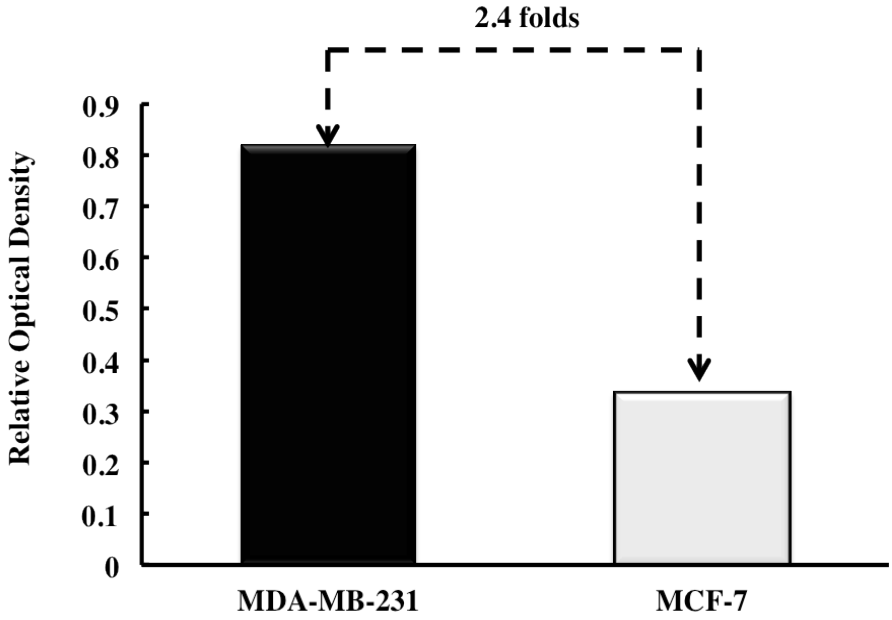

Figure 2-6: Representative immunoblots for constitutive expression levels of peroxisome proliferator-activated receptor γ (PPARγ) in MDA-MB-231 and MCF-7 [A]. [B] Quantitation of expression level in both breast cancer cells relative to β-actin is shown. Peroxisome proliferator-activated receptor γ (PPARγ) expression in MDA-MB-231 was 2.4-folds higher than MCF-7 in presence of 15d-PGJ2.

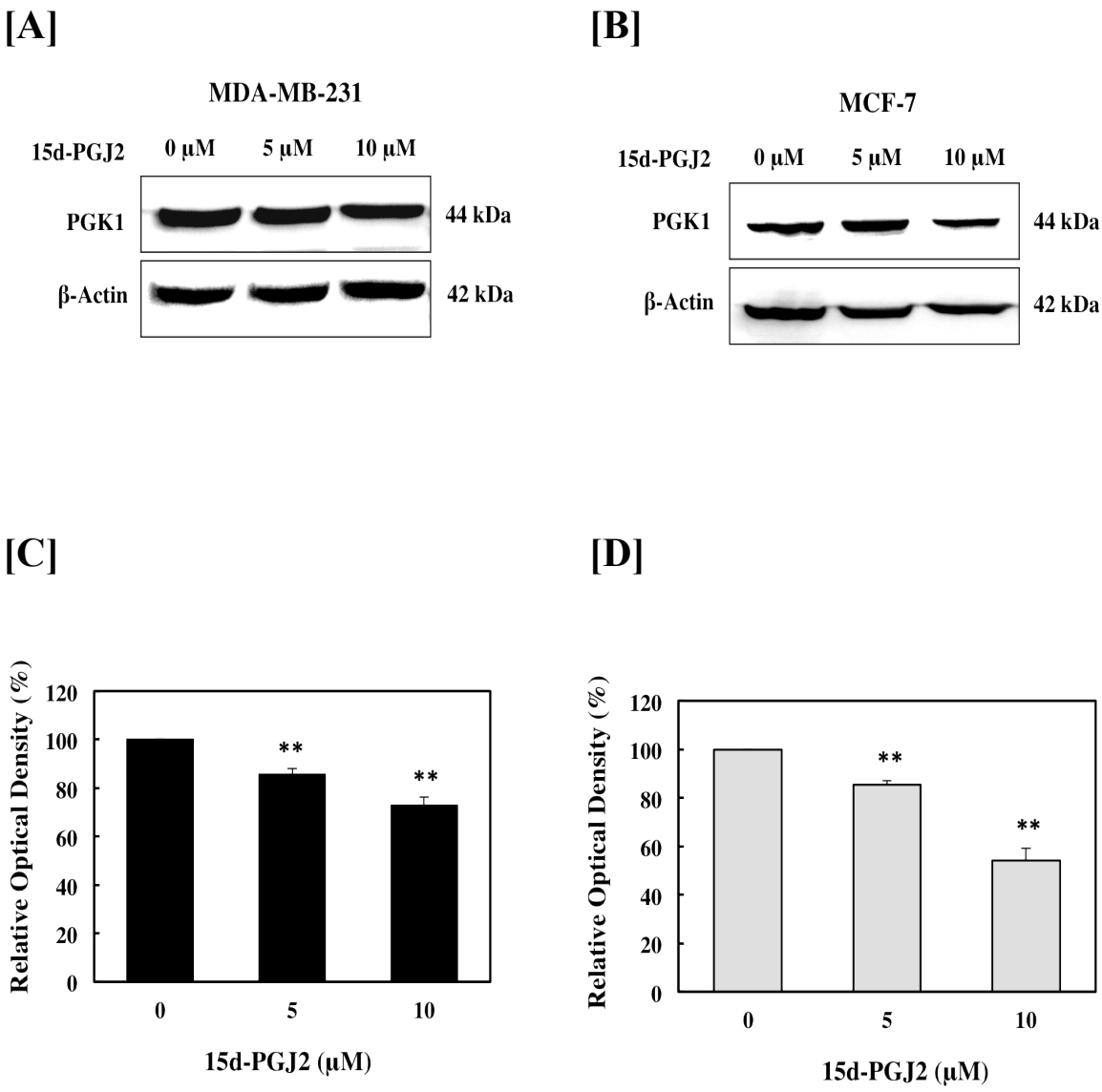

Figure 2-7: Representative western blots for protein PGK1 in (A) MDA-MB-231 and (B) MCF-7. (C, D) represents expression level of PGK1 in MDA-MB-231 and MCF-7 after 48 h of 15d-PGJ2 exposure. There was statistically difference of '**' ($p<0.005$) between control and test groups. Data are presented as mean ± SEM of three independent experiments.

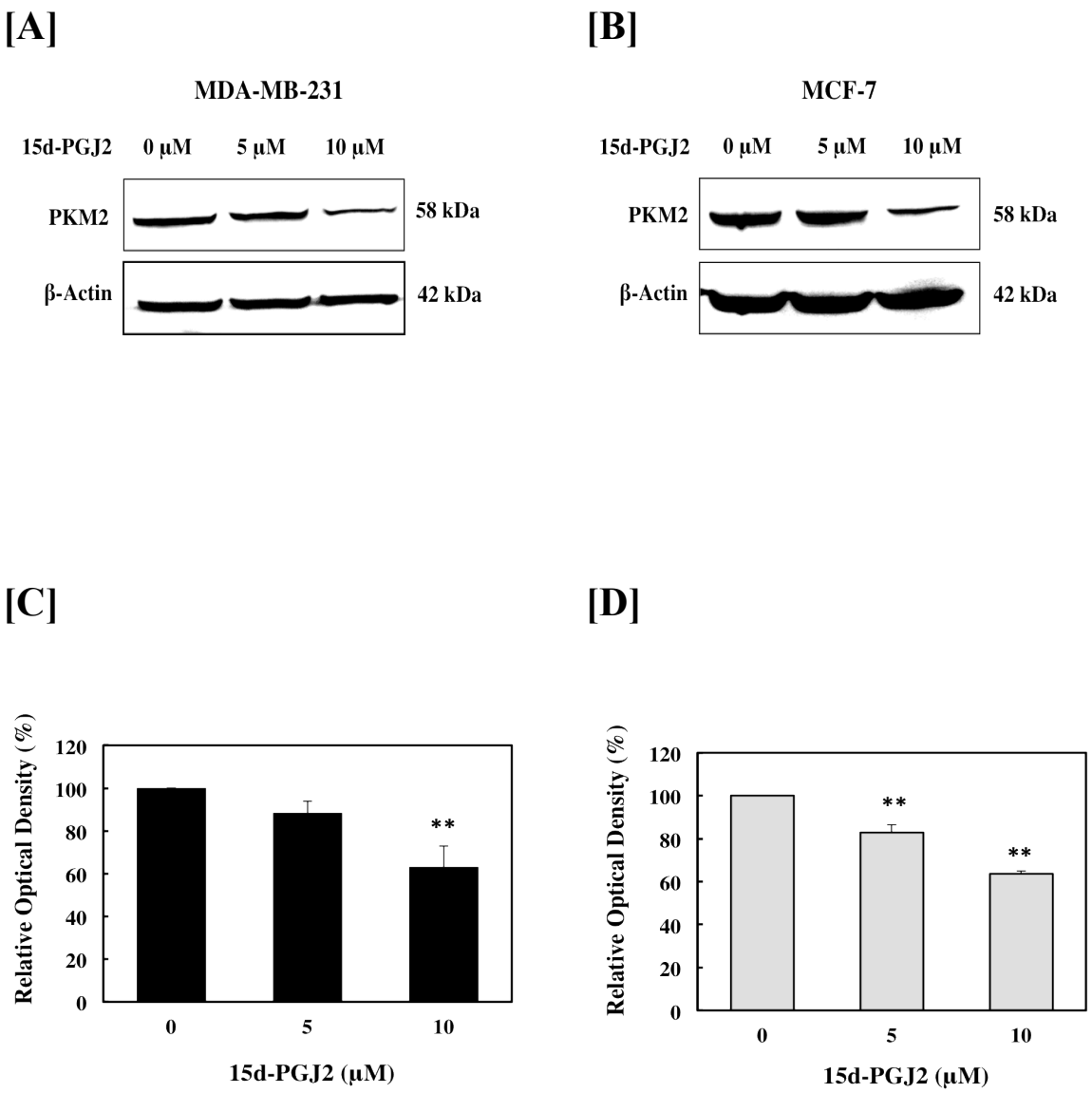

Figure 2-8: Representative western blots of PKM2 for (A) MDA-MB-231 and (B) MCF-7. Histograms (C, D) presenting expression level of PKM2 in MDA-MB-231 and MCF-7, respectively upon 48 h treatment of 15d-PGJ2. '**' ($p<0.005$) represents statistically difference between control and test groups. Data are presented as mean ± SEM of three independent experiments done.

[A]

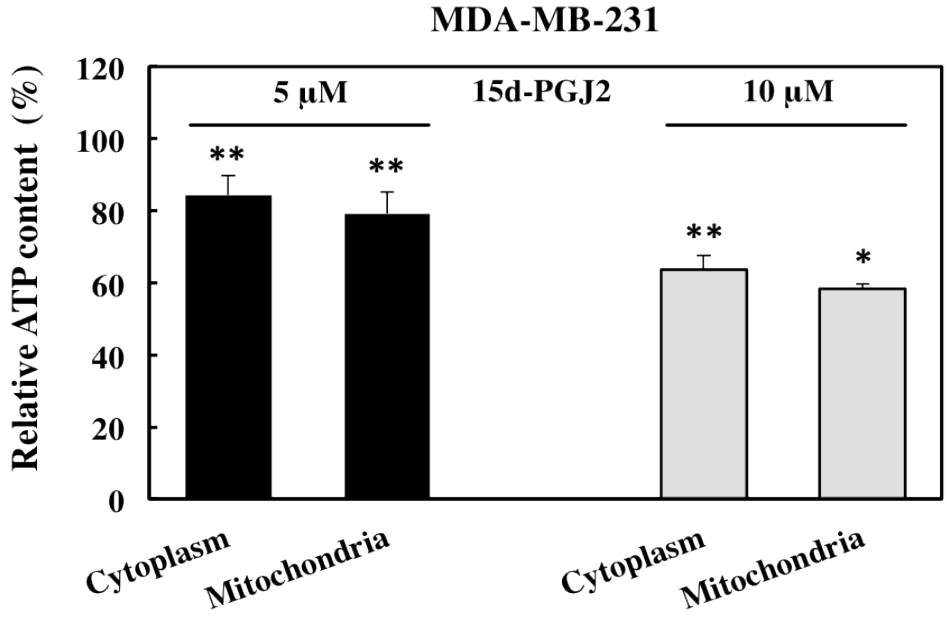

[B]

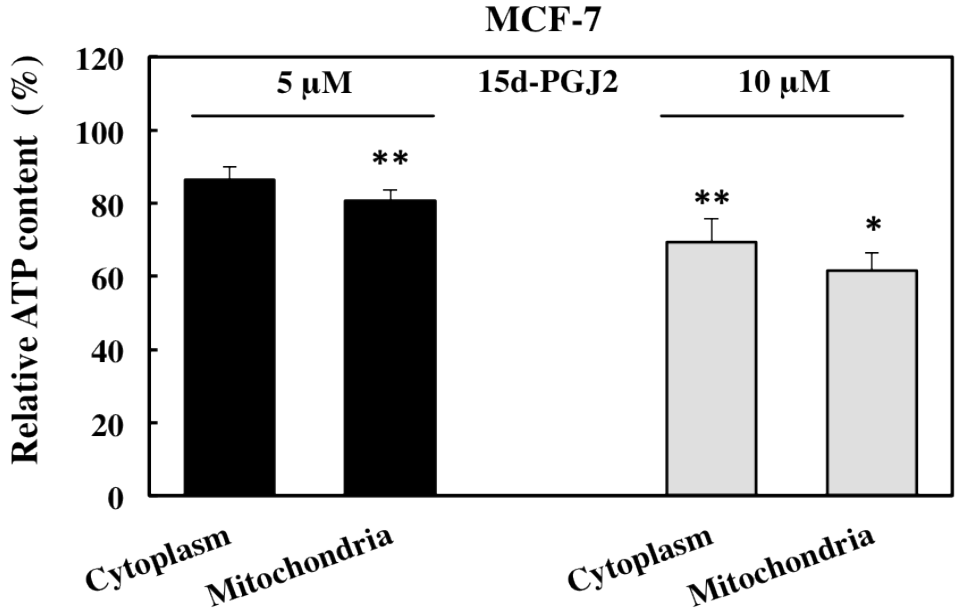

Figure 2-9: ATP depletion upon peroxisome proliferator-activated receptor γ (PPARγ) activation in (A) MDA-MB-231 and (B) MCF-7. Data are presented as mean ± SEM of thee independent experiments. '*' ($p < 0.001$) and '**' ($p<0.005$) represents statistically difference between control and test groups.

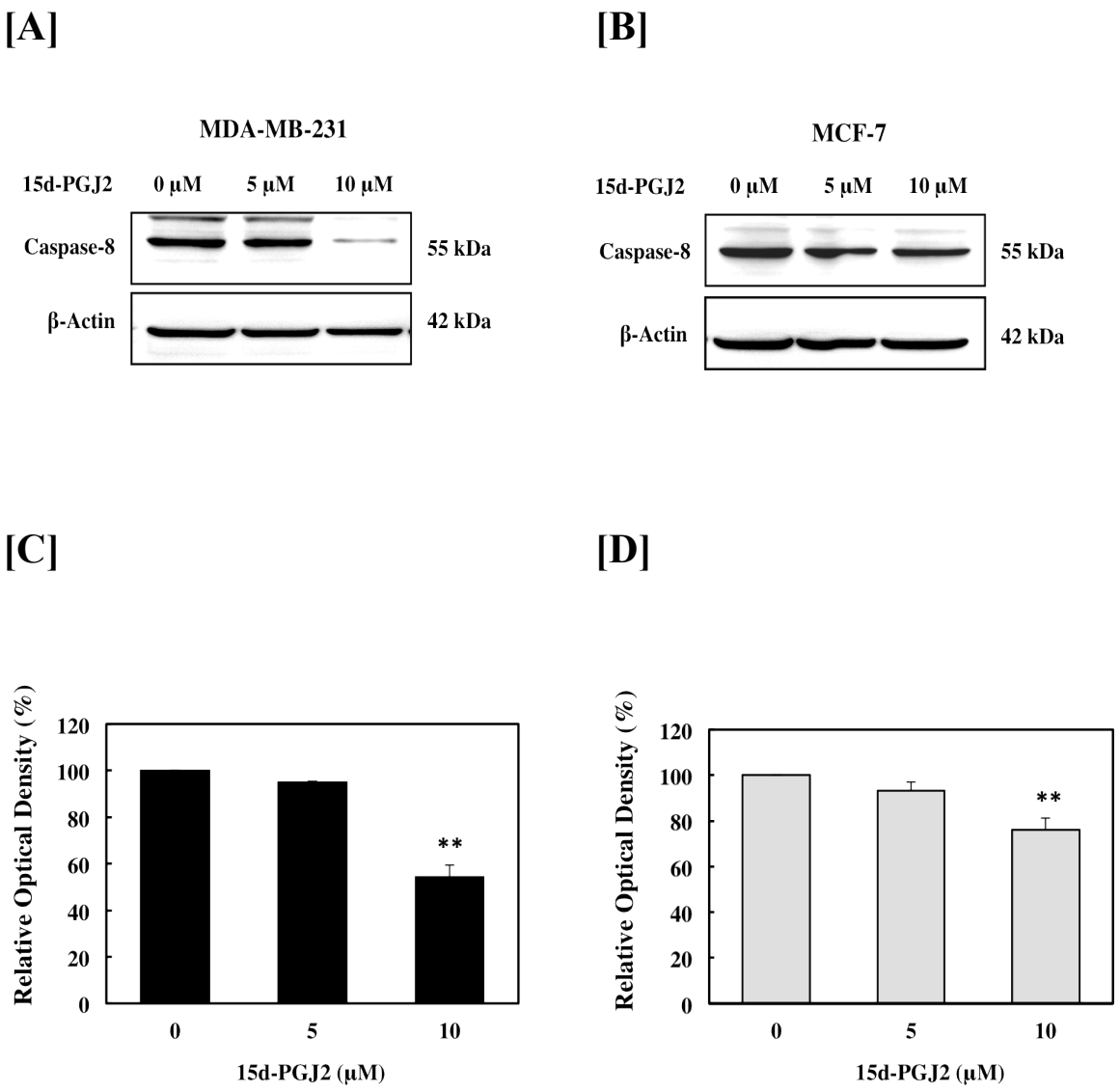

Figure 2-10: Representative western blots of proenzyme caspase-8 for (A) MDA-MB-231 and (B) MCF-7. (C, D) Histograms represent caspase-8 proenzyme's expression level in MDA-MB-231 and MCF-7, respectively upon 48 h treatment of 15d-PGJ2. Data are presented as mean ± SEM of three independent experiments. '**' ($p < 0.005$) represents statistically difference between control and test groups.

[A]

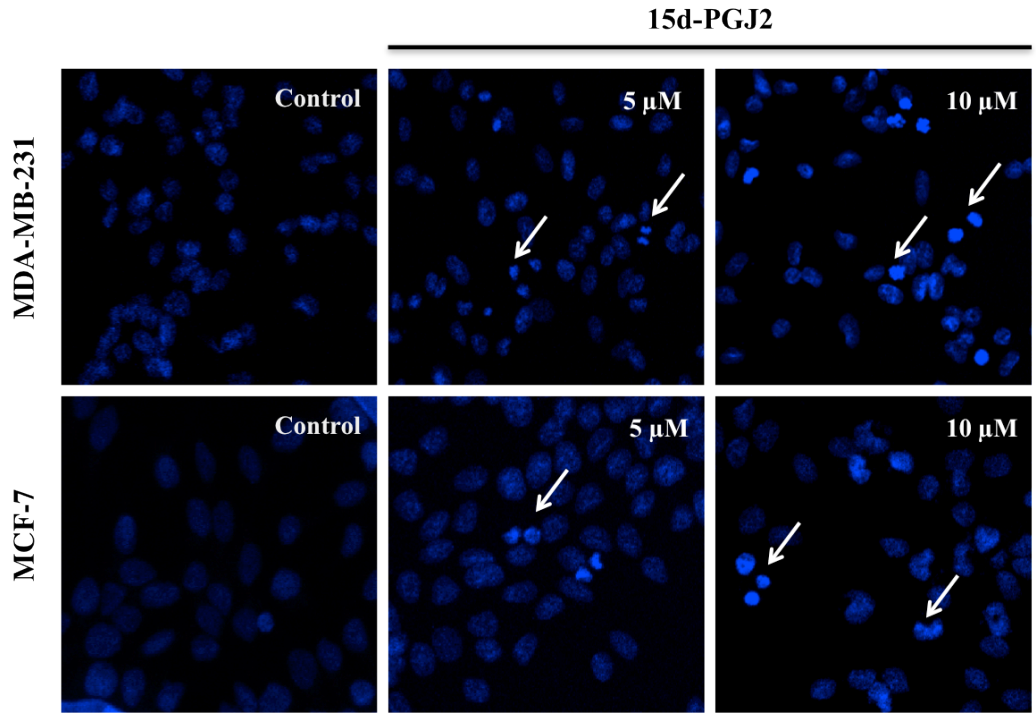

[B]

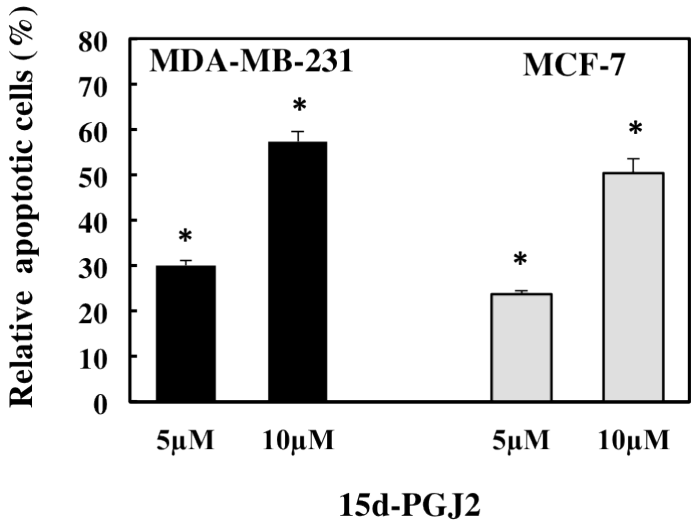

Figure 2-11: Hoechst staining of the (A) MDA-MB-231 and MCF-7 breast cancer cell lines. (B) Histogram represents the percentage (mean ± SEM) of apoptotic cells in MDA-MB-231 and MCF-7. Significant difference of '*' ($p < 0.001$) was observed in test groups of both cell lines as compared to control. Arrows indicate apoptotic cells.

[A]

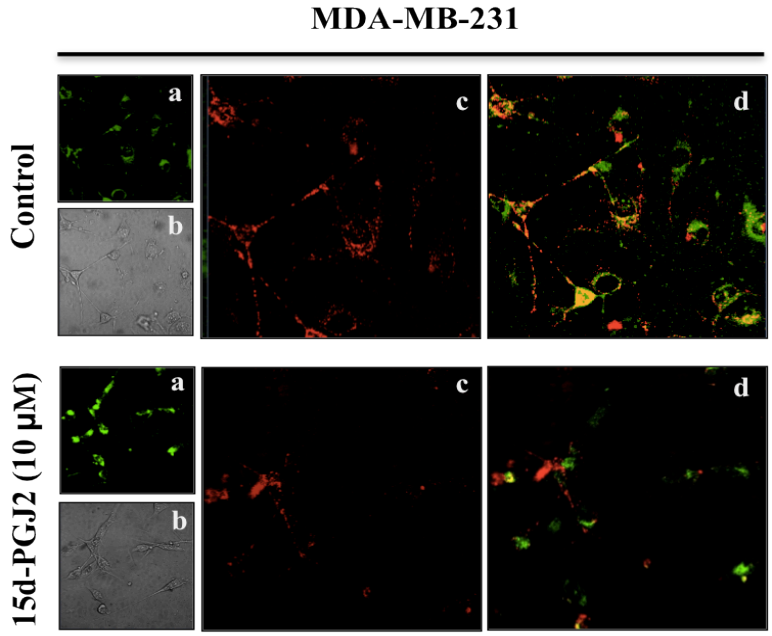

[B]

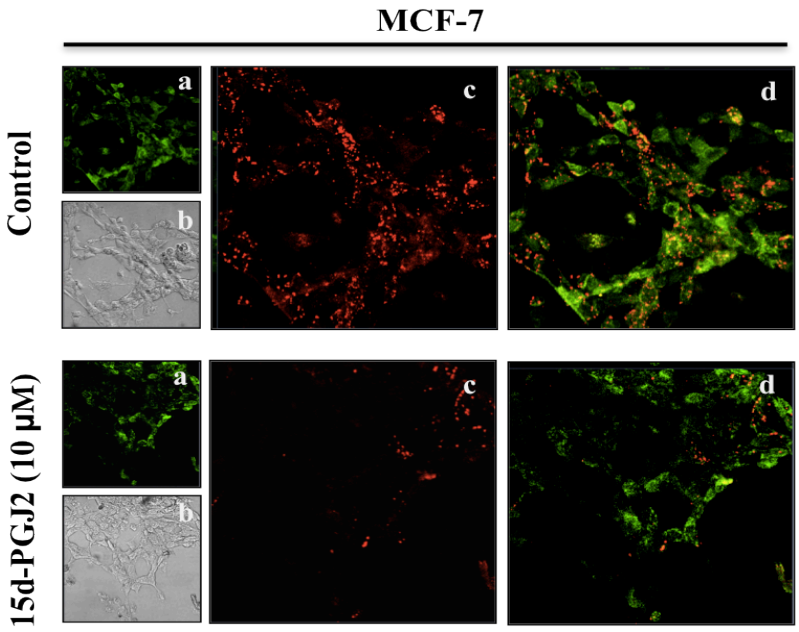

Figure 2-12: Disruption of mitochondrial membrane potential upon peroxisome proliferator-activated receptor γ (PPARγ) activation in (A) MDA-MB-231 and (B) MCF-7 breast cancer cell lines [JC-1 (a), Phase (b), JC-1 active mitochondria (c), Merge (d)]. The cells were treated with 10 µM concentration of 15d-PGJ2 for 48 h and stained with JC-1 dye. Untreated cells showed strong J-aggregrates of JC-1 dye and 10 µM 15d-PGJ2-treated cells showed majority of the cells stained in green due to loss in mitochondria membrane potential.

CHAPTER 3

COFFEE COMPONENT HYDROXYL HYDROQUINONE (HHQ) AS A PUTATIVE LIGAND FOR PPAR GAMMA AND IMPLICATIONS IN BREAST CANCER

3.1 INTRODUCTION

Coffee is one of the most widely consumed beverages in the world. The health-promoting properties of coffee are often attributed to its rich phytochemistry, including caffeine, chlorogenic acid, caffeic acid, hydroxyl hydroquinone (HHQ), etc. More recently, coffee consumption has been associated with reductions in the risk of several chronic diseases, including type 2 diabetes mellitus, Parkinson's disease and hepatocellular disease [126-128]. The association between coffee intake and breast cancer risk is biologically plausible because of its complex make-up of chemicals, e.g., caffeine and polyphenolic compounds such as flavonoids and lignans [129-131]. Among them, the relationship between coffee drinking and breast cancer risk holds great interest. Recent meta-analyses demonstrate inverse associations between coffee intake and the risk of colon, liver, breast, and endometrial cancer [132-135]. Also, a high daily intake of coffee has recently been reported to be associated with a statistically significant decrease in ER-negative breast (ER - Estrogen Responsive) cancer among postmenopausal women [136]. A number of previous epidemiologic studies have estimated the association between coffee consumption and breast cancer risk. However, the results are inconsistent [137]. Nevertheless, several reports in literature suggest that coffee consumption reduces the risk of cancer, but the molecular mechanisms of its chemopreventive effects remain unknown. Moreover, the interpretation of these data has often been limited to the role that caffeine plays [138,139].

HHQ is a natural constituent of coffee accounting for main dry matter constituent in roasted beans. Studies exploring the effects of this bioactive compound on mammalian cells are limited. HHQ was observed to dock and form hydrogen bonds with PDB ID - 2PRG (PDB 3-D crystal structure of the Ligand-binding domain of the human peroxisome proliferator activated receptor gamma solved in complexation with Rosiglitazone, the PPAR gamma agonist/ligand). The initial purpose of our

investigation is to determine whether HHQ alters the cell viability in estrogen dependent human breast cancer (MCF-7) and estrogen independent (MDA-MB-231) cells as a model system. HHQ was observed to decrease cell viability and colony formation in a dose-responsive manner and ROS was found to significantly increase in HHQ treated cells in a dose-dependent manner in both the cell lines.

3.2 EXPERIMENTAL SECTION

3.2.1 COMPUTATIONAL METHODOLOGY

Docking of HHQ into PPARγ structure

Docking studies were carried out using MolDock™ (Molegro virtual docker) which is based on a new heuristic search algorithm that combines differential evolution with a cavity prediction algorithm. The PDB file for the crystal structure of PPARγ (PDB ID - 2PRG) was downloaded from http://www.rcsb.org and transferred into the workspace keeping the orientation as a control. The energy between the existing ligand and protein was subsequently minimized. Both protein and ligands (Rosiglitazone and HHQ) were optimized in the workspace for docking by the addition of hydrogens. All structural water molecules were removed from the protein molecules using protein preparation wizard. Binding sites in the electrostatic surface of the protein was identified using the grid based cavity prediction algorithm. A total of five cavities were detected and the prepositioned ligand in the active site cavity was identified and the docking was constrained to the predicted active site cavity. MolDock™ scoring function is used for evaluating the energy between the ligand and the protein target. Grid resolution, number of runs, population size, maximum iterations, scaling factor, and cross over rate were set as 0.30 Å, 10, 50, 2000, 0.5, 0.9, respectively, for each run. Multiple poses were returned for each run with the RMSD threshold set to 1.00 Å. The pose with the highest rerank score was retained in the workspace for detailed evaluation of the ligand binding at the active site cavity. MVD was installed in Windows vista operating system on an Intel Core 2.

3.2.2 EXPERIMENTAL VALIDATION METHODOLOGY

Reagents

Dulbecco's modified eagle's medium (1000 mg/L glucose, L-glutamine and sodium bicarbonate), Fetal bovine serum, HHQ, GW9662 and crystal violet were purchased from Sigma-Aldrich (St Louis, MO, USA). Penicillin–Streptomycin–Neomycin antibiotic mixture, Hoechst 33258 and the Image-iTTM LIVE Green Reactive Oxygen Species (ROS) detection reagents were procured from Invitrogen (Eugene, OR, USA) and JC-1dye from Biotium (Hayword, CA, USA). Sodium chloride, Tris base, potassium chloride, sodium di hydrogen phosphate, glycine and sodium phosphate di basic were purchased from Wako Pure Chemical Industries (Osaka, Japan).

Cell culture and treatments

The human breast adenocarcinoma cell lines MCF-7 and MDA-MB-231 were purchased from the American Type Culture Collection (ATCC; Manassas, VA, USA). The carcinoma cultures were maintained in Dulbecco's modified eagle's medium supplemented with 10% fetal bovine serum and PNS antibiotic mixture 100 ng/mL at 37°C and 5% CO_2/95% O_2. Cultures at about 50% confluency were treated with 12.5 μM and 25 μM of HHQ concentration for 48 h at 37°C and for PPARγ activity inhibition studies, the breast cancer cells were pre-treated with GW9662 (10 μM, 4 h at 37°C) followed by HHQ (12.5 μM and 25 μM, 48 h at 37°C) and harvested for further use.

Cell Proliferation Assay and Morphological Study

HHQ was tested for its anti-proliferative activity on MDA-MB-231 and MCF-7 cells using the 3-(4, 5-dimethylthiazol-2-yl)-2, 5-diphenyltetrazolium bromides (MTT) test (Roche, Mannheim, Germany) following manufacturer's instructions. The MTT metabolic activity is a colorimetric cell proliferation assay that identifies living cells, and is based on the cellular conversion of a tetrazolium salt into insoluble formazan, which can be quantified by spectrophotometry. 5 x 10^3 cells/ well were plated in 96-well plates and grown for 24 h. The cells were then exposed to varying concentrations of HHQ for 48 h to find the half maximal inhibitory concentration (IC-50) values. The intensity of the reduced dye that corresponds to the viable cells was measured at reference wavelength of 570 nm by Thermo Scientific Varioskan Flash Multimode Reader. Morphological changes in breast cancer cells treated with 12.5 μM and 25 μM of HHQ concentration for 48 h were examined by phase contrast microscopy. All

experiments were performed in triplicates, and the relative cell viability (%) was expressed as a percentage relative to the untreated control cells.

Clonogenic assay

Colony formation potential of human breast cancer cells on exposure to HHQ was assessed by clonogenic assay. Clonogenic assay is a cell survival assay based on the ability of a single cell to grow into a colony. To determine long-term effects, breast cancer cells were treated with 12.5 μM and 25 μM of HHQ concentration for 48 h. At the end of treatment the breast cancer cells were then plated at a concentration of 100 cells/well in a new 6-well plate. The cells were allowed to grow for 14 days to form colonies. Fresh medium was replaced every third day. The colonies were washed with PBS and fixed in pre-chilled methanol: acetone mixture (1:1) for 10 min at room temperature. The colonies were then stained with crystal violet dye (0.5% in water) at room temperature for overnight. Cells were washed with water and plates were photographed with image scanner (EPSON GT-1500). Quantitative analysis of the total number of colonies was performed with Image J software (National Institutes of Health).

Detection of reactive oxygen species

The reactive oxygen species were detected by fluorescent staining using the Image-iTTM LIVE Green Reactive Oxygen Species (ROS) Detection Kit (Molecular Probes Inc, USA). The assay is based on a nonfluorescent and cell permeable 5-(and-6)-carboxy-2',7'-dichlorodihydrofluorescein diacetate (carboxy-H2DCFDA). The carboxy-H2DCFDA permeates the live cells and is deacetylated by intracellular esterases. The reduced fluorescein compound is oxidized by the cellular ROS and emits bright green fluorescence with excitation/ emission maxima of 495/529 nm. The cells were grown on glass cover slips placed in 12-well plate and were treated with 12.5 μM and 25 μM concentration of HHQ for 48 h. Subsequently, cells were fixed and then stained for ROS by following manufacturer's instructions. The images were analyzed with AxioVision software (version 4.4, Carl Zeiss).

Assessment of mitochondrial membrane potential

Mitochondrial transmembrane potential was investigated using a fluorochrome, JC-1 dye (Biotium). JC-1 (5,5',6,6'-tetrachloro-1,1',3,3' tetra ethyl benzimidazolyl carbo cyanine iodide) dye exhibits potential-dependent accumulation of red fluorescent J-

aggregates in energized mitochondria. JC-1 exists as a green fluorescent (535 nm) monomer and also accumulates as J-aggregates (595 nm) in the active mitochondria, which stain red. Consequently, healthy cells will exhibit high red/green fluorescence intensity ratio. In apoptotic cells, mitochondrial depolarization is indicated by a decrease in the red/green fluorescence intensity ratio. Therefore this fluorescence emission shift from green (~529 nm) to red (~590 nm) is indicative of mitochondrial depolarization occurring during apoptosis. After 48 h of 12.5 μM and 25 μM of HHQ treatment, the cells were incubated with 1X JC-1 dye at 37°C for 15 min followed by washes with assay buffer. The red fluorescence (excitation 550 nm, emission 600 nm) and green fluorescence (excitation 485 nm, emission 535 nm) were measured using fluorescence Thermo Scientific Varioskan Flash Multimode plate reader. The ratio of red fluorescence to green fluorescence was determined in JC-1 stained cells. The relative mitochondrial membrane potential (%) was expressed as a percentage relative to the untreated control cells.

Immunocytostaining

In order to find out the modulation of test proteins by HHQ through PPARγ, the test protein were immunostained. For immunostaining, cells were plated on glass coverslips in a 12-well plate (10^4 cells/coverslip). The cells were allowed to attach for 24 h and then exposed to 12.5 μM and 25 μM of HHQ for 48 h. At the end of treatment cells were washed with cold PBS three times and then fixed with pre-chilled methanol: acetone mixture (1:1) for 10 min at room temperature. Fixed cells were washed twice with PBS, permeabilized with 0.32% Triton X-100 in PBS (PBST) for 10 min and blocked with 2% bovine serum albumin (BSA) in PBS for 30 min. The cells were then probed with anti-PGK1 (1:250; Abcam, Cambridge, UK), anti-PKM2 (1:250; Abcam, Cambridge, UK), antibodies for overnight at 4°C. After primary antibody incubation the cells were washed thrice with 0.1% PBST, and then incubated with secondary antibodies (Alexa-594-conjugated goat anti-rabbit and Alexa 488-conjugated goat anti-mouse, (Molecular Probes, Eugene, OR) for 1 h at room temperature followed by 3 times washing with 0.1% PBST and then once with PBS. The coverslips were then mounted with ProLong+® Gold antifade reagent (Molecular Probes, Inc.) and observed under a microscope (Axiovert 200M; Carl Zeiss, Thornwood, NY). The experiment was carried out in duplicate in three independent experiments. The images were analyzed with Axio Vision software (version 4.4, Carl Zeiss).

Western blot analysis

Expression level of indicated proteins was examined by Western blotting. The control and treated cells were lysed in RIPA lysis buffer (25 mM Tris–HCl (pH 7.6), 1% NP-40, 1% sodium deoxycholate, 150 mM NaCl, 0.1% SDS) complemented with complete protease inhibitors (Roche) for 15 min on ice followed by centrifugation at 14,000 *g* for 15 min at 4°C. The protein concentration was determined using BCA reagents (Pierce, Rockford, IL, USA). Protein lysate (20 µg) was resolved in 10% in SDS-polyacrylamide gel under standard denaturing conditions according to Laemmli's method (1970) followed by transfer onto polyvinylidene difluoride membranes using a Trans-Blot SD (Bio-Rad, Lewes, E. Sussex, UK.) semi-dry electroblotter for 30 min at 20 V. Subsequently, the membranes were blocked for 45 min at room temperature with 2% bovine serum albumin in 0.1% PBST. The membranes were then probed with anti-PGK1 (1:1000; Abcam, Cambridge, UK), anti- PKM2 (1:500, Abcam), anti-caspase-8 (1:1000; Cell Signaling, Boston, MA, USA), Anti-Bax (1:1000; Cell Signaling) and anti-β-actin (1:20,000; Abcam) at 4°C overnight followed by three washes for 5 min each with 0.1% PBST. The membranes were then incubated with horseradish peroxidase conjugated secondary antibody (1:20,000; Abcam) for 45 min at RT and washed thrice for 5 min each with 0.1% PBST followed by chemiluminescent detection using Luminescent Image Analyzer equipped with charge-coupled device camera (LAS-4000 Ver. 2.1; Fuji Film, Tokyo, Japan).

Data Analysis

The captured images for ROS assay and immunostaining were analyzed using AxioVision software (version 4.4; Carl Zeiss). The analysis determined the overall density of ROS, PGK1 and PKM2 immunoreactivity in 5-8 randomly selected fields in each slide. The mean intensity of ROS, PGK1, and PKM2 immunoreactivity in control and treated cells were evaluated and presented as a histogram. Similarly the Relative Optical Density (%) for immunoreactive bands in western blotting for PGK1, PKM2 and Caspase-8 were analyzed using Image J software (National Institutes of Health).

Statistical Analysis

The quantitative data are representative of three independent experiments done in triplicates and expressed as mean ± SEM. Statistical analysis was performed using analysis of variance (one way analysis of variance) followed by Bonferroni's on test to determine differences in mean and $p < 0.05$ was considered as statistically significant.

3.3 RESULTS AND DISCUSSION

Understanding the molecular pathways that link tumor biology to the staggering array of pathologies and genes is of paramount scientific and medical importance. Though, the complexity of the underlying biochemical and molecular mechanisms of breast cancer make metabolic reprogramming and transformation in breast cancer unclear, many dietary compounds have been identified as potential chemopreventive agents. PPARγ is an interesting target for cancer therapy as its expression is elevated in tumors and also because PPARγ activation is reported to result in decreased cell proliferation, decreased G_0/G_1 to S phase progression, apoptosis and increased terminal differentiation [140-142]. Also, imbalances in expression of target genes forms the core of metabolic syndrome and cancer regulation through atherogenic metabolic triad/lipid triad metabolism modulation by PPARs [143]. Concurrently, increased levels of glycolytic proteins are observed in plasmas of women with breast cancer as a result of upregulation of glycolysis pathway [144].

In this paper, I for the first time report on the use of coffee component HHQ as a potential ligand for PPARγ and its role in induction of apoptosis in breast cancer cells by delineating the glycolytic pathway gene regulation by PPARγ activation.

3.3.1 Docking

The three-dimensional protein structures can be used to understand ligand binding and to rationally design novel ligands as prospective drug compounds. PPAR agonists typically possess a small polar region and a hydrophobic region that form hydrogen bonds and hydrophobic interactions, respectively, within the ligand binding domain. Several crystal structures of PPARγ in complexation with their ligands are available in the protein data bank (PDB). Here, I used the PDB crystal structure 2PRG (PPARγ with ligand Rosiglitazone) for structure-based identification of HHQ as a potential ligand for PPARγ in breast cancer therapeutics. I also compared the ligand binding properties of the two compounds Rosiglitazone (the known ligand) and HHQ (the proposed novel ligand). The rerank scores for the Rosiglitazone and HHQ were found to be -122.433 and -33.3562, respectively. The hydrogen bond energy values were -5.487 kcal/mol, and -9.460 kcal/mol for Rosiglitazone and HHQ. Rosiglitazone (the ligand in the crystal structure 2PRG) forms 3 hydrogen bonds with the 2PRG (Gln286, His449, Ser289) and HHQ forms 5 hydrogen bonds with 2PRG (Gln286, His449, Tyr473, Ser289, His323). Hydrogen bonding of the ligand to Tyr473 is

reported to be the key to the stabilization of the AF-2 region and it has also been shown that [145] agonistic activity of ligands disappears when Tyr473 is mutated. The importance of His323 and His449 has also been reported [146,147]. Our results show that both the ligands have hydrogen bond interactions with key residues - Tyr473 and His 449, thereby providing specificity of interaction that is a fundamental aspect of molecular recognition. The active site residues that interact with HHQ are shown in Table 3-1 and the hydrogen bonds between each compound and the 2PRG active site are shown in Figure 3-1.

3.3.2 HHQ inhibits cell proliferation and clonogenic survival

To investigate the potential cell growth inhibition of HHQ, I first examined the effect of HHQ on cell proliferation and clonogenic survival in human breast adenocarcinomas. I chose two breast adenocarcinoma cell lines, MDA-MB-231 (estrogen independent) and MCF-7 (estrogen dependent). MDA-MB-231 and MCF-7 were cultured in the control medium for 24 h, followed by 48 h treatment with different concentrations of HHQ for cytotoxic and anti-proliferative studies. HHQ led to decrease in relative density of viable cells as detected by MTT dye reduction assay. A dose-effect relationship was observed as shown in Figure 3-2. The IC-50 value for MDA-MB-231 and MCF-7 were found to be 25 μM and 50 μM, respectively. I proceeded with 12.5 μM and 25 μM of HHQ to investigate the comparable effects of same concentration on both the cell lines. At 12.5 μM the relative viability in MDA-MB-231 and MCF-7 was 58.2% and 76.3%, respectively, whereas at 25 μM the relative viability in MDA-MB-231 and MCF-7 was 50% and 60.7%, respectively. As morphological analyses depict the health of a cell, I next examined the cells for any altered morphology on treatment with HHQ. Cells cultured in the presence of HHQ (12.5 μM and 25 μM) show significant morphological changes and were found to be reduced in cell mass as well as number as compared to control (Figure 3-3). Also, HHQ treatment induced detachment and rounding in breast cancer cells as shown by phase contrast images in both the cell lines (12.5 μM and 25 μM). Furthermore, to examine the antitumor activity of HHQ on colony forming potential in breast cancer cells I performed clonogenic assay. This assay is an *in vitro* assay based on the ability of a single cell to proliferate and differentiate into colonies in response to various insults. HHQ severely affected the colony forming potential of human breast cancer cells - MDA-MB-231 and MCF-7. As shown in Figure

3-4, clonogenicity of both the breast cancer lines were found to be significantly reduced in a concentration-dependent manner after exposure to HHQ.

3.3.3 HHQ induces intracellular ROS generation and cytotoxicity

Reactive oxygen species (ROS) is a universal entity mediating apoptosis [148]. ROS act as a secondary messenger in cell signaling and are essential for various biological processes in normal cells. Disturbances in redox balance relate to human pathogenesis including cancers. ROS are constantly generated and eliminated in the biological system, and play important roles in a variety of normal biochemical functions and abnormal pathological processes. Growing evidence suggests that cancer cells exhibit increased intrinsic ROS stress, due in part to oncogenic stimulation, increased metabolic activity, and mitochondrial malfunction. Since ROS are chemically active and can inflict severe cellular damage, the very fact that cancer cells are under increased intrinsic ROS stress may also provide a unique opportunity to kill the malignant cells based on their vulnerability to further ROS insults caused by exogenous agents [149]. HHQ is earlier reported to generate reactive oxygen species (ROS) by autoxidation [150].

Therefore, to get further insights to HHQ induced cytotoxicity in breast cancer cells; I examined the intracellular ROS generation. As shown in Figure 3-5, intracellular ROS formation was found to be significantly increased in HHQ treated cells as compared to control cells in a dose-dependent manner. The effective enhancement of ROS production by HHQ correlates to its cytotoxicity nature. Since the mitochondrial respiratory chain (electron transport chain) is a major source of ROS generation in the cells, the vulnerability of the mitochondrial DNA to ROS mediated damage has been suggested to be a mechanism to amplify ROS stress in cancer cells [151]. One major effect is to generate increased intracellular ROS causing loss of outer mitochondrial membrane permeability and induction of apoptosis [152,153]. Another possible mechanism by which cancer cells generate increased amounts of ROS may involve malfunction of the mitochondrial respiratory chain. The fact that cancer cells exhibit an increased dependency on glycolysis to meet their ATP need (the Warburg effect) may reflect an inefficient ATP generation in mitochondria, or “respiration injury” [154]. A correlation between mtDNA mutations and increased ROS contents in primary leukemia cells isolated from patients has been shown [155]. Because the mitochondrial respiratory chain is the major site of ROS generation due to electron transfer,

malfunction of the mitochondrial respiratory chain associated with mtDNA mutations is likely to result in more free radical production due to increased "leakage" in mitochondrial membrane.

3.3.4 HHQ induces mitochondrial dysfunctioning

Mitochondria are central players in the determination of cell life and death. Their main physiological function is energy production by the oxidative phosphorylation pathway. This process not only involves production of cell energy currency, ATP but also increases the production of reactive oxygen species (ROS) as by-products of aerobic metabolism. Mitochondria are also the main regulators of apoptotic cell death by mediating extrinsic and intrinsic apoptotic pathways. Oxidative stress may cause oxidative damage to various cellular components and may lead to lipid peroxidation, protein oxidation, mitochondrial DNA mutations, initiation of apoptosis cascade by decrease in mitochondrial membrane potential and release of apoptogenic factor cytochrome c into the cytosol [156]. Thus, the oxidative damage and the associated mitochondrial dysfunction may lead to energy depletion, accumulation of cytotoxic mediators, apoptosis and ultimately cell death.

Therefore to investigate the effect of HHQ induced oxidative stress on mitochondria and apoptosis cascade initiation, I undertook mitochondrial membrane potential analysis using potential sensitive, cationic dye JC1. This dye exhibits potential-dependent accumulation in mitochondria, indicated by a fluorescence emission shift from green (525 nm) to red (590 nm). Consequently, live cells have higher red/green intensity ratio as compared to cells undergoing apoptosis. As shown in Figure 3-6, I observed that the breast cancer cells when treated with HHQ show loss of mitochondria membrane potential (MMP) in a dose-dependent manner. This decrease in MMP at 25 μM of HHQ was significant in both the cell lines. Furthermore, I found that the level of pro-apoptotic protein Bax, significantly increased in a concentration-dependent manner in both the breast cancer cells (Figure 3-7). The expression levels of Bax correlates with the MMP loss in breast cancer cells on treatment with HHQ. This protein is involved in the mitochondrial apoptotic signaling pathway. The activation of the proapoptotic Bcl-2 family member Bax, induces permeabilization of the mitochondrial outer membrane and release of cytochrome c leading to caspase dependent apoptosis [157,158]. Together, these data demonstrate that there is disruption in mitochondrial potential, permeability and functioning upon PPARγ activation by HHQ.

3.3.5 Induction of Caspase dependent apoptosis by HHQ

Caspase-8 activation is one of the early events leading to apoptosis. PPAR synthetic ligands are known to activate intrinsic and extrinsic apoptotic cascade [159,160]. In order to understand the mechanism of cell death, I hypothesized that PPARγ ligand HHQ may initiate apoptosis cascade via PPARγ dependent pathway. To examine the above hypothesis I undertook the expression analysis of apoptotic protein, caspase-8. Interestingly, I observed that on treatment with HHQ the level of procaspase-8 decreases significantly in both the cancer cells. This demonstrates that caspase-8 proenzyme is being cleaved to active caspase-8 fragments in a dose-dependent manner (Figure 3-8). Concurrent increase in proapototic protein Bax, loss of mitochondrial membrane potential and activation of caspase-8 demonstrate PPARγ dependent apoptotic cascade activation by HHQ.

3.3.6 PPARγ dependent modulation of glycolytic enzymes

In 1930, Otto Warburg discovered the unknown link between highly proliferative nature of cancer cells and glycolysis [91]. The phenomenon involved was described as the "Warburg Effect" which is characterized by increased glucose uptake and dependence on glycolysis for ATP production even in the presence of oxygen source. The glycolytic rate of rapidly proliferating tumor cells was found to be 200 times higher than those of their normal tissues of origin. Altenberg and Greulich (2004) found over expression of glycolytic genes in 24 different types of cancer including breast cancer. Two such glycolytic genes are phosphoglycerate kinase 1 (PGK1) and tumor specific pyruvate kinase muscle 2 (PKM2) [161,162]. PGK1 and PKM2 catalyze the sixth and ninth step, respectively, in the glycolysis pathway generating two ATPs each. PGK1 also functions as a polymerase alpha cofactor protein (primer recognition protein) and is involved in DNA synthesis. PKM2 on the other hand is also a metabolic regulator and is also reported to be involved in channelization of glucose carbons to biosynthetic processes and hence control glycolysis. Hence, down regulating these enzymes would not only starve the cells for ATP but also lead to biosynthetic metabolite starvations, as they are important for tumor cell proliferation and survival. Earlier, I reported that both phosphoglycerate kinase 1 (PGK1) and pyruvate kinase M2 (PKM2) are repressed by PPARγ in the breast cancer cell lines MDA-MB-231 and MCF-7 [163]. Further analysis suggested that this repression leads to decrease in ATP levels and apoptosis. Here, I

hypothesized (based on docking results) that HHQ can modulate the expression of PGK1 and PKM2 via PPARγ dependent pathway.

Therefore, to test this hypothesis, I undertook expression analysis of these metabolic enzymes. I observed that the expression of glycolytic genes, PGK1 and PKM2 was significantly reduced in both the breast cancer cells on treatment with HHQ in dose-dependent manner, (Figure 3-9 and 3-10). Further, to confirm the repression of glycolytic genes, PGK1 and PKM2 through HHQ induced PPARγ activation, I utilized GW9662, an irreversible PPARγ antagonist which acts by binding to the human ligand-binding domain (region E/F). As shown in Figure 3-11, no significant repression of PGK1 and PKM2 was seen on pre-treating the breast cancer cells with GW9662 (10 μM, 4h at 37°C) followed by HHQ (12.5 μM and 25 μM, 48h at 37°C). GW9662 showed no effect of HHQ on expression of PGK1 and PKM2, thereby suggesting that the activation of PPARγ is required for repression of these enzymes. Conversely, these data suggests that HHQ represses the expression of glycolytic enzymes via PPARγ dependent pathway. Down regulation of PGK1 and PKM2 decreases ATP production in the cytoplasm and mitochondria, initiating apoptosis and suppressing cancer metabolism. ATP depletion, used in combination with chemotherapy and/or radiation, has a variety of effects on cancer cells including inducing apoptosis in multi-drug resistant cells and decreasing tumor promotion. Cellular ATP level has been reported as an important determinant of cell death [164]. Though the exact mechanisms of these effects have not been fully elucidated, these investigations suggest on the role of HHQ as an anti-cancer agent. However, further work is required to establish the exact nature and behavior of this molecule in conjunction with other coffee components and to determine its relevance to the biological role of PPARγ breast cancer progression and therapeutics.

3.4 CONCLUSION

My results have established previously unknown novel cross-link between HHQ, PPARγ, ROS and glycolysis; thereby adding a new dimension to therapeutic potential of PPARγ ligands. Although the exact mechanism remains unclear and further studies are still needed to clarify the potential role and molecular basis of action of PPARγ in breast carcinogenesis, my investigation open a new direction for development HHQ in breast cancer treatment. Further investigations on these could possibly help us in

understanding the molecular mechanisms by which PPARγ regulates disease targets specifically in breast cancer and the use of its ligands in breast cancer therapeutics. Despite several advancements that have been made on the subject, there is still much to be clarified regarding PPARγ signaling in breast cancer and several important questions remain unanswered. Many intriguing avenues of PPARγ research have been opened and hold the potential to ultimately lead to newer classes of more selective molecules.

Table 3-1: Docking results for HHQ and Rosiglitazone.

Drugs	Hydrogen bond score (kcal.mol-1)	Number of hydrogen bonds	Residues of PPARγ binding site interacting with the ligands	Rerank score
HHQ	-9.46033	5	Gln286, His449, Tyr473, Ser289, His323	-33.3562
Rosiglitazone	-5.48771	3	Gln286, His449, Ser289	-122.433

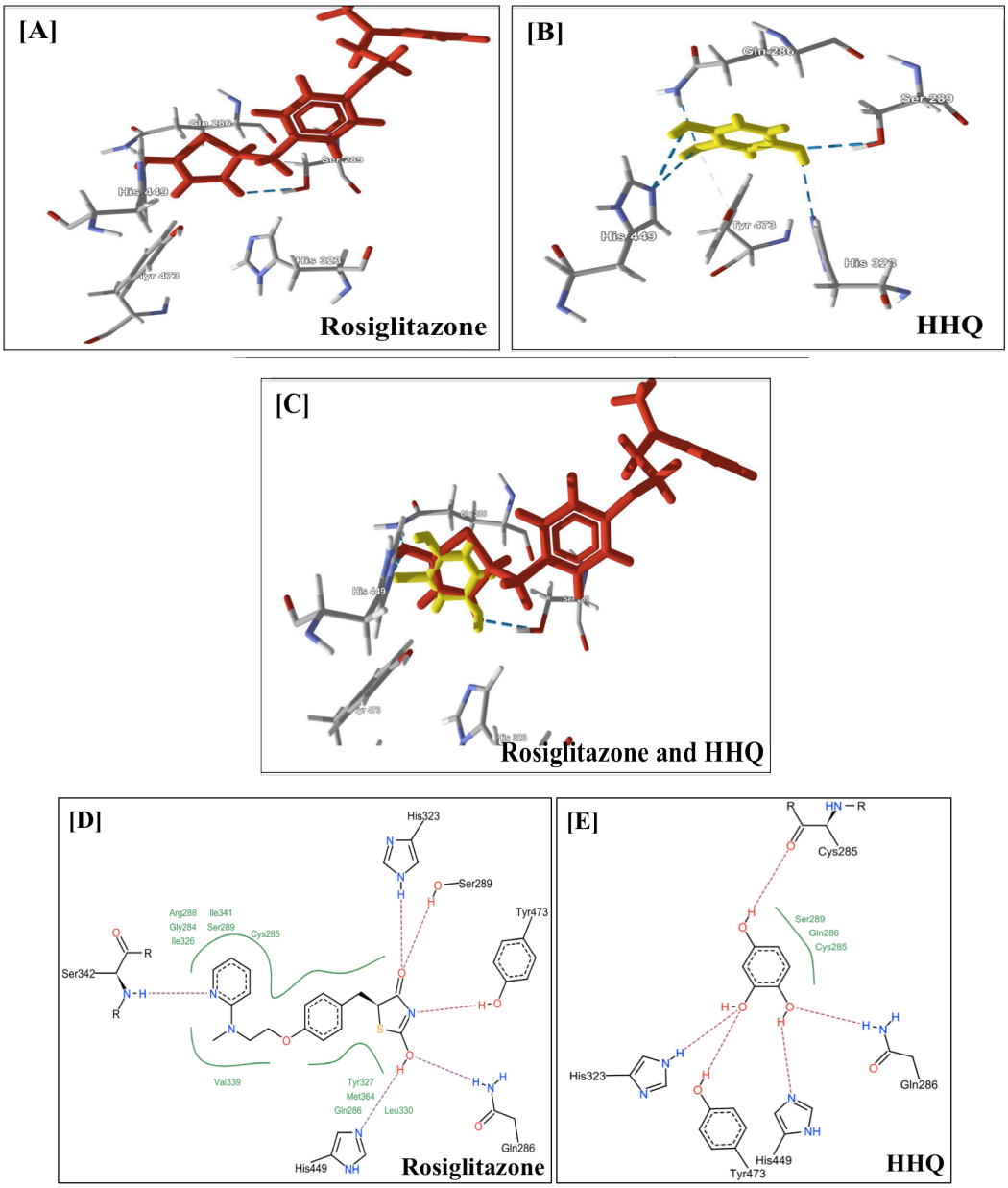

Figure 3-1: HHQ docked in the ligand binding domain of PPARg protein crystal structure for PDB solved in conjunction with Rosiglitazone (PDBID: 2PRG). [A] Represents hydrogen bonds (in black dotted line) observed for Rosiglitazone (in red) with the active site residues in the ligand binding domain of PPARg (2PRG). [B] Represents hydrogen bonds (in black dotted line) observed for HHQ (in yellow) with the active site residues in the ligand binding domain of 2PRG. [C] Represents superposition of the best conformation of Rosiglitazone (in red) and HHQ (in yellow) in the ligand binding domain of 2PRG. [D] and [E] represents the chemical bond between rosiglitazone and HHQ with 2PRG, respectively.

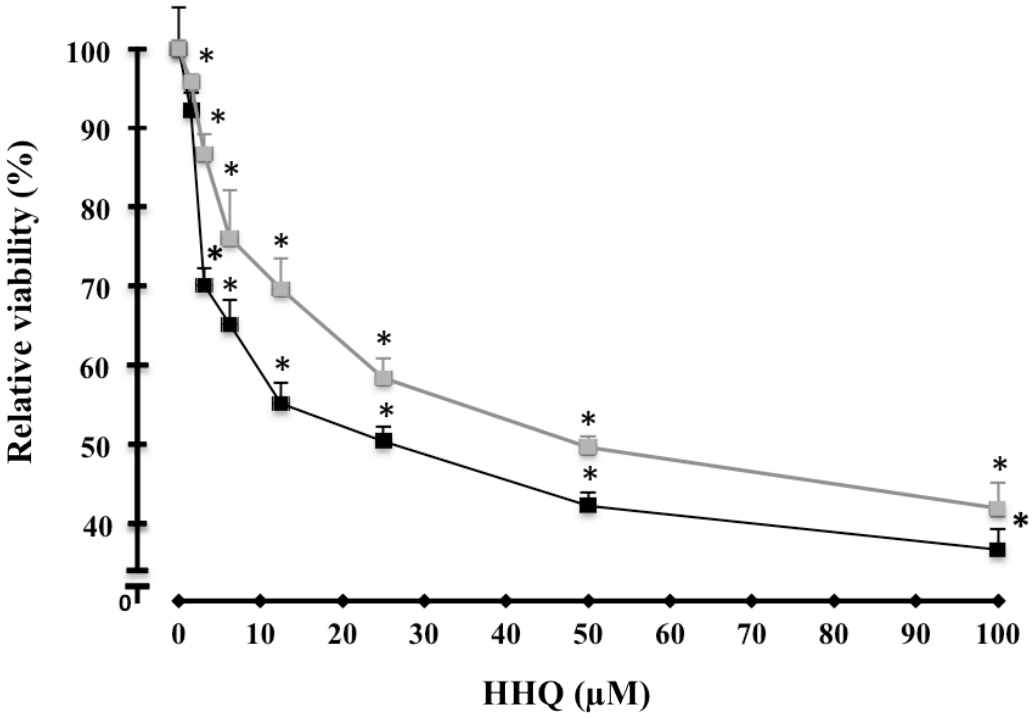

Figure 3-2: Growth curve inhibition as assessed by MTT assay in human breast cancer cells (MDA-MB-231 (black line) and MCF-7 (grey line)). The breast cancer cells were exposed to different doses of HHQ for 48 h at 37°C. The cell viability in breast cancer cells decreased in dose-dependent fashion. The IC-50 value for MDA-MB-231 and MCF-7 were observed to be 25 μM and 50 μM, respectively. Data are representative of three independent experiments done in triplicates and expressed as mean ± S.E.M. '*' ($p < 0.005$) represents statistical significant difference between control and HHQ test groups.

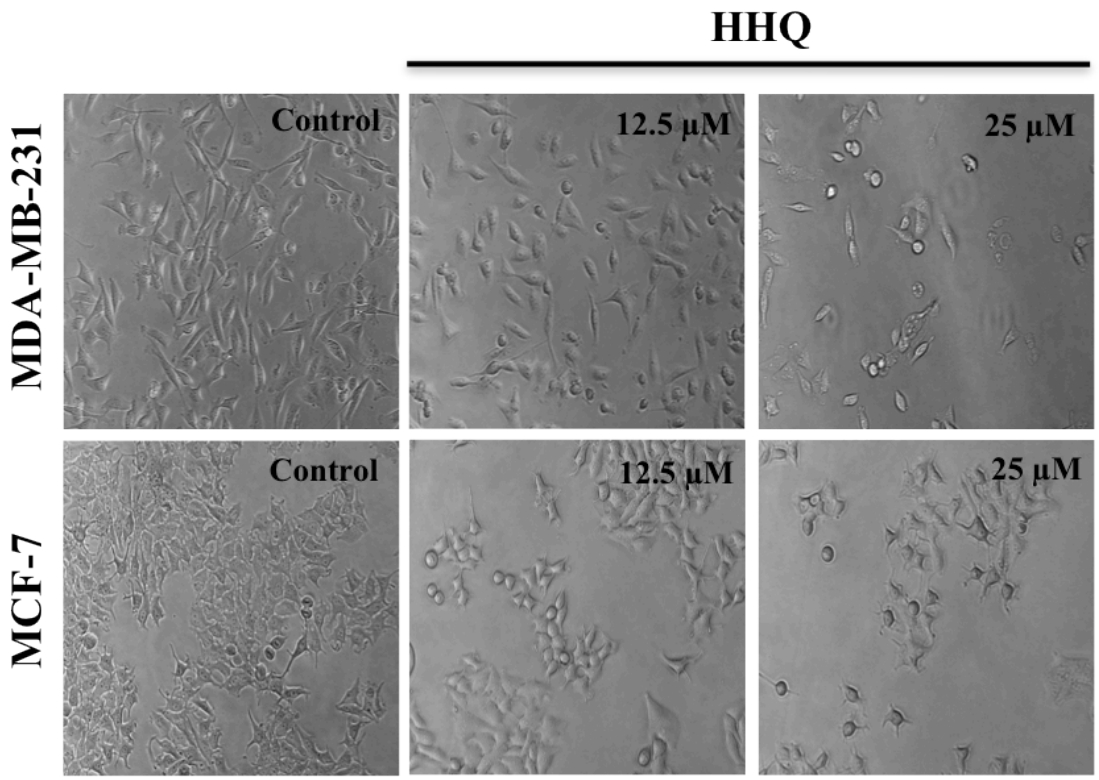

Figure 3-3: Phase contrast images of human breast cancer cells (MDA-MB-231 and MCF-7). The breast cancer cells were exposed to 12.5 µM and 25 µM concentration of HHQ for 48 h at 37°C. HHQ treated groups did not retain their normal morphology. HHQ induced cell rounding and detachment in breast cancer cells.

[A]

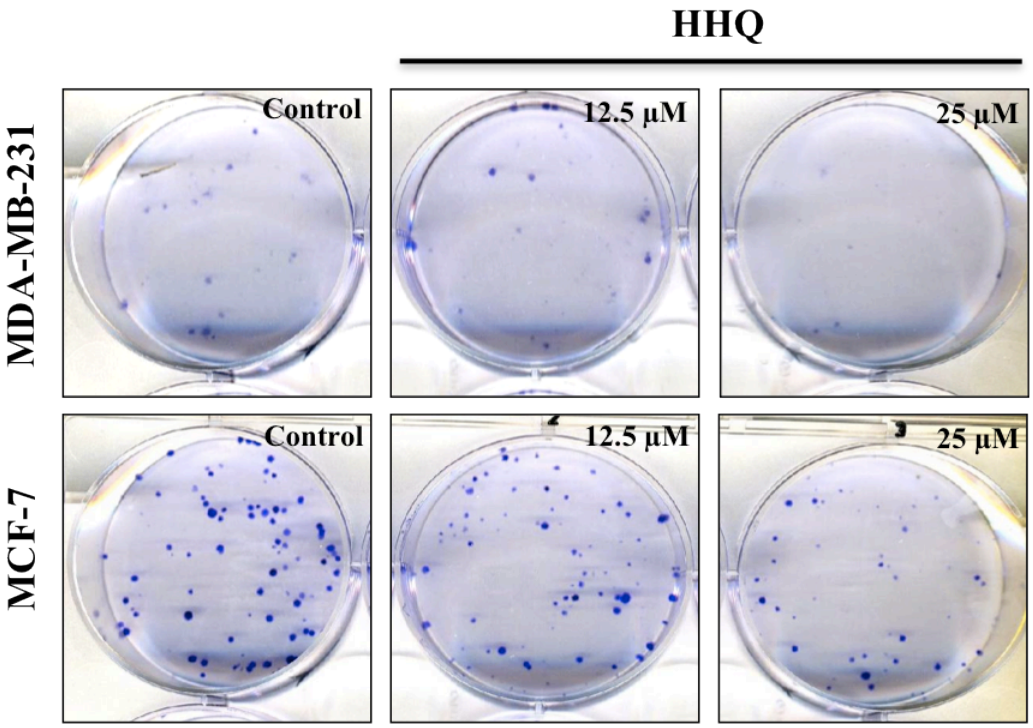

[B]

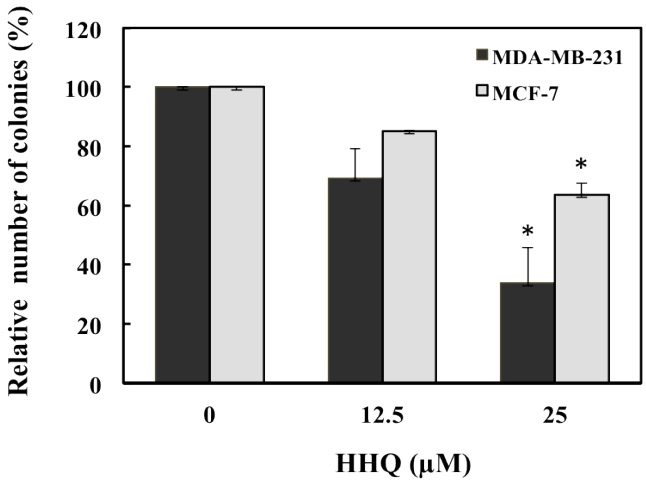

Figure 3-4: The inhibitory effects of HHQ on colony formation in human breast cancer cells (MDA-MB-231 and MCF-7) as evaluated by clonogenic assay. The breast cancer cells were exposed to 12.5 µM and 25 µM concentration of HHQ for 48 h at 37°C. [A] Representative plates; [B] graph of the number of colonies formed (the result of three independent experiments, expressed as mean ± S.E.M). Decrease in number of colonies in HHQ treated groups were statistically significant '*' ($p < 0.005$).

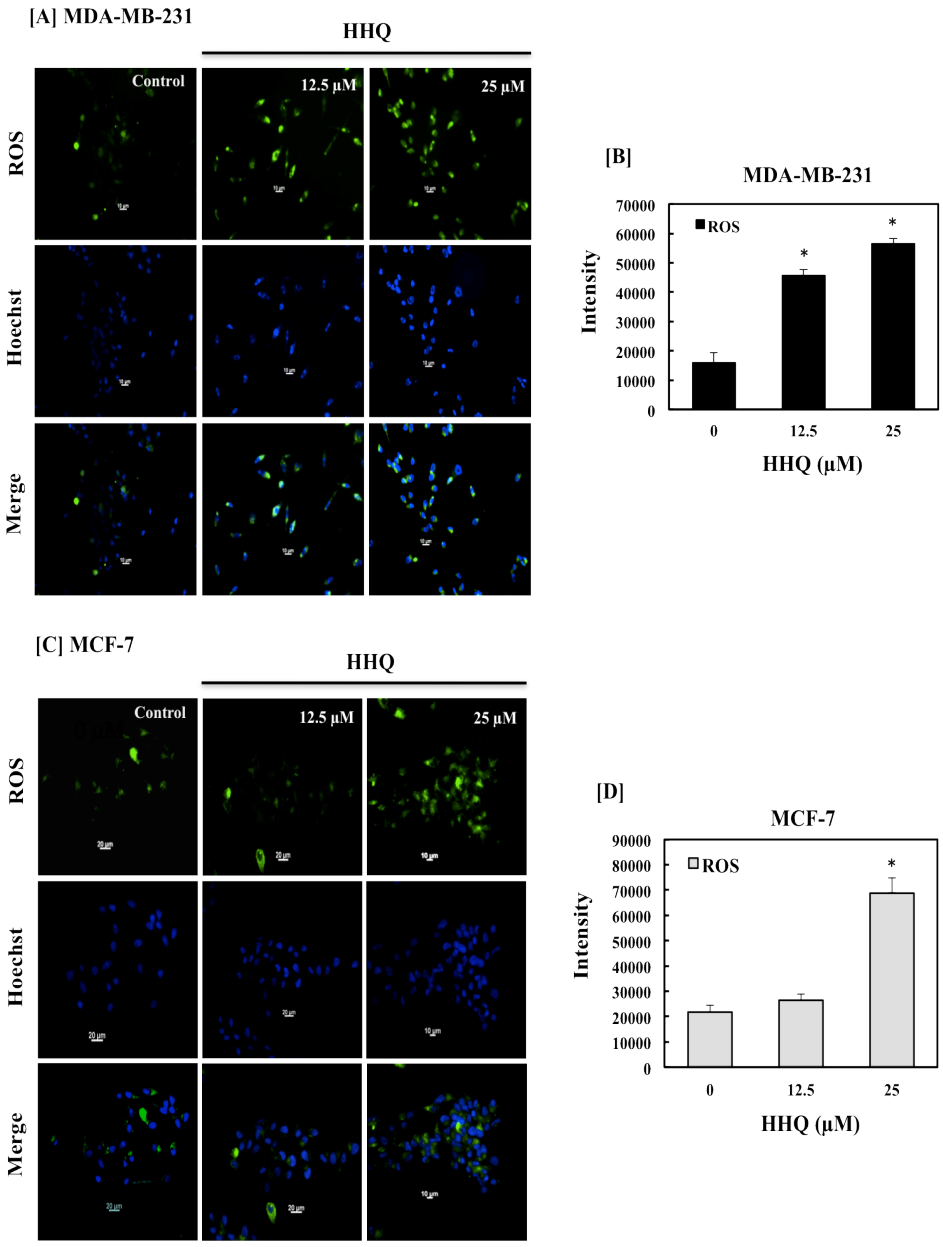

Figure 3-5: HHQ induced intracellular ROS production in human breast cancer cells, MDA-MB-231 [A] and MCF-7 [C]. The breast cancer cells were treated with 12.5 µM and 25 µM of HHQ for 48 h at 37°C, intracellular ROS was detected by a fluorescent microscope. Quantitation of the ROS signals in MDA-MB-231 and MCF-7 is shown in [B] and [D], respectively. Significant increase in ROS level was observed in HHQ treated cells. Data are representative of three independent experiments done in triplicates and expressed as mean ± S.E.M. Increase in ROS generation in HHQ treated groups with 12.5 µM and 25 µM were statistically significant '*' ($p < 0.005$).

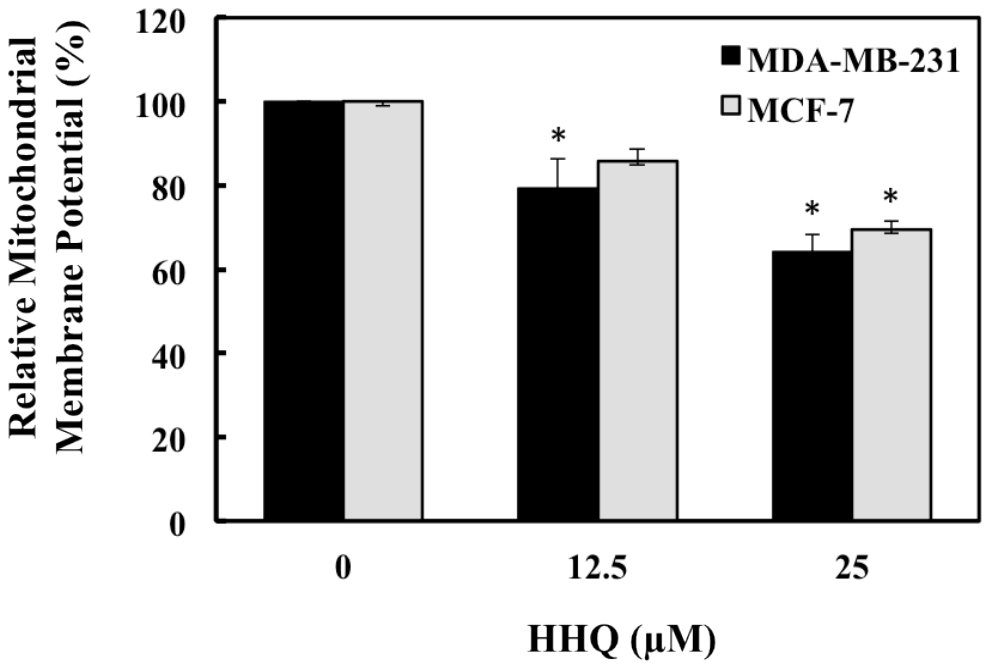

Figure 3-6: HHQ induced loss in mitochondrial membrane potential (MMP) in human breast cancer cells (MDA-MB-231 and MCF-7). The breast cancer cells were treated with 12.5 μM and 25 μM of HHQ for 48 h at 37°C and then immunostained for JC1. HHQ treated cells showed loss of MMP comparable to that of the control cells. Data are representative of three independent experiments done in triplicates and expressed as mean ± S.E.M. '*' ($p < 0.005$) represents statistical significant difference between control and HHQ test groups.

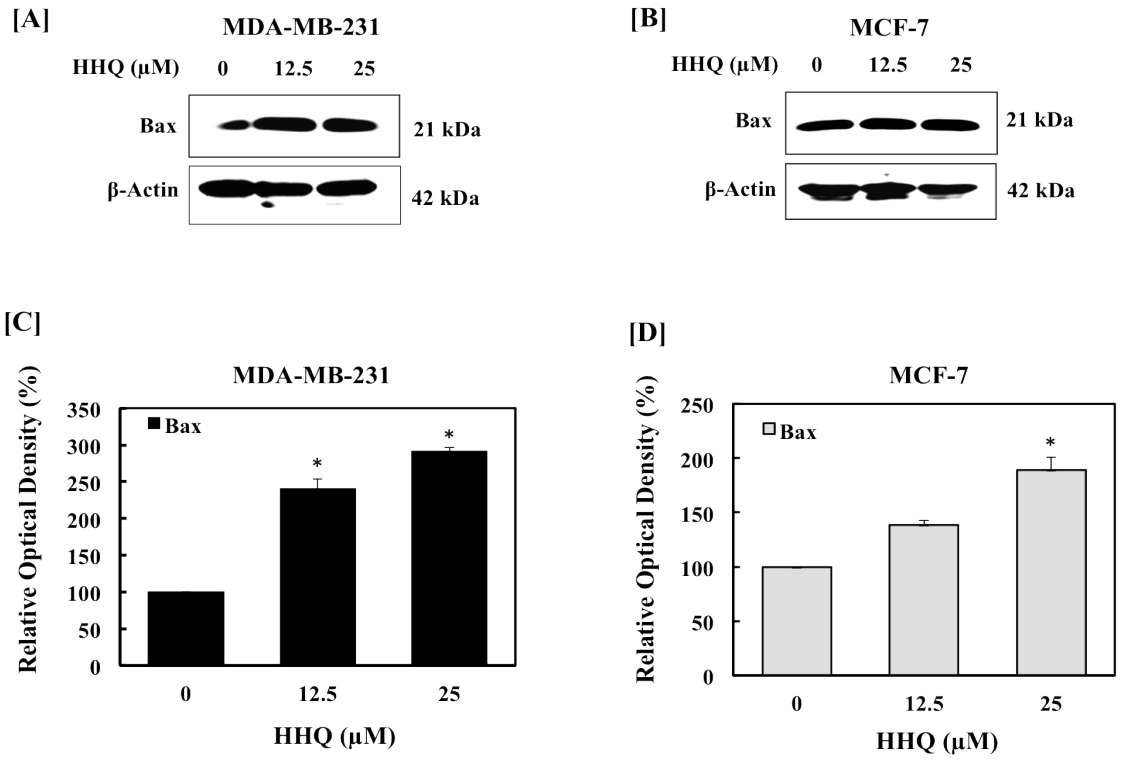

Figure 3-7: Expression analyses of pro-apoptotic protein Bax in response to HHQ treatment in human breast cancer cells (MDA-MB-231 and MCF-7). The breast cancer cells were treated with 12.5 μM and 25 μM of HHQ for 48 h at 37°C. Representative western blot hybridization signals of Bax for MDA-MB-231 [A] and MCF-7 [B] and the quantitation of the signals is shown in [C] and [D], respectively. Significant increase in Bax expression was observed in HHQ treated cells. Data are presented as mean ± S.E.M. of three independent experiments. '*' ($p < 0.005$) represents statistical significant difference between control and HHQ test groups.

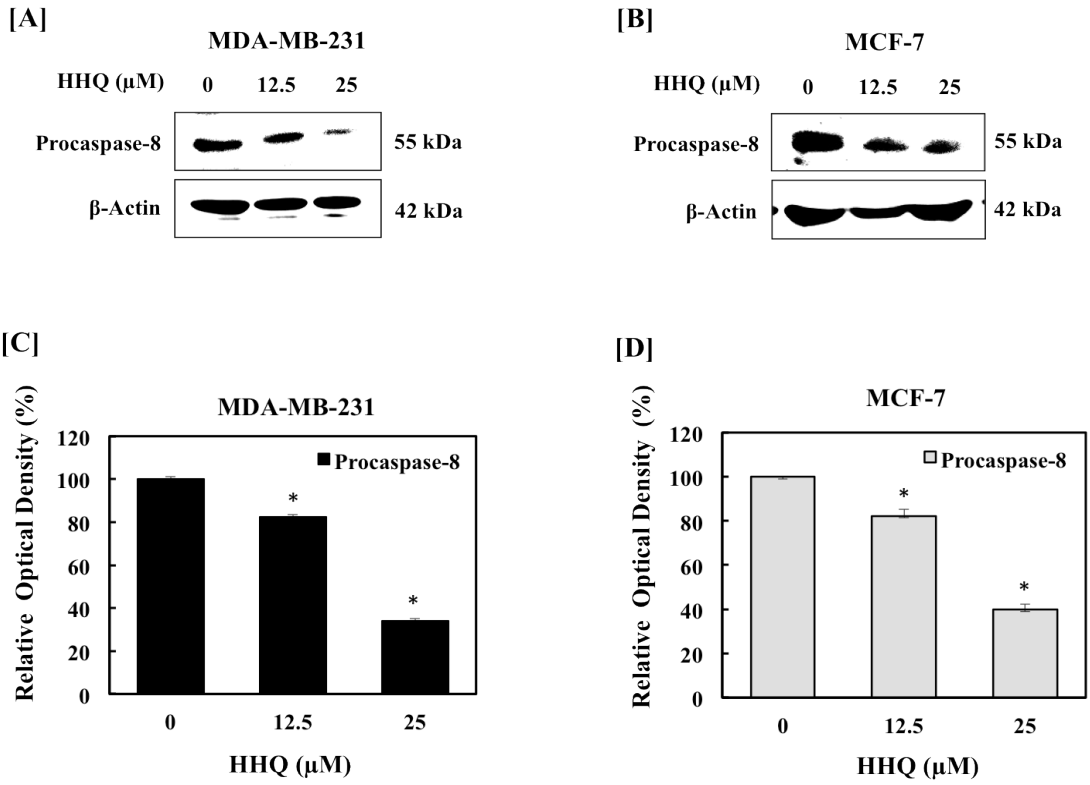

Figure 3-8: Expression analyses of proenzyme caspase-8 in response to HHQ treatment in human breast cancer cells (MDA-MB-231 and MCF-7). The breast cancer cells were treated with 12.5 μM and 25 μM of HHQ for 48 h at 37°C. Representative western blot hybridization signals for proenzyme caspase-8 for MDA-MB-231 [A] and MCF-7 [B] and the quantitation of the signals are shown in [C] and [D], respectively. Significant decrease in expression of proenzyme caspase-8 was observed in HHQ treated cells. Data are presented as mean ± S.E.M. of three independent experiments. '*' ($p < 0.005$) represents statistically difference between control and HHQ test groups.

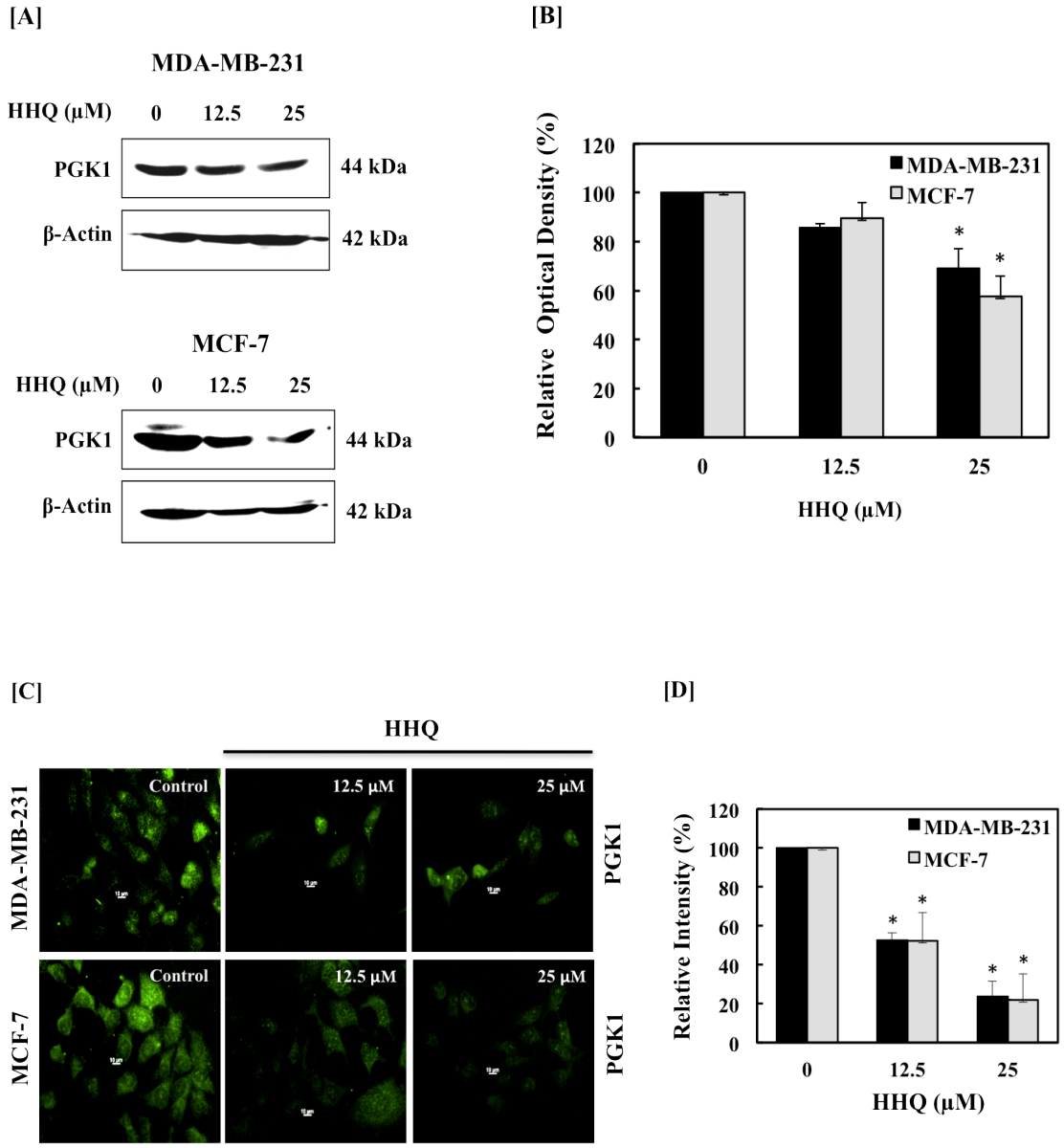

Figure 3-9: Expression analyses of glycolytic enzyme phosphoglycerate kinase 1 (PGK1) in response to HHQ treatment in human breast cancer cells, MDA-MB-231 and MCF-7. The breast cancer cells were treated with 12.5 μM and 25 μM of HHQ for 48 h at 37°C. Representative western blot hybridization signals for PGK1 [A] and the quantitation of the signals is shown in [B]. Immunofluorescent detection of PGK1 is shown in [C] and the relative intensity measurement of immunofluorescence is shown in [D]. Significant decrease in PGK1 expression was observed in HHQ treated cells. Data are representative of three independent experiments done in triplicates and expressed as mean ± S.E.M.' '*' represents the statistical significant ($p<0.05$) difference between control and HHQ treated group

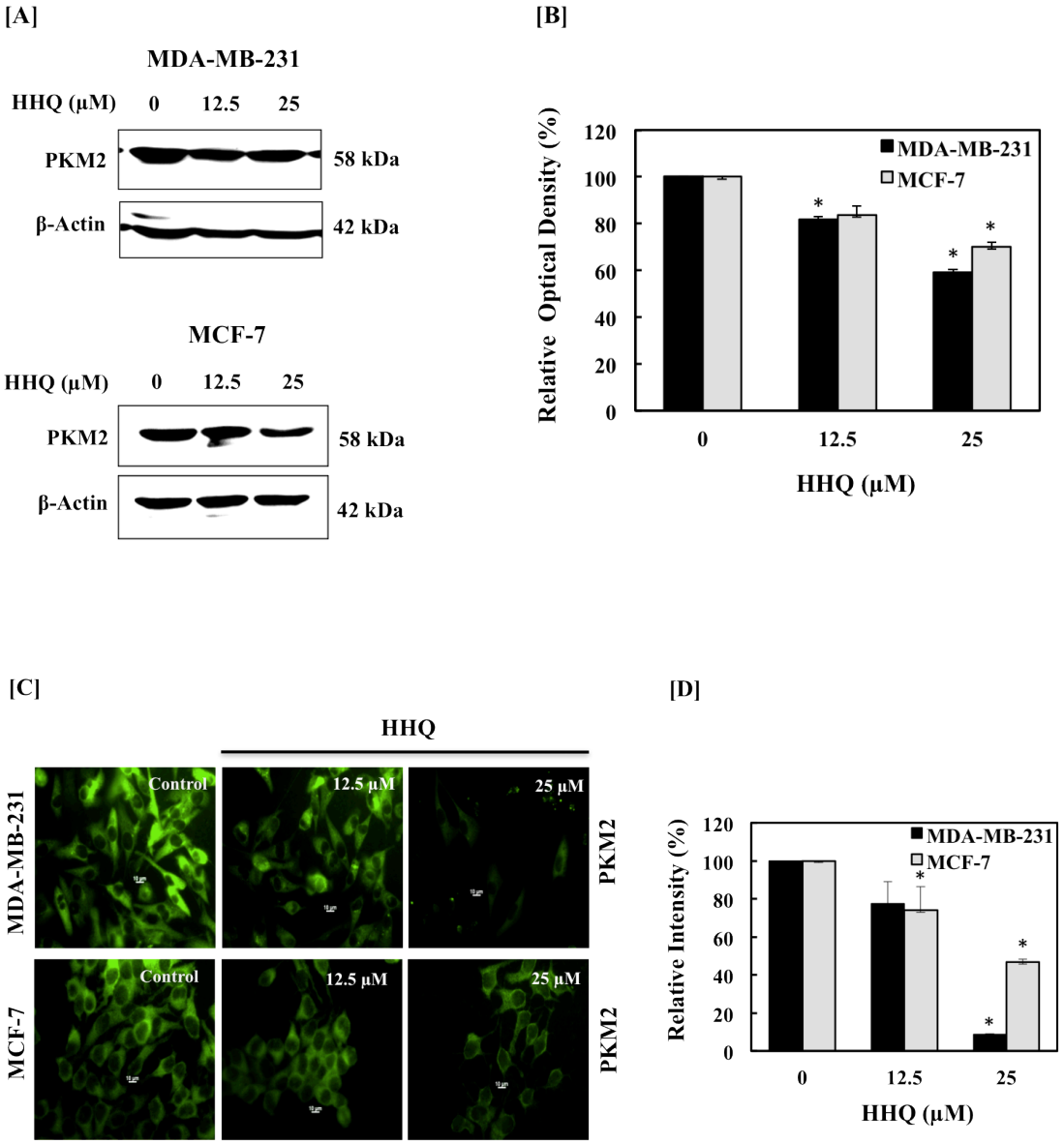

Figure 3-10: Expression analyses of glycolytic enzyme pyruvate kinase-muscle 2 (PKM2) in response to HHQ treatment in human breast cancer cell, MDA-MB-231 and MCF-7. The breast cancer cells were treated with 12.5 µM and 25 µM of HHQ for 48 h at 37°C. Representative western blot hybridization signals for PKM2 [A] and the quantitation of the signals is shown in [B]. Immunofluorescent detection of PKM2 is shown in [C] and the relative intensity measurement of immunofluorescence is shown in [D]. Significant decrease in PKM2 expression was observed in HHQ treated cells. Data are representative of three independent experiments done in triplicates and expressed as mean ± S.E.M. '*' represents the statistical significant ($p<0.05$) difference between control and HHQ treated groups.

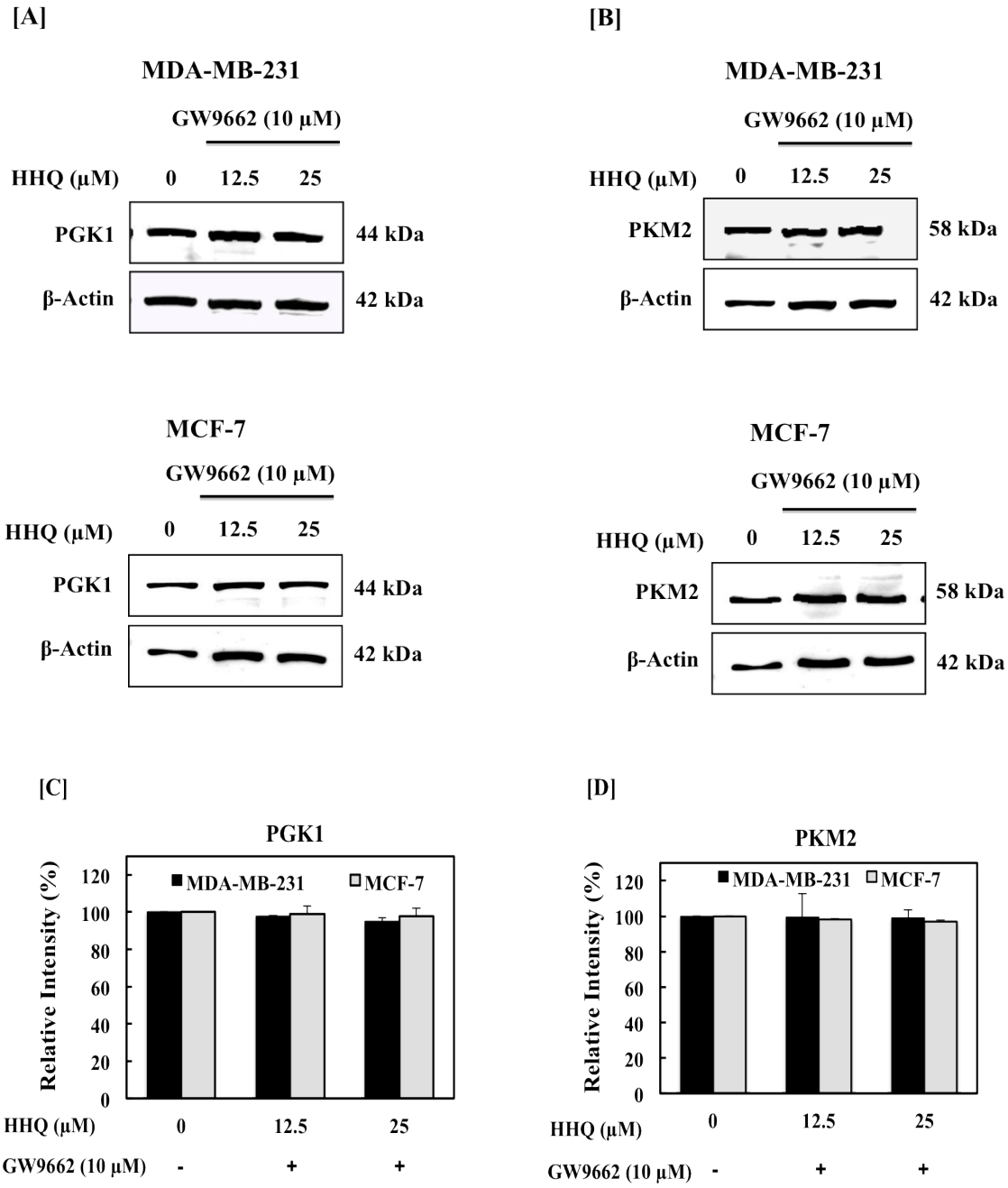

Figure 3-11: PPARγ dependent repression of glycolytic enzymes PGK1 and PKM2 by HHQ in human breast cancer cells, MDA-MB-231 and MCF-7. The breast cancer cells were pre-treated with a potent PPARγ antagonist, GW9962 (10 μM) for 4 h at 37°C, followed by treatment with 12.5 μM and 25 μM of HHQ for 48 h at 37°C. Representative western blot hybridization signals for PGK1 [A] and PKM2 [B] for both the breast cancer cell lines and the quantitation of the signals is shown in [C] and [D], respectively. GW9662 showed no effect of HHQ on expression of PGK1 and PKM2, thereby suggesting that the activation of PPARγ is required for repression of these enzymes. Data are representative of three independent experiments and expressed as mean ± S.E.M.

CHAPTER 4

IBRUTINIB TARGETS GLYCOLYTIC ENZYMES THROUGH PPAR GAMMA DEPENDENT SIGNAL PATHWAY - THERAPEUTIC INTERVENTION IN HUMAN BREAST CANCER

4.1 INTRODUCTION

Breast cancer is the fifth most common cancer globally and accounts for the highest morbidity and mortality. It is the second highest occurring cancer in women and one of the leading causes of death [165]. Although anti-estrogens have provided an effective endocrine therapy, a significant proportion of patients have acquired resistance to these drugs, while others are intrinsically resistant [166]. Hence, there is a requirement for alternative therapeutics to treat breast cancer. Development of anticancer agents with therapeutic selectivity based on the biological differences between normal and cancer cells is essential to improve therapeutic selectivity, sensitivity and specificity [167].

It is prudent to note that the metabolic phenotype of cancer is distinct from that of normal cells. Rapidly proliferating cancer cells alter their metabolism to support continuous cell growth and proliferation [168]. These alterations in cellular bioenergetics are thus the hallmarks of cancer [169]. Increased aerobic glycolysis and the dependency on glycolytic pathway for ATP generation, and elevated oxidative stress are prominent metabolic alterations frequently observed in cancer cells, as shown by the Warburg hypothesis [170]. The altered metabolism in cancer cells may be due to mitochondrial defects and malfunction, adaptation to hypoxic tumor microenvironment, oncogenic signaling and abnormal expression of metabolic enzymes [167]. Altenberg et al. [171] found overexpression of glycolytic genes in 24 cancer cell lines including breast cancer. *RAS*, *SRC* and *MYC* oncogenes have been found to enhance glycolysis by regulating the expression of glycolytic enzymes and glucose transporters [172]. Moreover, transcription factor hypoxia-inducible factor (HIF), which is frequently deregulated in cancer, also regulates the expression of glycolytic genes [173].

It has been reported that dysregulated cellular metabolism is linked to drug resistance in cancer therapy [174,175]. It has been found that glycolytic enzymes, lactate dehydrogenase A and pyruvate dehydrogenase kinase 3 contributes to

paclitaxel/trastuzumab resistance in breast cancer and hypoxia-induced drug resistance in cervical and colon cancer, respectively [168]. In addition, cisplatin resistance is linked to glutaminolysis via mammalian target of rapamycin complex 1 (mTORC1) signaling pathway in gastric cancer and fatty acid synthase is linked to acquired docetaxel/trastuzumab/adriamycin resistance in breast cancer [168]. Hypoxic tumours have generally been known to evolve into invasive and metastatic tumors as compared to those with normal oxygen levels due to increased glycolysis requirements in hypoxia [176]. These results demonstrate the clinical importance of glucose metabolism in treatment of cancer. Thus, the increased dependence of cancer cells on glycolytic pathway for metabolic demands provides basis for the design of therapeutic strategies to selectively and efficiently kill cancer cells by pharmacological inhibition of glycolysis.

As described earlier, many oncogenes and transcriptional factors regulate glycolytic enzymes. One such popular transcriptional factor is peroxisome proliferator-activated receptors (PPARs). The peroxisome proliferator-activated receptors (PPARs) are ligand activated transcription factors, belonging to the nuclear receptor superfamily, that control the expression of genes involved in organogenesis, cell differentiation, inflammation, proliferation, lipid, and carbohydrate metabolism [177]. PPARs once activated by ligands, heterodimerize with retinoid X receptor (RXR) and bind to peroxisome proliferator response elements (PPREs) and/or PPAR-associated conserved motif (PACM) motifs, in the promoter of the target genes [178,179]. The PPRE motif consists of a direct repeat of the consensus sequence AGGTCA separated by a single/double nucleotide (DR-1 site/DR-2 site) [180]. Recently, a PACM motif of width 15 bp with the consensus TTCATTTGGACATTG was discovered. It is reported that PACM motifs are more common than PPREs [181]. Three isoforms (α, β and γ) for PPAR have been identified so far in Xenopus, mouse, rats hamsters and human and is encoded by a different gene, performs different functions and exhibits different tissue localizations in many parts of the human body [182]. The peroxisome proliferator-activated receptor γ (PPARγ) is the most extensively studied subtype of the PPARs. PPARγ is expressed in adipose tissue, colon, immune system, and hematopoietic cells and is involved in lipid anabolism, adipocyte differentiation, inflammation control and macrophage maturation [183]. Activation of PPARγ by selected ligands has shown anti-proliferation effect in many cancer cell lines including breast [184], colon [185], prostate [186], and non-small-cell lung cancer [187].

PPARγ can be activated by polyunsaturated fatty acids (e.g. linoleic acid, linolenic acid and arachidonic acid) and eicosanoids (e.g. prostaglandin J2 derivatives) [188, 189]. Currently however, synthetic ligands such as Thiazolidinediones (TZDs) and tyrosine agonists remain the most potent known activators of PPARγ. Its role in cancer development and potential as a target for cancer prevention and treatment strategies has been noted in recent years. PPARγ agonists e.g Thiazolidinediones (TZDs), and tyrosine based agonists show cytotoxicity by inducing apoptosis of malignant cells, arresting the cells at G0/G1 phase, up regulation of the tumor suppressor p53 etc. [190]. Recently, I reported the presence of PPRE and PACM motifs in glycolytic genes, phosphoglycerate kinase 1 (PGK1) and tumor specific pyruvate kinase muscle 2 (PKM2). I experimentally validated the repression of PGK1 and PKM2 by PPARγ natural ligand, 15d-PGJ2 [179] and also by novel PPARγ ligand, Hydroxy hydro Quinone (HHQ) [201] and since both the enzymes are involved in ATP synthesis, with repression in PGK1 and PKM2, the ATP level was found to be lowered in both of the breast cancer cell lines. The main physiological function of PGK1 and PKM2 is to catalyze sixth and ninth step, respectively in glycolysis generating one molecule of ATP each. PGK1 and PKM2 are reported to be over expressed in many cancers [161, 192] accounting for their pivotal role in most fundamental metabolic alterations [170].

Ibrutinib (formerly named as PCI-32765) is an anti-cancer drug targeting B cell malignancies such mantle cell lymphoma (MCL) and chronic lymphocytic leukemia (CLL) [193]. Ibrutinib targets chronic lymphocytic leukemia inhibition of bruton tyrosine kinase (BTK) tyrosine phosphorylation and have also found to limit downstream survival pathways activated BTK such ERK1/2, PI3K, and NF-κB and has found to induce apoptosis by activation of caspase-3 and PARP. Ibrutinib shows no T-cell cytotoxicity and decreases the production of several anti-inflammatory cytokines such as IL-6 and IL-10 that enhance CLL cell survival [194].

The main objective of this chapter is to investigate the anti-proliferative effect of Ibrutinb, and the possible mechanism of modulatory effect on expression of glycolytic genes, PGK1 as PKM2 in breast cancer cell lines. Further investigations on these could possibly help us in understanding the molecular mechanisms by Ibrutinib targets genes involved in breast cancer pathophysiology and its use in breast cancer therapeutics.

4.2 EXPERIMENTAL SECTION

4.2.1 Reagents

Dulbecco's modified eagle's medium (1000 mg/L glucose, L-glutamine and sodium bicarbonate), Fetal bovine serum, GW9662 and crystal violet were purchased from Sigma-Aldrich (St Louis, MO, USA). Ibrutinib (PCI-32765) was procured from Selleck Chemicals (Houston, Texas, USA). Penicillin–Streptomycin–Neomycin antibiotic mixture, Hoechst 33258 and the Image-iTTM LIVE Green Reactive Oxygen Species (ROS) detection reagents were procured from Invitrogen (Eugene, OR, USA) and JC-1dye from Biotium (Hayword, CA, USA), Tris base, potassium chloride, Sodium chloride, sodium di hydrogen phosphate, glycine and sodium phosphate di basic were purchased from Wako Pure Chemical Industries (Osaka, Japan).

4.2.2 Methodology

Cell culture and treatments

The human breast adenocarcinomas - MDA-MB-231 and MCF-7 were purchased from the American Type Culture Collection (ATCC; Manassas, VA, USA). The breast cancer cell lines were maintained in Dulbecco's modified eagle's medium supplemented with 10% fetal bovine serum and PNS antibiotic mixture 100 ng/ml at 37°C and 5% CO_2/95% O_2. Cultures at about 70% confluency were treated with various concentration of Ibrutinib for cytotoxic assay to calculate median inhibitory concentration (IC-50) and for other experiments, 6 µM and 12µM of Ibrutinib concentration for 48 h at 37°C. For PPARγ activity inhibition studies, the breast cancer cells were pre-treated with GW9662 (10 µM, 4 h at 37°C) followed by Ibrutinib (6 µM and 12µM, 48 h at 37°C) and harvested for future use.

Cytotoxicity/growth inhibition assay

Ibrutinib was tested for its anti-proliferative activity on MDA-MB-231 and MCF-7 cells using the 3-(4, 5-dimethylthiazol-2-yl)-2, 5-diphenyltetrazolium bromides (MTT) test (Roche, Mannheim, Germany) following manufacturer's instructions. The MTT is a colorimetric cell proliferation assay that identifies living cells based on the cellular conversion of a tetrazolium salt by enzyme dehydrogenases into insoluble formazan, which can be quantified by spectrophotometry. 1 $x10^4$ cells/well were plated in 96-well plates and grown for 24 h. The cells were then exposed to varying concentrations of Ibrutinib for 48 h to find the median inhibitory concentration (IC-50) values. The intensity of the reduced dye that corresponds to the viable cells was measured at

reference wavelength of 570 nm by Thermo Scientific Varioskan Flash Multimode Reader. All experiments were performed in triplicates, and the relative cell viability (%) was expressed as a percentage relative to the untreated control cells.

Morphological Studies

The cells were cultured in 24-well plates. At about 50% confluency cells were treated with 6 μM and 12 μM of Ibrutinib concentration. After 48 h morphological changes in breast cancer cells were examined by phase contrast microscope (Nikon, Japan). The plates were stained with crystal violet and scanned for records. All experiments were performed in triplicates, and the relative cell viability (%) was expressed as a percentage relative to the untreated control cells.

Clonogenic assay

Clonogenic assay is a cell survival assay based on the ability of a single cell to grow into a colony. Effect of Ibrutinib on colony formation potential of human breast cancer cells was assessed by clonogenic assay. To determine long-term effects, breast cancer cells were treated with 6 μM and 12 μM of Ibrutinib concentration. After 48 h of treatment, the breast cancer cells were then plated at a concentration of 200 cells/well in a new 6-well plate. The cells were then allowed to grow for 15 days to form colonies. Fresh medium was replaced every third day. After 15 days, the colonies were once washed with PBS and then fixed in pre-chilled methanol: acetone mixture (1:1) for 10 min at room temperature. The colonies were then stained with crystal violet dye (0.5% in water) at room temperature for overnight. Cells were washed with water and plates were photographed with image scanner (EPSON GT-1500). Quantitative analysis of the total number of colonies was performed with Image J software (National Institutes of Health).

Detection of reactive oxygen species

The reactive oxygen species were detected by fluorescent staining using the Image-iTTM LIVE Green Reactive Oxygen Species (ROS) Detection Kit (Molecular Probes Inc, USA). The assay is based on a nonfluorescent and cell permeable 5-(and-6)-carboxy-2',7'-dichlorodihydrofluorescein diacetate (carboxy-H2DCFDA that permeates the live cells and is deacetylated by intracellular esterases. The reduced fluorescein compound is oxidized by the cellular ROS and emits bright green fluorescence with excitation/ emission maxima of 495/529 nm. The cells were grown on glass cover slips placed in 12-well plate and were treated with 6 μM and 12 μM of Ibrutinib

concentration. Subsequently, after 48 h cells were fixed and then stained for ROS by following manufacturer's instructions. The images were analyzed with AxioVision software (version 4.4, Carl Zeiss).

Assessment of mitochondrial membrane potential

Mitochondrial transmembrane potential was investigated using a fluorochrome, JC-1 dye (Biotium). JC-1 (5,5',6,6'-tetrachloro-1,1',3,3' tetra ethyl benzimidazolyl carbo cyanine iodide) dye exhibits potential-dependent accumulation of red fluorescent J-aggregates in energized mitochondria. JC-1 exists as a green fluorescent (535 nm) monomer and also accumulates as J-aggregates (595 nm) in the active mitochondria, which stain red. Consequently, healthy cells will exhibit high red/green fluorescence intensity ratio. In apoptotic cells, mitochondrial depolarization is indicated by a decrease in the red/green fluorescence intensity ratio. Therefore this fluorescence emission shift from green (~529 nm) to red (~590 nm) is indicative of mitochondrial depolarization occurring during apoptosis. After 48 h of 6 μM and 12 μM of Ibrutinib treatment, the cells were incubated with 1X JC-1 dye at 37°C for 15 min followed by washes with assay buffer. The red fluorescence (excitation 550 nm, emission 600 nm) and green fluorescence (excitation 485 nm, emission 535 nm) were measured using fluorescence Thermo Scientific Varioskan Flash Multimode plate reader. The ratio of red fluorescence to green fluorescence was determined in JC-1 stained cells. The relative mitochondrial membrane potential (%) was expressed as a percentage relative to the untreated control cells.

ATP depletion studies

In order to examine the extent of ATP depletion due to PPARγ activation I next examined ATP concentration in cytosol and mitochondria. ATP concentration was quantified using commercially available luciferin–luciferase bioluminescence assay kit (Molecular Probes, Inc., Eugene, OR, USA). The assay is based on luciferase's requirement for ATP in producing light (emission maximum ~560 nm at pH 7.8). The total ATP level was estimated according to manufacturer's instructions. The amount of ATP in the experimental samples was calculated from standard curve prepared with ATP (1–100 μM) and expressed as percentage of ATP in cells. Light emission was monitored using a luminometer (Wallac 1420 Victor 2 multiplate counter system; Perkin Elmer Life Science, Inc., Gaitherburg, MD, USA).

Western blot analysis

Expression level of indicated proteins was examined by Western blotting. The control and treated cells were lysed in RIPA lysis buffer (25 mM Tris–HCl (pH 7.6), 1% NP-40, 1% sodium deoxycholate, 150 mM NaCl, 0.1% SDS) complemented with complete protease inhibitors (Roche) for 15 min on ice followed by centrifugation at 14,000 *g* for 15 min at 4°C. The protein concentration was determined using BCA reagents (Pierce, Rockford, IL, USA). Protein lysate (20 µg) was resolved in 10% in SDS-polyacrylamide gel under standard denaturing conditions followed by transfer onto polyvinylidene difluoride membranes using a Trans-Blot SD (Bio-Rad, Lewes, E. Sussex, UK.) semi-dry electroblotter for 30 min at 20 V. Subsequently, the membranes were blocked for 45 min at room temperature with 2% bovine serum albumin in 0.1% PBST. The membranes were then probed with anti-PGK1 (1:1000; Abcam, Cambridge, UK), anti- PKM2 (1:500, Abcam), anti-caspase-8 (1:1000; Cell Signaling, Boston, MA, USA), Anti-Bax (1:1000; Cell Signaling) and anti-β-actin (1:20,000; Abcam) at 4°C overnight followed by three washes for 5 min each with 0.1% PBST. The membranes were then incubated with horseradish peroxidase conjugated secondary antibody (1:20,000; Abcam) for 45 min at RT and washed thrice for 5 min each with 0.1% PBST followed by chemiluminescent detection using Luminescent Image Analyzer equipped with charge-coupled device camera (LAS-4000 Ver. 2.1; Fuji Film, Tokyo, Japan).

Data Analysis

The captured images for ROS assay and immunostaining were analyzed using AxioVision software (version 4.4; Carl Zeiss). The analysis determined the overall density of ROS, PGK1 and PKM2 immunoreactivity in 5-8 randomly selected fields in each slide. The mean intensity of ROS, PGK1, and PKM2 immunoreactivity in control and treated cells were evaluated and presented as a histogram. Similarly the Relative Optical Density (%) for immunoreactive bands in western blotting for PGK1, PKM2 and Caspase-8 were analyzed using Image J software (National Institutes of Health).

Statistical Analysis

The quantitative data are representative of three independent experiments done in triplicates and expressed as mean ± SEM. Statistical analysis was performed using analysis of variance (one way analysis of variance) followed by Bonferroni's on test to determine differences in mean and $p < 0.05$ and $p < 0.001$ was considered as statistically significant.

4.3 RESULTS AND DISCUSSIONS

4.3.1 Ibrutinib inhibits cell proliferation and clonogenic survival of human breast cancer cell lines

To investigate the cytotoxic effect of Ibrutinib, I first examined the effect of Ibrutinib on cell proliferation and colony forming potential in human breast adenocarcinomas, MDA-MB-231 (estrogen independent) and MCF-7 (estrogen dependent). The breast cancer cell lines, MDA-MB-231 and MCF-7 were cultured in the control medium for 24 h, followed by 48 h of treatment with different concentrations of Ibrutinib for cytotoxic and anti-proliferative studies. The cell viability was detected by MTT dye reduction assay. As shown in Figure 4-1A, Ibrutinib was observed to inhibit the proliferation of breast cancer cell lines in a dose dependent manner. The median inhibitory concentration (IC-50) value of Ibrutinib for MDA-MB-231 and MCF-7 were found to be 12 μM and 10 μM, respectively. I proceeded with 6 μM and 12 μM of Ibrutinib to investigate the comparable effects of same concentration on both the breast cancer cell lines. As observed through cytotoxicity graph of Ibrutinib, at 6 μM the relative viability in MDA-MB-231 and MCF-7 was 66.9 ± 1.6 % and 59.3 ± 0.5 %, respectively, whereas at 12 μM the relative viability in MDA-MB-231 and MCF-7 was 50.0 ± 1.1 % and 44.1 ± 0.4 %, respectively. At 100 μM of Ibrutinb concentration (the highest dose taken for the viability study), the relative viable cell percentage was observed to be 20.3 ± 0.5 % and 18.7 μM ± 0.2 % in MDA-231 and MCF-7, respectively. In order to confirm these cytotoxicity results, a comparative viability assays was performed. Breast cancer cell lines were cultured in 24-well culture dishes and treated with 6 μM and 12 μM of Ibrutinib concentration. 48 h post-treatment the cells were fixed and stained with crystal violet. As shown in Figure 4-1B, Ibrutinib treatment caused decreased in cell viability in MDA-MB231 and MCF-7 in dose dependent manner. However it was prudent to note the cytotoxicity of Ibrutinib more effective in case of estrogen dependent MCF-7, suggesting the possible potential cytotoxic and anti-proliferative implications of Ibrutinib on estrogen dependent breast cancer cell lines. Morphological analyses of cells on treatment with various insults usually, depicts the health of a cell, therefore I next examined the cells for any altered morphology on treatment with Ibrutinib. Treatment with Ibrutinib (6 μM and 12 μM) showed significant morphological changes in breast cancer cell lines and were found to be reduced in cell mass and cell number with respective to control. Ibrutinib treatment

induced cell detachment and rounding in breast cancer cells and seemed to undergo apoptotic cell death as shown by phase contrast images in both the breast cancer cell lines in 48 h as shown in Figure 4-1C. The phase contrast micrographs supported the viability results. Significant decrease in cell density, rounding and detachment induced by Ibrutinib was observed in dose dependent fashion.

Furthermore, to examine the antitumor activity of Ibrutinb on colony forming potential in breast cancer cells I performed clonogenic potential assay. Clonogenic assay is an *in vitro* assay based on the ability of a single cell to survive and proliferate into colonies in response to various insults. Ibrutinib treatment was found to severely retard the cell survival and colony forming potential of human breast cancer cells - MDA-MB-231 and MCF-7. As shown in Figure 4-2A, the clonogenicity of both the breast cancer lines was found to be significantly reduced in a concentration-dependent manner after exposure to Ibrutinib. For MDA-MB-231, the relative number of colonies (%) were observed to be 71 ± 2 % and 50 ± 1 % for 6 μM and 12 μM of Ibrutinib, respectively, whereas for MCF-7, the relative number of colonies (%) were observed to be 63 ± 1 % and 37 ± 1.5 % for 6 μM and 12 μM of Ibrutinib, respectively (Figure 4-2B). Ibrutinib was more effective in limiting the colony forming ability of MCF-7 as compared to MDA-MB-231. The finding again confirms the results of viability assay, involving increased cytotoxicity of Ibrutinib to estrogen positive breast cancer cell lines, MCF-7.

4.3.2 Ibrutinib down regulates glycolytic enzymes through PPARγ dependent signaling pathway.

In 1930, Otto Heinrich Warburg [170] discovered that highly proliferative cancer cells' metabolism is quite different than the one of normal adult cells. The unknown link was thus termed as "Warburg Effect". Warburg effect is a phenomenon involved which is characterized by increased glucose uptake and dependence on glycolysis for ATP production even in the presence of oxygen source. It was found that the glycolytic rate of rapidly proliferating tumor cells was 200 times higher than those of their normal tissues of origin [170]. Highly proliferating cancer cells cope up with the increased metabolic demand by up regulating glycolytic enzymes, thereby leading to increase in glycolysis. Altenberg and Greulich [171] found over expression of glycolytic genes in 24 different types of cancer including breast cancer.

Glycolytic genes, phosphoglycerate kinase 1 (PGK1) and tumor specific pyruvate kinase muscle 2 (PKM2) [171,195] are also found to be overexpressed in breast cancer

cells. PGK1 catalyzes conversion of 1,3-diphosphoglycerate to 3-phosphoglycerate, which is the sixth step of glycolysis and generates 1 molecule of ATP. In addition to its role as a glycolytic enzyme, PGK1 also functions as a polymerase alpha cofactor protein (primer recognition protein) and is involved in DNA synthesis. On the other hand, PKM2 catalyze the rate-limiting ninth step of glycolysis converting phosphoenol pyruvate (PEP) to pyruvate with production of one ATP molecule.

To cope up with rapid cell proliferation, tumor cells have to maintain a budget of metabolic intermediates that is adequate enough to ensure energy regeneration as well as synthesis of building blocks in sufficient amounts. PKM2 is a key regulator of the metabolic budget system in tumor cells which promotes the Warburg effect as well as tumor growth and it is also reported to be involved in channelization of glucose carbons to biosynthetic processes and hence control glycolysis [196]. This tumor specific PKM2 can be switched between dimeric and tetrameric forms in cancer cells. In tumor cells, PKM2 determines whether glucose is converted to lactate for regeneration of energy by active tetrameric form or used for the synthesis of cell building blocks (inactive dimeric PKM2). Dimeric inactive PKM2 has higher Km value for the substrate PEP than the tetrameric form of PKM2. Switching of tetrameric PKM2 to dimeric PKM2, leads to accumulation of energy rich phospho metabolites upstream of glycolytic pathway which are then channeled to macromolecule biosynthesis via pentose phosphate pathway (PPP) involving pyrimidine, glycerol, and serine/glycine biosynthesis thereby promoting cancer cell proliferation and tumor growth [197,198]. Hence therapeutic strategies to down regulating these enzymes which not only starve the cells for ATP but also lead to biosynthetic metabolite starvations, as they are important for tumor cell proliferation and survival.

In order to investigate the effect of Ibrutinib on glycolysis, I undertook expression analysis of glycolytic enzymes, PGK1 and PKM2. I observed that the expression levels of PGK1 and PKM2 were significantly down regulated in both the breast cancer cells on treatment with Ibrutinib for 48 h in dose-dependent manner, as shown in Figure 4-3A. Since both enzymes, PGK1 and PKM2 are involved directly (glycolysis) and indirectly (intermediates for metabolic pathways such as pentose phosphate pathway, citric acid cycle etc.) in production of energy rich molecule, ATP henceforth; I next investigated the effect of down regulation of glycolytic enzymes, PGK1 and PKM2 by Ibrutinib on ATP levels. As shown in Figure 4-3B, the total ATP levels were significantly reduced in MDA-MB-231 and MCF-7 cell lines on treatment with Ibrutinib in concentration

dependent manner. In MDA-MB-231, relative ATP level (%) were decreased to 80.6 ± 2.9 % and 61.6 ± 4.8 % at 6 μM and 12 μM of Ibrutinib, respectively. Whereas in MCF-7, the relative ATP level (%) were decreased to 79.3 ± 5.8 % and 58.3 ± 1.5 % at 6 μM and 12 μM of Ibrutinib, respectively. Down regulation of PGK1 and PKM2 and decrease in ATP level corroborated with viability assays and apoptotic assay, suggesting that down regulating these enzymes starved the cells for ATP ultimately leading to cell death. Earlier, I reported that both PGK1 and PKM2 have PPRE and PACM binding sites for PPARγ and are repressed in the breast cancer cell lines MDA-MB-231 and MCF-7 through PPARγ dependent signal pathway by natural ligand 15d-PGJ2 [179]. Further the same glycolytic enzymes were found to down regulated by novel PPARγ ligand HHQ through PPARγ dependent signal pathway. Further analysis suggested that this repression leads to decrease in ATP levels and initiates apoptosis [191].

Here, I hypothesized that the repression of Ibrutinib can modulate the expression of PGK1 and PKM2 via PPARγ dependent pathway. Therefore, to test this hypothesis, I undertook expression analysis of these metabolic enzymes using GW9662, an irreversible PPARγ antagonist that acts by binding to the human ligand-binding domain (region E/F). The breast cancer cells were pre-treated with GW9662 (10 μM, 4 h at 37°C) followed by Ibrutinib (6 μM and 12 μM, 48 h at 37°C). As shown in Figure 4-4, no significant repression of PGK1 and PKM2 was observed. GW9662 showed no effect of Ibrutinib on expression of PGK1 and PKM2, thereby suggesting that the activation of PPARγ is required for repression of these enzymes.

4.3.3 Ibrutinib induces mitochondrial dysfunctioning in human breast cancer cell lines

Mitochondria are the powerhouse of a cell. They lie at the focal of many biosynthetic pathways but the main physiological function of the mitochondria is production of cell energy currency, adenosine triphosphate (ATP) by the oxidative phosphorylation pathway [199]. In addition to production of cellular energy, mitochondria also regulate mitochondrial and cellular redox status, are also crucial for the regulation of intracellular Ca^{2+} homeostasis and are the main regulators of apoptotic cell death by mediating extrinsic and intrinsic apoptotic pathways. They can initiate apoptosis by the activation of the mitochondrial permeability transition pore, which leads to loss of mitochondrial membrane potential [200]. Henceforth, mitochondria are considered as the central players in the determination of cell survival and death. Similar

to normal cells, functional mitochondria are essential for survival of the cancer cell.

Cancer cells synthesize ATP mainly through aerobic glycolysis, which is linked to high glucose uptake [170]. In cancer cells, increased glycolysis not only leads to increased production of ATP, but also produces metabolites used for synthesizing cell building blocks such as nucleotides, lipids and proteins via pentose phosphate pathway and tricarboxylic acid cycles [201]. In addition, the upregulated metabolic process which takes place in the mitochondria produces increased reactive oxygen species (ROS) and acidification of the tumor microenvironment. ROS are regulators of many physiological processes in cancer cells whereas acidification of tumor environment has been found to be associated with tumor invasion [202]. Furthermore, elevated production of NADPH and glutathione through pentose phosphate shunt are associated with increased resistance of tumor cells against oxidative insults and few chemotherapeutic agents [203].

As mitochondrial health is critical for cancer cell survival, I next investigated the effect of Ibrutinib on mitochondria in MDA-MB231 and MCF-7 by mitochondrial membrane potential analysis using potential sensitive, cationic dye JC1. This dye exhibits potential-dependent accumulation in mitochondria, indicated by a fluorescence emission shift from green (525 nm) to red (590 nm). Consequently, live cells have higher red/green intensity ratio as compared to cells undergoing apoptosis. As shown in Figure 4-5A, control breast cancer cells show increased red fluorescence due to accumulation of J-aggregate by the concentrated JC-1 dye, indicating the regions of high mitochondrial polarization in MDA-MB-231 and MCF-7, whereas on treatment with Ibrutinib at 12 μM for 48 h showed depolarized regions with increased green fluorescence of the JC-1 monomers. To further confirm these results, a fluorometric analysis was carries out. The cells were cultured in 96-well plate and treated with Ibrutinib at 12 μM. Forty eight hours of post treatment, cells were stained with JC-1 and observed for red fluorescence (excitation 550 nm, emission 600 nm) and green fluorescence (excitation 485 nm, emission 535 nm). As shown in Figure 4-5B, on treatment with Ibrutinib cells showed significant loss of mitochondria membrane potential (MMP) in both of the breast cancer cell lines. Breast cancer cell line, MDA-MB-231 showed 72.2 % loss of mitochondrial membrane potential with total mitochondrial membrane potential level accounting to 27.8 ± 9.9 %, where as in case of MCF-7, the percentage of loss of mitochondrial membrane potential was 92.35 %, with

total mitochondrial membrane potential level accounting to 7.7 ± 4.01%, suggesting the enhanced mitochondrial dysfunctioning of Ibrutinib on estrogen positive MCF-7. This data corroborated with the results of viability assays. Since disruption of active mitochondria is a distinctive feature of the early stages of programmed cell death [204], these findings suggested that Ibrutinib causes alterations to the oxidation–reduction potential of the mitochondria, ultimately leading to the mitochondrial disruption and possible induction of apoptosis.

4.3.4 Ibrutinib induces of caspase dependent apoptosis in human breast cancer cell lines

Apoptosis, or programmed cell death, is a mechanism by which cells undergo death to control cell proliferation or in response to any DNA damage [205]. It is found that, in cancer cells oncogenic mutations causes more malignant phenotype by disrupting apoptosis that leads to tumor initiation, progression, metastasis and resistance to therapeutic regimes [206]. Hence forth, there is a need of development of strategies designed to selectively induce apoptosis in cancer cells or sensitize them to established cytotoxic agents and radiation therapy.

Ibrutinib (formerly PCI-32765) is a highly potent bruton's tyrosine kinase (BTK) pathway inhibitor. The BTR signaling regulates cell proliferation, differentiation, and apoptosis of B-lymphocytes and plays a crucial role in the pathogenesis of B-cell malignancies such as Mantle cell lymphoma (MCL) and Chronic lymphocytic leukemia (CLL). It was found that Ibrutinib induces apoptosis selective for B cells, mediated by the caspase pathway in MCL. It also found to alter the immunogenicity of T cells by inhibiting production of interleukins - IL-6, IL-10 and tumor necrosis factor-alpha (TNF α) by T cells without affecting the cell survival [192,193,207].

In order to determine if the inhibition of cell growth by Ibrutinib involves cellular apoptotic pathways in human breast cancer cell lines, I undertook apoptosis studies. As morphological analysis is important to study the cellular organization and the physiological state of the cells, therefore I first examined the effect of Ibrutinib on morphology of breast cancer cell lines. The breast cancer cells lines were treated with 6 μM and 12 μM of Ibrutinib for 48 h. Ibrutinib treatment induced noticeable morphologic changes in MDA-MB-231 and MCF-7. The morphology of the cells showed apoptotic characteristics. The Ibrutinb treated cells were round, detached and cellular disintegrated as shown in Figure 4-6A.

Apoptosis leads to activation of series of biochemical events that alter cell characteristics [208]. One of these important changes is chromatin condensation and nuclear fragmentation [209]. To further confirm these apoptotic changes, the cells, MDA-MB-231 and MCF-7 were subsequently analyzed for nuclear condensation by staining the nucleus with nucleic acid specific stain Hoechst stain. Ibrutinib treatment showed marked apoptosis with increased condensed nuclei in dose-dependent fashion. A total of 22.8 % and 42.5 % of apoptotic cells were observed in MDA-MB-231 on treatment with 6 μM and 12 μM Ibrutinib, respectively. On the other hand, in MCF-7 treatment induced 30 % and 46.5% of relative percentage of apoptotic cells at 6 μM and 12 μM Ibrutinib, respectively (Figure 4-6A and 4-6B).

In order to understand the mechanism of cell death induced by Ibrutinib, I undertook the expression analysis of apoptotic proteins, capase-8, bax, and cytochrome c in human breast cancer cell lines. Caspase-8 belongs to the family of cysteine proteases that plays a critical role in the regulation of apotosis. Activation of caspase-8 is one of the early events leading to apoptosis [210,211]. Activated caspase-8 is known to initiate the apoptotic signal by directly cleaving and activating downstream effector caspases (extrinsic apoptotic pathway) or by cleaving the BH3 Bcl2-interacting protein, which leads to the release of cytochrome c from mitochondria (Intrinsic apoptotic pathway) [212]. Furthermore, PPAR agonists also have known to induce intrinsic and extrinsic apoptotic cascade by activating caspase-8 [213]. Interestingly, I observed that on treatment with Ibrutinib the level of procaspase-8 decreases significantly in both the cancer cells. This demonstrates that caspase-8 proenzyme is being cleaved to active caspase-8 fragments in a dose-dependent manner (Figure 4-6). In addition level of cleaved active part-10 of procaspase-8 was also found to be significantly increased in both the breast cancer cell line which corroborated with decrease in procaspase-8.

Previous mitochondrial membrane permeability results suggested that Ibrutinib causes mitochondrial dysfunctioning, there fore in order to get further insights I next examined the expression level of apoptotic proteins involved with mitochondrial dysfunctioning. I investigated the expression level of Bax and cytchrome c in MDA-MB-231 and MCF-7. Bax is a pro-apoptotic protein belonging to Bcl-2-family [214]. Bax translocates from its predominantly cytoplasmic location to the mitochondria upon apoptosis induction and inserts its C-terminal hydrophobic domain into the mitochondrial membrane [215,216]. This leads to increase in mitochondrial membrane

permeability, loss of mitochondrial membrane potential and release of cytochrome c, thereby activating APAF-1 dimerization and the apoptotic cascade [217,218]. As shown in Figure 4-7 there was significant increase in bax level upon Ibrutinb treatment in dose dependent fashion. Bax is found to induce cytochrome c release from mitochondria by increasing the mitochondrial membrane permeability. It was observed that Ibrutinib treated cells had increased expression of cytochrome c. This result corroborated with increase bax level upon Ibrutinib treatment, suggesting the bax induced cytochrome c release.

It is prudent to note that the increased expression levels of bax and cytochcrome c correlates with the mitochondrial membrane potential loss in breast cancer cells on treatment with Ibrutinib. Together, these findings suggests that Ibrutinib induces mitochondrial dysfunctioning by upregulated bax expression, caspase-dependent apotosis by activated caspase-8 and bax induced cytochrome c release, ultimately leading to breast cancer cell death by induction of apoptosis.

4.4 CONCLUSION

Metabolic characteristic of cancer cells are significantly diverse than normal cells. The dysregulated metabolism has been to linked to therapeutic resistance in cancer treatment. Thus, inhibition of metabolic enzymes might be a promising strategy to overcome therapeutic resistance and improve the efficacy of cancer therapy. My results have established previously unknown novel cross-link between Ibrutinib, PPARγ, and glycolysis; thereby adding a new dimension to therapeutic potential of Ibrutinib. Although the exact mechanism remains unclear and further studies are still needed to clarify the potential role and molecular basis of action of Ibrutinib and PPARγ in breast carcinogenesis, my investigation open a new direction for development Ibrutinib in breast cancer treatment.

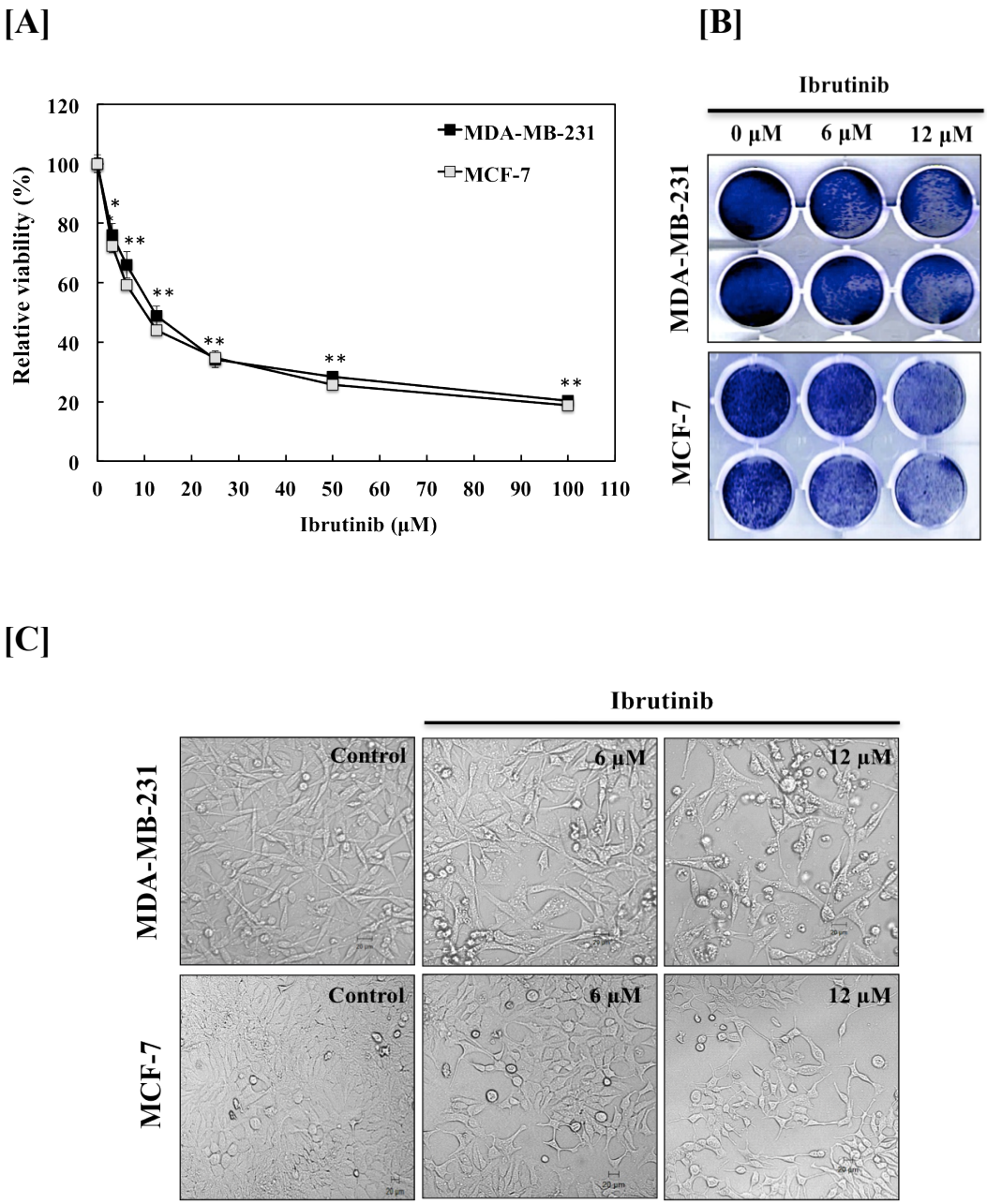

Figure 4-1: Cytotoxic effect of Ibrutinib on human breast cancer cell lines, MDA-MB-231 and MCF-7. Growth curve inhibition was assessed by MTT assay in MDA-MB-231 (grey line) and MCF-7 (blue line) [A]. The breast cancer cells were exposed to different doses of Ibrutinib for 48 h at 37°C. The cell viability decreased in dose-dependent fashion. The IC-50 value for MDA-MB-231 and MCF-7 were observed to be 12 µM and 10 µM, respectively. The breast cancer cells were treated with 6 µM and 12 µM of Ibrutinib and stained with crystal violet confirmed toxicity to cancer cells [B]. Morphological analyses revealed that Ibrutinib treated cells did not retain their normal morphology and induced rounding and detachment in breast cancer cells [C]. Data are representative of three independent experiments done in triplicates and expressed as mean ± S.E.M. '*' ($p < 0.005$) represents statistical significant difference between control and Ibrutinib test groups.

[A]

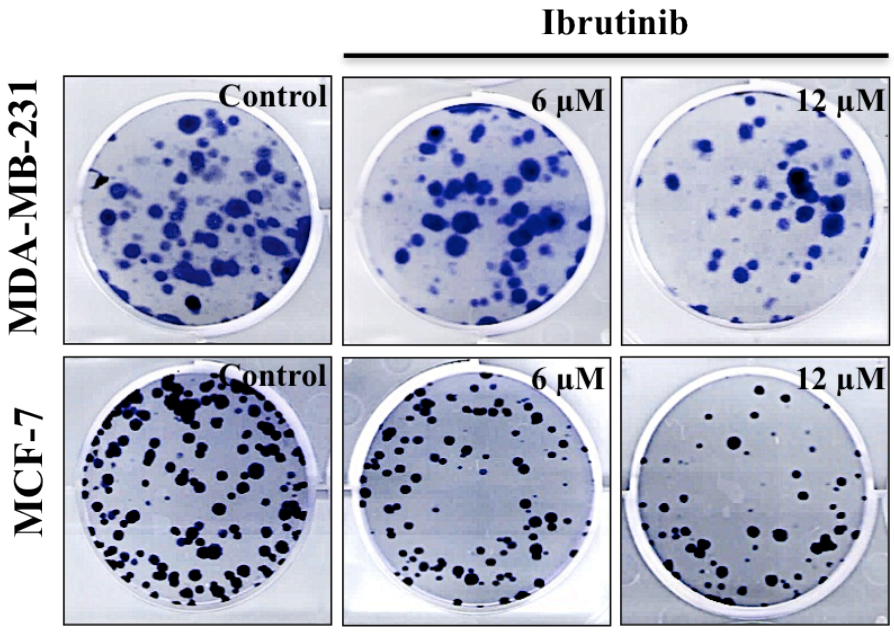

[B]

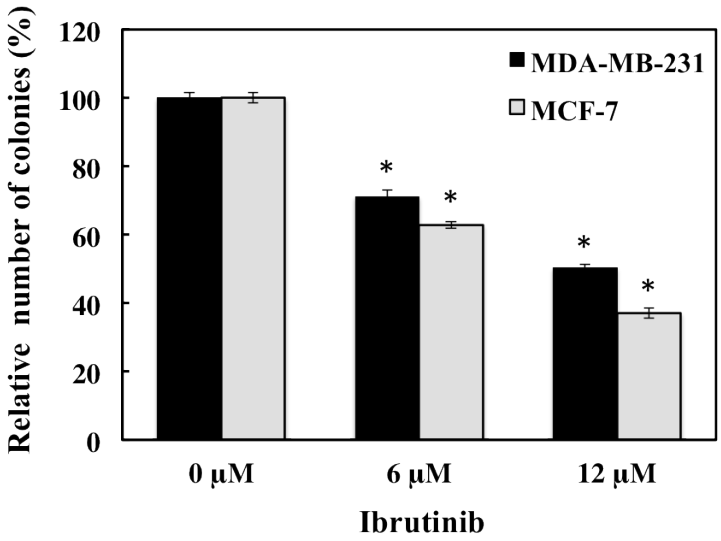

Figure 4-2: The inhibitory effects of HHQ on colony formation in human breast cancer cells (MDA-MB-231 and MCF-7) as evaluated by clonogenic assay. The breast cancer cells were exposed to 6 µM and 12 µM concentration of Ibrutinib for 48 h at 37°C. [A] Representative plates; [B] graph of the number of colonies formed (the result of three independent experiments, expressed as mean ± SEM). Decrease in number of colonies in Ibrutinib treated groups were statistically significant '*' ($p < 0.005$).

[A]

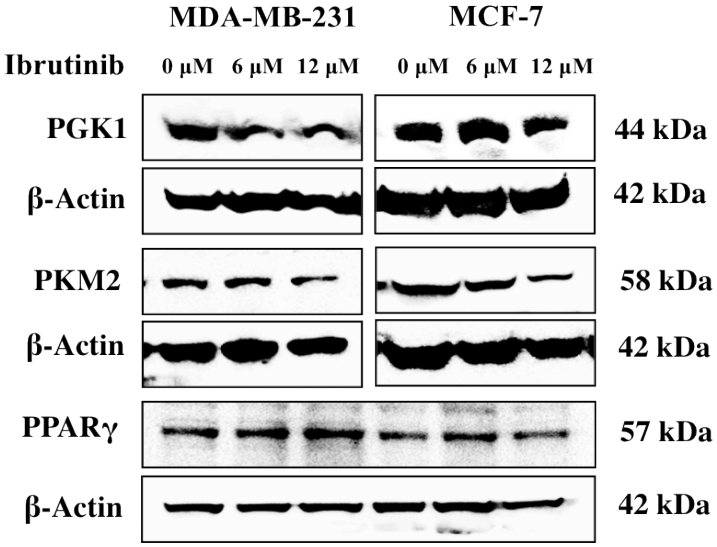

[B]

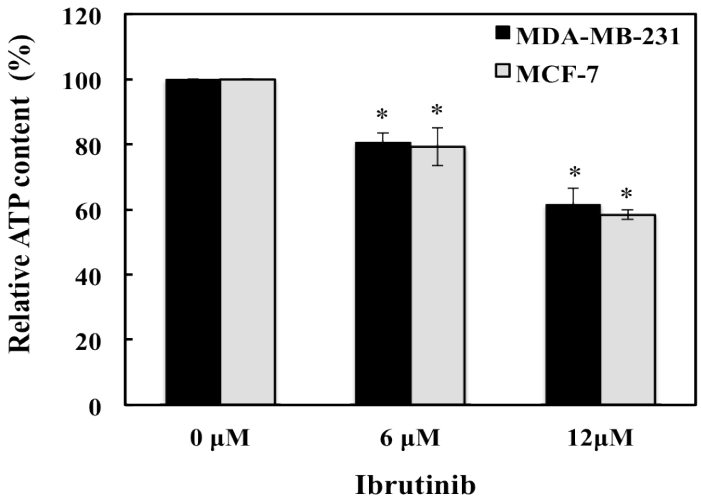

Figure 4-3: Expression analyses of the glycolytic enzymes, phosphoglycerate kinase 1 (PGK1), pyruvate kinase muscle 2 (PKM2) and transcriptional factor PPARγ in response to Ibrutinib treatment in human breast cancer cells, MDA-MB-231 and MCF-7. The breast cancer cells were treated with 6 µM and 12 µM of Ibrutinib for 48 h at 37°C. Representative western blot hybridization signals for PGK1, PKM2 and PPARγ [A]. Significant decrease in PGK1 and PKM2 and increase in PPARγ expression was observed with Ibrutinib treatment. Also repression of glycolytic enzymes corroborated with decrease in ATP levels in Ibrutinib treated cells [B]. Data are representative of three independent experiments done in triplicates and expressed as mean ± S.E.M.‘’*’’ represents the statistical significant ($p<0.05$) difference between control and Irutinib treated groups.

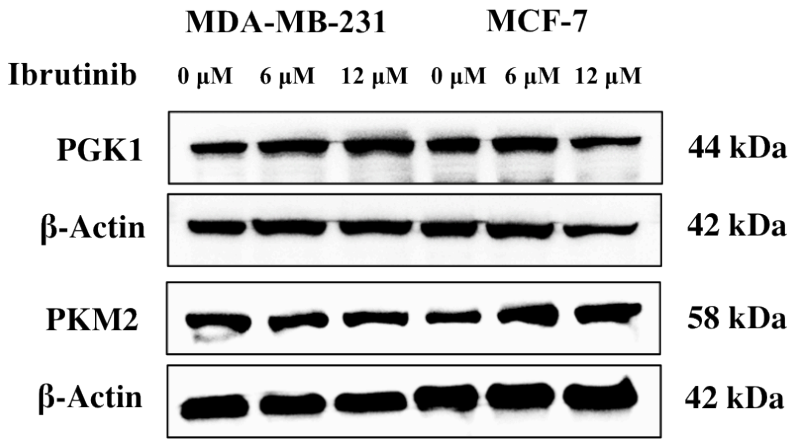

Figure 4-4: Ibrutinib represses PGK1 and PKM2 by PPARγ dependent pathway in MDA-MB-231 and MCF-7. The breast cancer cells were pre-treated with a potent PPARγ antagonist, GW9962 (10 µM) for 4 h at 37°C, followed by treatment with 6 µM and 12 µM of Ibrutinib for 48 h at 37°C. Representative western blot hybridization signals for PGK1 and PKM2 is shown. GW9662 showed no effect of Ibrutinib on expression of PGK1 and PKM2, thereby suggesting that the activation of PPARγ is required for repression of these enzymes.

[A]

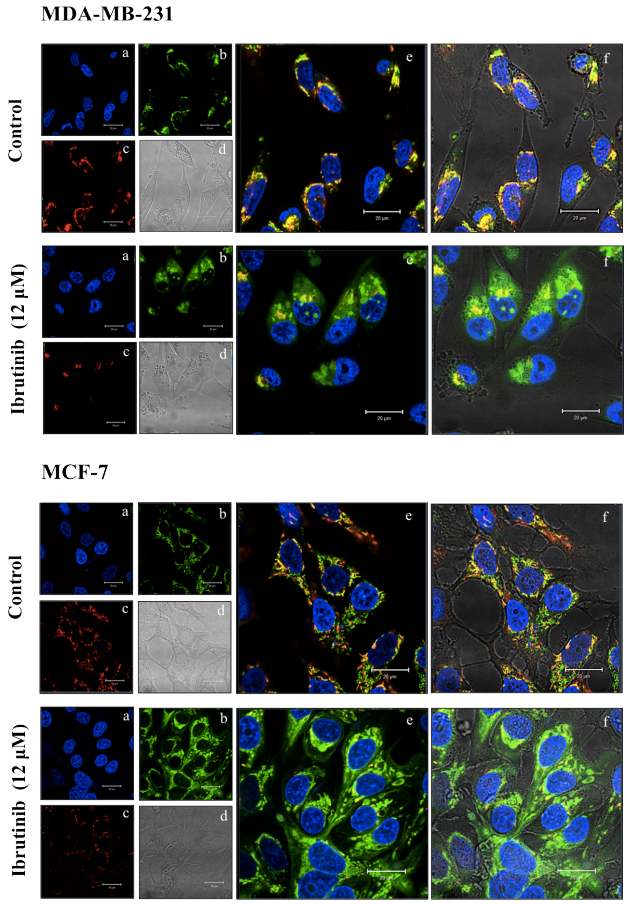

[B]

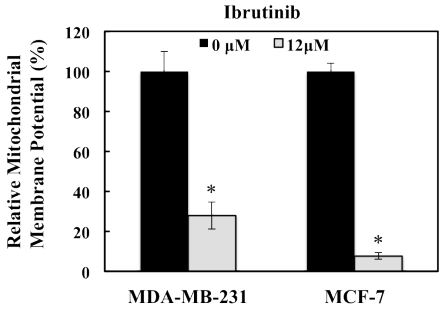

Figure 4-5: Ibrutinib induced loss in mitochondrial membrane potential (MMP) in human breast cancer cells (MDA-MB-231 and MCF-7). The breast cancer cells were treated with 6 µM and 12 µM of Ibrutinib for 48 h at 37°C and then stained by JC1. Ibrutinib treated cells showed loss of MMP comparable to that of the control cells [A- (a) Hoechst, (b) JC-1 529 nm (Green), (c) JC-1 590 nm (Red), (d) bright field, (e) fluorescence merge and (f) Overlay] and quantitation of florescence intensity is shown in [B]. Data are representative of three independent experiments done in triplicates and expressed as mean ± S.E.M. '*' ($p < 0.005$) represents statistical significant difference between control and Ibrutinib test groups.

[A]

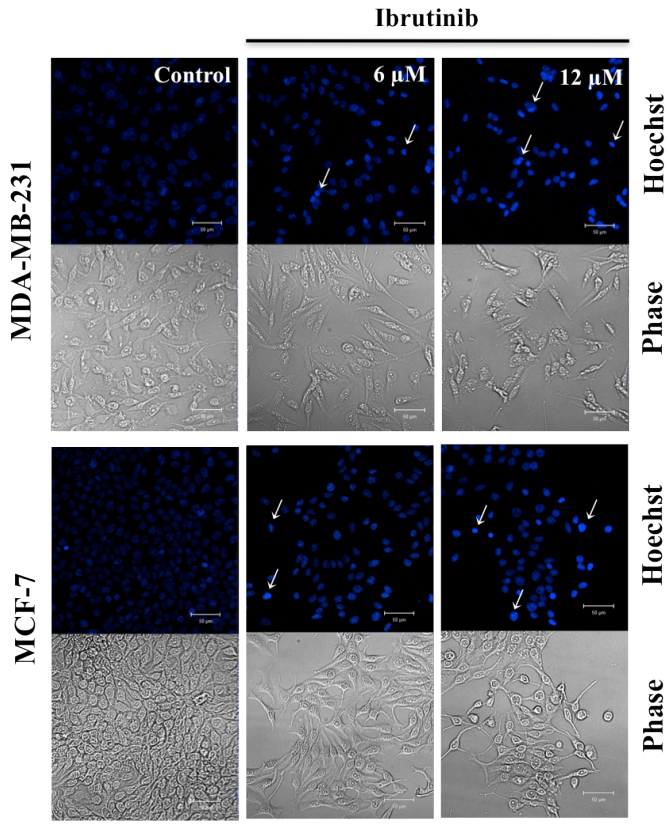

[B]

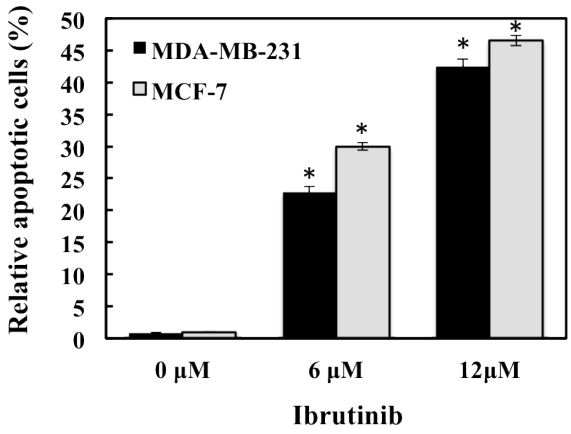

Figure 4-6: Ibrutinib induced nuclear condensation, a hallmark in apoptosis in MDA-MB-231 and MCF-7. Cells were treated with 6 µM and 12 µM of Ibrutinib for 48 h at 37°C were morphologically examined for nuclear condensation. Ibrutinib treated cells showed marked cell nuclear shrinkage, fragmentation and budding [A] and quantitation of relative number of apoptotic cells (%) is shown in [B]. Micrographs and quantitative data are representative mean ± S.E.M. '*' ($p < 0.005$) represents statistical significant difference between control and Ibrutinib test groups.

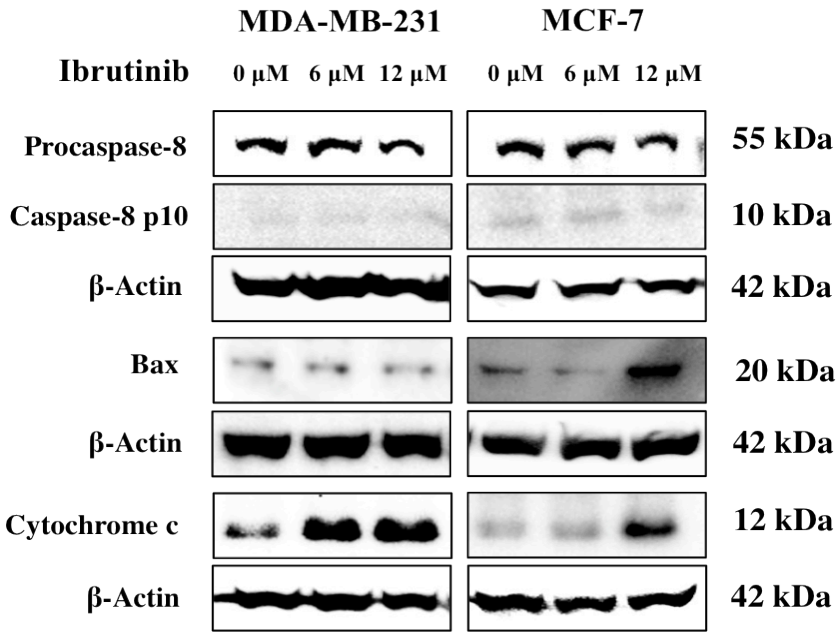

Figure 4-7: Ibrutinib induces caspase dependent apoptosis in the human breast cancer cell lines, MDA-MB-231 and MCF-7.

CHAPTER 5

5.1 CONCLUSION

The purpose of the present study was to identify novel transcriptional of nuclear hormone receptor - peroxisome proliferator activated receptor gamma (PPARγ) involved in breast cancer pathophysiology and functionally validate the identified PPARγ novel targets by its natural ligand 15-Deoxy-Δ12, 14-prostaglandin J (15d-PGJ2) and PPARγ novel ligand/ activator (HHQ and Ibrutinib).

Chapter 1 focuses on the background of the research. A brief introduction to breast cancer burden in the world, current therapies for breast (radiation therapy, chemotherapy, endocrine therapy and surgery), reasons for need of alternate breast cancer therapy such as adverse effects of chemotherapy and radiation therapy, available drugs for breast cancer and the details of resistance acquired by breast cancer is discussed. Furthermore, role of PPARγ in tumorigenesis, its mechanism of action, known PPARγ ligands and its transcriptional targets are also discussed in detail.

In chapter 2, I computationally identified PPARγ binding motifs, PPRE and PACMs in the whole human genome by PPRE search tool. A total of 217 genes were identified with PPRE and PACM sites involved in breast cancer pathphysiology. As complex global network of protein interactions dictates cellular behavior, therefore 217 putative PPARγ targeted breast cancer genes were mapped to the BioGRID to identify the their interacting partners and these protein interaction network were visualized by Cytoscape. The average value of the node degree, betweenness and stress was 3.7, 6242.74, and 46561.29, respectively. BRCA1 scored the highest for all the three centrality parameters Furthermore, the putative targets were mapped on to PANTHER database, to classify genes according to gene ontology classes: molecular function, biological process and cellular component. The analysis revealed that cell cycle (52), cell–cell signaling (30), and signal transduction (28) were the most common GO categories representing biological processes. A total of 280 classifications were identified under the molecular function with transcription factor activity, protein kinase activity, and transmembrane protein kinase activity in the top three. Further functional disease ontology was performed to find the enrichment of predicted PPARγ breast cancer target gene set in various disease profiles. All the genes were found to be associated with diseases. The

disease gene network showed predominant role of PPARγ in cancer in general (18.5%), followed by breast cancer (10.1%), and prostate cancer (8.9%). Cancer and SERPEINE had the highest centrality pararaeters in protein–protein interaction network disease and gene network. Also based on the protein and protein interaction network of 217 PPARγ predicted gene targets, glycolytic enzymes PGK1 and PKM2 were chosen for the functional validation in human adenocarcinomas, MDA-MB-231 and MCF-7. PGK1 and PKM2, PPARγ regulation were functionally validated by PPARγ natural ligand, 15d-PGJ2. It was observed that PPARγ activation by 15d-PGJ2 led to significant down regulation of glycolytic enzymes-PGK1 and PKM2. Since these glycolytic enzymes are involved in ATP synthesis, their down regulation resulted in decrease in level of cytoplasmic and mitochondrial ATP. It was also observed that PPARγ activation also induced caspase dependent apoptosis, which were evident by activation of caspase-8 and loss of mitochondrial membrane potential in MDA-MB-231 and MCF-7. Based upon this work I conclude that the glycolytic enzymes, PGK1 and PKM2 are potential therapeutic transcriptional targets of PPARγ involved in breast cancer pathophysiology.

In chapter 3, I identified HHQ as a novel ligand for PPARγ. I confrmed by docking procedures that HHQ docks to the PPARγ ligand binding domain and compared the docking parameters (ligand binding propertis) with the standard PPARγ ligand rosiglitazone. The rerank scores and the hydrogen bond energy values for the Rosi- glitazone and HHQ were found to be -122.433, -33.3562 and 5.487 kcal/mol, -9.460 kcal/mol respectively. In addition Rosiglitazone formed 3 hydrogen bonds (Gln286, His449, Ser289) and HHQ forms 5 hydrogen bonds (Gln286, His449, Tyr473, Ser289, His323) with ligand binding domain of PPARγ. Additional hydrogen bond between HHQ and ligand binding domain of PPARγ indicates increased specificity of interaction, which is a fundamental aspect of molecular recognition. Once the docking was confirmed, HHQ then was functionally validated with identified PPARγ transcriptional targets, PGK1 and PKM2 in human breast adenocarcinoma, MDA-MB-231 and MCF-7. It was found that HHQ induced activation of PPARγ down regulated PGK1 and PKM2 expressions significantly. Furthermore HHQ also induced caspase dependent apoptosis, which were quite evident with activation of caspase-8, increased bax levels, increase in ROS level and loss of mitochondrial membrane potential. Based upon this work I conclude that coffee component HHQ is a potential PPARγ ligand and may have potential

implication in breast cancer therapeutics.

In chapter 4, I identified Ibrutinib (formerly PCI-32765), highly potent bruton's tyrosine kinase (BTK) pathway inhibitor, as an activator of PPARγ and its anti-cancer effect on human breast adenocarcinoma, MDA-MB-231 and MCF-7. Dose dependent relation was observed between cytotoxicity and Ibrutinib dose. In addition the cytotoxic effect was more on estrogen positive MCF-7. Furthermore, the effect of Ibrutinib on glycolytic transcriptional targets of PPARγ was also investigated. I observed that the expression levels of PGK1 and PKM2 were significantly down regulated in both the breast cancer cells, where as on pretreating with PPARγ antagonist GW9962 no significant repression was observed, suggesting the down regulation of glycolytic enzymes, PGK1 and PKM2 through PPARγ dependent pathway by Ibrutinib. Since both enzymes, PGK1 and PKM2 are involved in production of energy rich molecule, ATP henceforth; I next investigated the effect of down regulation of glycolytic enzymes, PGK1 and PKM2 by Ibrutinib on ATP levels. The total ATP levels were significantly reduced in MDA-MB-231 and MCF-7 cell lines on treatment with Ibrutinib in concentration dependent manner. Down regulation of PGK1 and PKM2 and decrease in ATP level corroborated with viability assays and apoptotic assay, suggesting that down regulating these enzymes starved the cells for ATP ultimately leading to cell death. Further, I investigated the mechanism of cell death induced by Ibrutinib in MDA-MB-231 and MCF-7. Significant loss of mitochondrial membrane potential, activation of caspase-8, proapototic protein bax and cytochrome c was observed in Ibrutinib treated cells, suggesting caspase-dependent apoptosis induced by Ibrutinib in MDA-MB-231 and MCF-7. Together, these findings suggests that Ibrutinib induces mitochondrial dysfunctioning by upregulated bax expression, caspase-dependent apoptosis by activated caspase-8 and bax induced cytochrome c release, ultimately leading to breast cancer cell death by induction of apoptosis.

My results have established previously unknown novel crosslink between PPARγ, glycolysis, HHQ, Ibrutinib and breast cancer thereby adding a new dimension to therapeutic potential of PPARγ ligands/activators. Although the exact mechanism remains unclear and further studies are still needed to clarify the potential role and molecular basis of action of PPARγ in breast carcinogenesis, my investigation open a new direction for development of novel therapeutic method by

targeting PGK1 and PKM2 and use of PPARγ ligands/activators in breast cancer therapy.

5.2 SUMMARY

With increase in complications in treatment of breast cancer, currently, target therapies involving modulation of transcriptional targets are become quite popular to overcome the adverse effects of cancer therapy and drug resistance. Transcriptional factors control gene expression patterns resulting in tumor formation and progression as well as metastasis thereby playing critical roles in tumorigenesis. These can be used as molecular therapeutic tools in cancer development and progression to regulate transcriptional levels of genes associated with disease, verify gene function and to validate target genes for drug design.

This research was completely based on the molecularly targeted cancer therapeutics. I examine the efforts to specifically target the transcription factors for therapeutical interference in cancer development and progression *in vitro.*

Below are the summarized results of the research.

1. I established previously unknown novel crosslink between PPARγ and glycolysis via PGK1 and PKM2.
2. I found out that by targeting PGK1 and PKM2, apoptosis is induced in human breast adenocarcinomas.
3. I also identified novel PPARγ ligands-coffee component HHQ.

This report also established the unknown link between coffee and breast cancer.

4. Furthermore I also identified another PPARγ modultaor, Ibrutinib and its cytotoxic effects on human breast adenocarcinomas by down regulating PPARγ targets and induction of apoptosis.

These findings add a new dimension to therapeutic potential of PPARγ ligands/activators and increase the understanding of molecular mechanisms by which PPARγ regulates disease targets specifically in breast cancer.

5.3 FUTURE DIRECTIONS

Cancer therapy involving targeting specific proteins such as transcriptional factors, which may have important role in tumorigenesis, could overcome the limitations of other cancer therapies such as surgery, chemotherapy, radiation therapy and endocrine therapy. One such popular transcriptional factor is PPARγ. It is prudent to note that PPARγ is overexpressed in many cancers including breast cancer indicating its importance in tumor development and progression. Taking advantage of its overexpression and prudent role in expression of many genes required for cell survival these transcriptional targets could serve as a potential molecular therapeutics targets in cancer.

Epidemiologic evidence suggests that people with diabetes are at significantly higher risk for many forms of cancer including breast cancer [219-221]. Obesity has also been reported as a risk factor for breast cancer and type- 2 diabetes [222]. The possible association could be due to link between diabetes and cancer in metabolic syndrome. PPARγ agonist are commonly used to treat patients with type 2 diabetes who share metabolic abnormalities, act as insulin sensitizers and mediate in vitro and in vivo pleiotropic anticancer effects, suggesting PPARγ as the possible link between these diseases [223].

Computational analyses by us and generation of gene-disease network suggests that PPARγ is implicated in pathology of several diseases including cancer, diabetes, and obesity (Figure 5-1) [224]. These results are in accordance with several isolated reports on their involvement in individual disorders. These computational findings may open new doors to using PPARγ as a therapeutic target for multiple diseases.

In addition with extension to our previous findings it would be interesting to see the mechanism of cell death and anti-metastatic effect of HHQ and Ibrutinib in *in vivo* and *in vivo* cancer models. These finding may open a new direction for development of PPARγ ligands-HHQ and Ibrutinib in breast cancer therapeutics.

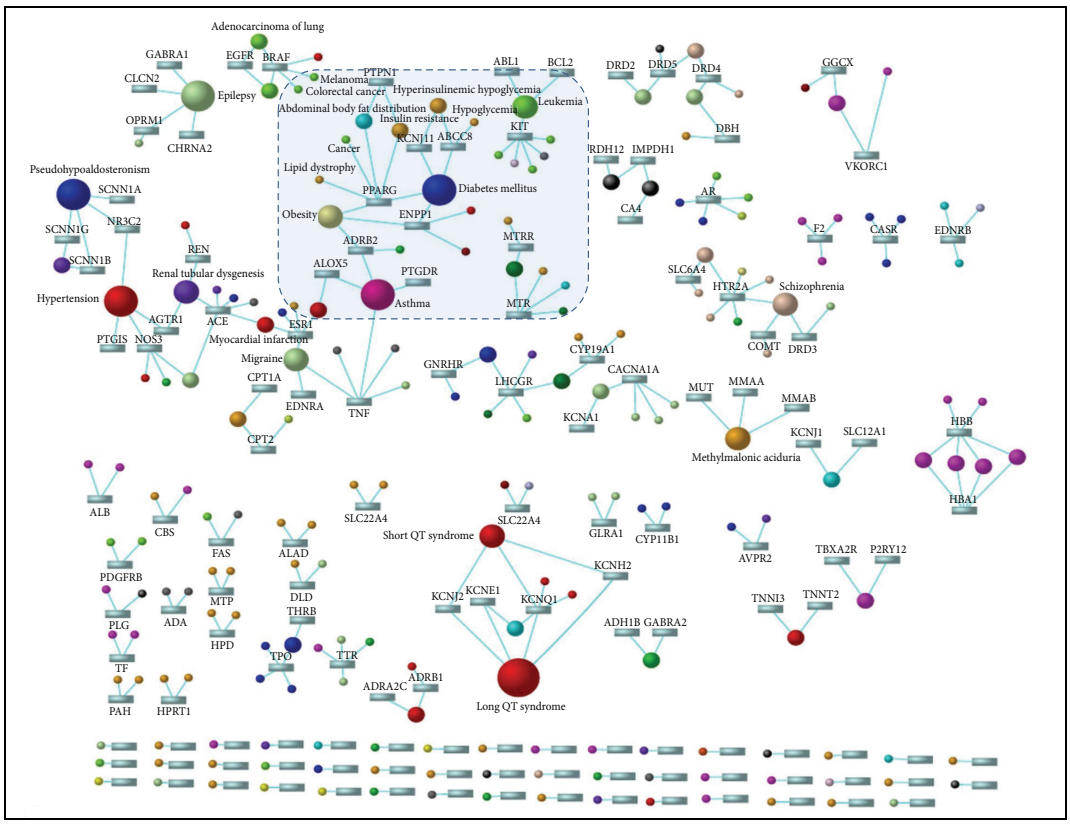

Figure 5-1: PPAR gamma disease gene network. Rectangles represent genes and circles represent diseases. Only genes involved in more than one disease are shown.

REFERENCES

[1] **Global Health Estimates**, WHO, 2013.

[2] Margolese R. G., Fisher B., Hortobagyi G. N. and Bloomer W. D., (2000). "**Neoplasms of the Breast".** *Holland-Frei Cancer Medicine*, 5th edition, ch 118.

[3] Lacey J. V., Kreimer A. R., Buys S. S., Marcus P.M., Chang S.C., Leitzmann M.F, Hoover R.N., Prorok P.C., Berg C.D. and Hartge P., (2009). "**Breast cancer epidemiology according to recognized breast cancer risk factors in the Prostate, Lung, Colorectal and Ovarian (PLCO) Cancer Screening Trial Cohort".** *BMC Cancer,* 9: 84.

[4] Early Breast Cancer Trialists' Collaborative Group. (1992). **"Systemic treatment of early breast cancer by hormonal, cytotoxic, or immune therapy, 133 randomised trials involving 31,000 recurrences and 24,000 deaths among 75,000 women".** *Lancet*, 339: 71-85.

[5] Osborne C. K., (1998). **"Tamoxifen in the treatment of breast cancer"**. *N. Engl. J. Med.*, 339: 1609-1618.

[6] Early Breast Cancer Trialists' Collaborative Group, (1992). "**Systemic treatment of early breast cancer by hormonal, cytotoxic, or immune therapy".** *Lancet*, 339: 71-85.

[7] Osborne C. K. and Fuqua S. A., (1994). "**Mechanisms of tamoxifen resistance"**. *Breast Cancer Res. Treat.*, 32: 49-55.

[8] Osborne C. K., Jarman M., McCague R., Coronado E. B., Hilsenbeck S. G. and Wakeling A. E., (1994). **"The importance of tamoxifen metabolism in tamoxifen-stimulated breast tumor growth"**. *Cancer Chemother. Pharmacol.*, 34: 89-95.

[9] Osborne C. K., Coronado E., Allred D. C., Wiebe V. and DeGregorio M, (1991). **"Acquired tamoxifen resistance: correlation with reduced breast tumor levels of tamoxifen and isomerization of trans-4-hydroxytamoxifen".** *J. Natl. Cancer Inst. (Bethesda)*, 83: 1477-1482.

[10] Nicholson R. I., Gee J. M. W., Barrow D., Pamment J. S., Knowlden J. M. and McClelland R., (1991). **"Endocrine resistance in breast cancer can involve a switch towards EGFR signaling pathways and a gain of sensitivity to an EGFR-selective tyrosine kinase inhibitor".** *AACR-NCI-EORTC International Conference on Molecular Targets and Cancer Therapeutics,* ZD1839.

[11] Kato S., Endoh H., Masuhiro Y., Kitamoto T., Uchiyama S., Sasaki H., Masushige S., Gotoh Y., Nishida E., Kawashima H., Metzger D. and Pierre Chambon P., (1995). **"Activation of the estrogen receptor through phosphorylation by mitogen-activated protein kinase".** *Science*, 270: 1491-1494.

[12] Lee H., Jiang F., Wang Q., Nicosia S. V., Yang J., Su B. and Bai W., (2000). **"MEKK1 activation of human estrogen receptor alpha and stimulation of**

the agonistic activity of 4-hydroxytamoxifen in endometrial and ovarian cancer cells". *Mol. Endocrinol.*, 14: 1882-1896.

[13] Campbell R. A., Bhat-Nakshatri P., Patel N. M., Constantinidou D., Ali S. and Nakshatri H., (2001). **"Phosphatidylinositol 3-kinase/AKT-mediated activation of estrogen receptor alpha: a new model for anti-estrogen resistance"**. *J. Biol. Chem.*, 276: 9817-9824.

[14] Schiff R., Reddy P., Ahotupa M., Coronado-Heinsohn E., Grim M., Hilsenbeck S. G., Lawrence R., Deneke S., Herrera R., Chamness G. C., Fuqua S. A., Brown P. H. and Osborne C. K., (2000). **"Oxidative stress and AP-1 activity in tamoxifen-resistant breast tumors in vivo".** *J. Natl. Cancer Inst. (Bethesda)*, 92: 1926-1934.

[15] Shou J., Weigel N. L., Osborne C. K. and Schiff R., (2000). **"Onset of endocrine resistance in breast cancer is associated with increased active p38 MAPK".** *24th San Antonio Breast Cancer Symposium*, San Antonio, 254.

[16] Benz C. C., Scott G. K., Sarup J. C., Johnson R. M., Tripathy D., Coronado E., Shepard H. M. and Osborne C. K., (1993). **"Estrogen-dependent, tamoxifen-resistant tumorigenic growth of MCF-7 cells transfected with HER2/neu".** *Breast Cancer Res. Treat.*, 24: 85-95.

[17] Piccart M., Lohrisch C., Di Leo A. and Larsimont D., (2000). **"The predictive value of HER2 in breast cancer".** *Oncology*, 61*:* 73-82.

[18] Font de Mora J. and Brown M., (2000). **"AIB1 is a conduit for kinase-mediated growth factor signaling to the estrogen receptor".** *Mol. Cell. Biol.*, 20: 5041-5047.

[19] Issemann I. and Green S., (1990). **"Activation of a member of the steroid hormone receptor superfamily by peroxisome proliferators".** *Nature,* 347: 645–650.

[20] Reddy J. K. and Mannaerts GP., (1994). **"Peroxisomal lipid metabolism"**. *Annu Rev Nutr.,* 14: 343–370.

[21] Feige J. N., Gelman L., Michalik L., Desvergne B. and Wahli W., (2006). **"From molecular action to physiological outputs: peroxisome proliferator-activated receptors are nuclear receptors at the crossroads of key cellular functions".** *Prog Lipid Res*, 45(2): 120-159.

[22] Michalik L., Auwerx J., Berger J. P., Chatterjee V. K., Glass C. K., Gonzalez F. J., Grimaldi P. A., Kadowaki T., Lazar M. A., O'Rahilly S., Palmer C. N. A., Jorge Plutzky J., Reddy J. K., Spiegelman B. M., Staels B. and Wahli W., (2006). **"International Union of Pharmacology. LXI. Peroxisome proliferator-activated receptors".** *Pharmacol Rev.,* 58(4): 726-741.

[23] Zhu Y, Qi C., Korenberg J. R., Chen X. N., Noya D., Rao M. S. and Reddy J. K., (1995). **"Structural organization of mouse peroxisome proliferator-activated receptor gamma (mPPAR gamma) gene: alternative promoter use and different splicing yield two mPPAR gamma isoforms",** *Proc Natl Acad Sci USA,* 92(17): 7921-7925.

[24] Chandra V., Huang P., Hamuro Y., Raghuram S., Wang Y., Burris T. P., and Rastinejad F., (2008). **"Structure of the intact PPAR-gamma-RXR- nuclear receptor complex on DNA,"** *Nature*, 456: 350–356.

[25] Venkatachalam G., Kumar A. P., Sakharkar K. R., Thangavel S., Clement M. V. and Sakharkar M. K., (2011). **"PPARγ disease gene network and identification of therapeutic targets for prostate cancer,"** *J Drug Target*, 19: 781–796.

[26] Gervois P., Chopin-Delanno S., Fadel A., Dubois G., Kosykh V., Fruchart J., Najib J. and Laudetand V., (1999). **"Bart staels fibrates increase human REV-ERBα expression in liver via a novel peroxisome proliferator-activated receptor response element".** *Mol Endocrin.,* 13: 400.

[27] Lemay D. G. and Hwang D. H., (2006). **"Genome-wide identification of peroxisome proliferator response elements using integrated computational genomics".** *J Lipid Res*, 47: 1583–1587.

[28] Lapillonne H., Konopleva M., Tsao T., Gold D., McQueen T., Sutherland R. L., Madden T. and Andreeff M., (2003). **"Activation of peroxisome proliferator-activated receptor gamma by a novel synthetic triterpenoid 2-cyano-3, 12-dioxooleana-1, 9-dien-28-oic acid induces growth arrest and apoptosis in breast cancer cells".** *Cancer Res*., 63(18): 5926-5939.

[29] Huang J. T., Welch J. S., Ricote M., Christoph J., Willson T. M., Kelly C., Joseph W. L., Colin D. F., Douglas C. and Glass C.K., (1999). **"Interleukin-4-dependent production of PPAR-γ ligands in macrophages by 12/15-lipoxygenase".** *Nature*, 400(6742): 378–382.

[30] Nagy L., Tontonoz P., Alvarez J. G. A., Chen H. and Evans R. M., (1998). **"Oxidized LDL regulates macrophage gene expression through ligand activation of PPARγ",** *Cell*, 93(2): 229–240.

[31] Berger J., Bailey P., Biswas C., Cullinan A., Doebber T. W., Hayes N.S., Saperstein R., Smith G. R. and Leibowitz., (1996). **"Thiazolidinediones produce a conformational change in peroxisomal proliferator-activated receptor-γ: binding and activation correlate with anti-diabetic actions in db/db mice".** *Endocrinology*, 137(10): 4189–4195.

[32] Lehmann J. M., Moore L. B., Smith-Oliver T. A., Wilkison W. O., Willson T. M. and Kliewer S. A., (1995). **"An anti-diabetic thiazolidinedione is a high affinity ligand for peroxisome proliferator-activated receptor γ (PPARγ)".** *The Journal of Biological Chemistry*, 270(22): 12953–12956.

[33] Lambe K. G. and Tugwood J. D., (1996). **"A human peroxisome-proliferator-activated receptor-γ is activated by inducers of adipogenesis, including thiazalidinedione drugs,"** *European Journal of Biochemistry*, 239(1): 1–7.

[34] Unwin R. D., Craven R. A., Harnden P., Hanrahan S., Totty N., Margaret Knowles M., Eardley I., Selby P.J. and Banks R. E., (2003). **"Proteomic changes in renal cancer and co-ordinate demonstration of both the**

glycolytic and mitochondrial aspects of the Warburg effect". *Proteomics,* 3(8): 1620–1632.

[35] Mukhopadhyay S., Das S. K. and Mukherjee S., (2006). **"Expression of Mn-superoxide dismutase gene in nontumorigenic and tumorigenic human mammary epithelial cells".** *Journal of Biomedicine and Biotechnology*, 2004(4): 195–202.

[36] Bonofiglio D., Aquila S., Catalano S., Gabriele S., Belmonte M., Middea E., Qi H., Morelli C., Gentile M., Maggiolini M. and Andò S., (2006). **"Peroxisome proliferator-activated receptor-γ activates p53 gene promoter binding to the nuclear factor-κB sequence in human MCF7 breast cancer cells".** *Molecular Endocrinology*, 20(12): 3083–3092.

[37] M. Pignatelli, C. Cocca, A. Santos, and A. Perez-Castillo, (2003). **"Enhancement of BRCA1 gene expression by the peroxisome proliferator-activated receptor γ in the MCF-7 breast cancer cell line".** *Oncogene,* 22(35): 5446–5450.

[38] Lin M. S., Chen W. C., Bai X. and Wang Y. D., (2007). "**Activation of peroxisome proliferator-activated receptor gamma inhibits cell growth via apoptosis and arrest of the cell cycle in human colorectal cancer".** *J. Dig. Dis.*, 8: 82–88.

[39] Elstner E., Williamson E. A., Zang C., Fritz J., Heber D., Fenner M., Possinger K. and Koeffler H. P., (2002). **"Novel therapeutic approach: ligands for PPAR gamma and retinoid receptors induce apoptosis in bcl-2-positive human breast cancer cells".** *Breast Cancer Res. Treat*, 74: 155–165.

[40] Rubin G. L., Zhao Y., Kalus A. M. and Simpson E. R., (2000). **"Peroxisome proliferator-activated receptor gamma ligands inhibit estrogen biosynthesis in human breast adipose tissue: possible implications for breast cancer therapy".** *Cancer Res.*, 60: 1604–1608.

[41] Motomura W., Okumura T., Takahashi N., Obara T. and Kohgo Y., (2000). **"Activation of peroxisome proliferator-activated receptor γ by troglitazone inhibits cell growth through the increase of $p27^{Kip1}$ in human pancreatic carcinoma cells".** *Cancer Res*., 60: 5558–5564.

[42] Yu H. N., Lee Y. R., Noh E. M., Lee K. S., Kim J.S., Song E. K., Han M.K., Lee Y.C., Kwon K.B., Lee S. J., Youn H. J. and Jung S.H., (2008). **"Induction of G1 phase arrest and apoptosis in MDA-MB-231 breast cancer cells by troglitazone, a synthetic peroxisome proliferator-activated receptor γ (PPARγ) ligand".** *Cell Biology International*, 32(8): 906–912,

[43] Sakharkar M. K., Shashni B., Sharma K., Kaur S., Ranjekar P. and Sakharkar K. R., (2013). **"Therapeutic Implications of Targeting Energy Metabolism in Breast Cancer".** *PPAR Res.*, 2013(109285): 11.

[44] Putney L. K., Denker S. P. and Barber D. L., (2002). **"The changing face of the Na^+/H^+ exchanger, NHE1: structure, regulation, and cellular actions".** *Annual Review of Pharmacology and Toxicology,* 42: 527–552.

[45] Reshkin S. J., Bellizzi A., Caldeira S. Albarani V., Malanchi I., Poignee M., Alunni-Fabbroni M., Casavola V. and Tommasino M., (2000). **"Na^+/H^+ exchanger-dependent intracellular alkalinization is an early event in malignant transformation and plays an essential role in the development of subsequent transformation-associated phenotypes".** *The FASEB Journal*, 1414: 2185–2197.

[46] Grinstein S. and Dixon S. J., (1989). **"Ion transport, membrane potential, and cytoplasmic pH in lymphocytes: changes during activation".** *Physiological Reviews*, 69(2): 417–481.

[47] Bell S. M., Schreiner S. M., Schultheis P. J., Miller M. L., Evans R. L., Vorhees C. V., Shull G. E. and Scott W. J., (1999). **"Targeted disruption of the murine NHE1 locus induces ataxia, growth retardation, and seizures".** *American Journal of Physiology*, 276: 788–795.

[48] Pouyssegur J., Franchi A. and Pages G., (2001). **"pHi, aerobic glycolysis and vascular endothelial growth factor in tumour growth,"** Novartis Foundation Symposium, 240:186–196.

[49] Reshkin S. J., Bellizzi A., Caldeira S. Albarani V., Malanchi I., Poignee M., Alunni-Fabbroni M., Casavola V. and Tommasino M., (2000). **"Na^+/H^+ exchanger-dependent intracellular alkalinization is an early event in malignant transformation and plays an essential role in the development of subsequent transformation-associated phenotypes".** *The FASEB Journal*, 1414: 2185–2197.

[50] Akram S., Teong H. F. C., Fliegel L., Pervaiz S. and Clément M. V., (2006). **"Reactive oxygen species-mediated regulation of the Na^+-H^+ exchanger 1 gene expression connects intracellular redox status with cells' sensitivity to death triggers".** *Cell Death and Differentiation*, 13(4): 628–641.

[51] Pelicano H., Carney D. and Huang P., (2004). **"ROS stress in cancer cells and therapeutic implications".** *Drug Resistance Updates*, 7(2): 97–110.

[52] Storey K. B., (1996). **"Oxidative stress: animal adaptations in nature".** *Brazilian Journal of Medical and Biological Research*, 29(12): 715–1733.

[53] Miranda A., Janssen L., Bosman Coen B., Duijn W. V., Marjan M., Ruit O., Kubben F. J. G. M., Griffioen G., Lamers C. B. H. W., Han J., Krieken J. M. V., Velde C. J. H. and Verspaget H. W., (2000). **"Superoxide dismutases in gastric and esophageal cancer and the prognostic impact in gastric cancer".** *Clinical Cancer Research*, 6(8): 3183–3192.

[54] Punnonen K., Ahotupa M., Asaishi K., Hyöty M., Kudo R. and Punnone R., (1994). **"Antioxidant enzyme activities and oxidative stress in human breast cancer".** *Journal of Cancer Research and Clinical Oncology*, 120(6): 374–377.

[55] Klement R. J. and Kämmerer U., (2011). **"Is there a role for carbohydrate restriction in the treatment and prevention of cancer?"** *Nutrition & Metabolism*, 8: 75.

[56] Bi X., Lin Q., Foo T. W., Joshi S., You T., Shen H. M., Ong C. N., Cheah P. Y., Eu K. W., Hew C. L., (2006). **"Proteomic analysis of colorectal cancer**

reveals alterations in metabolic pathways: mechanism of tumorigenesis". *Molecular & Cellular Proteomics*, 5: 1119–1130.

[57] Unwin R. D., Craven R. A., Harnden P., Hanrahan S., Totty N., Knowles M., Eardley I., Selby P. J. and Banks R. E., (2003). **"Proteomic changes in renal cancer and co-ordinate demonstration of both the glycolytic and mitochondrial aspects of the Warburg effect".** *Proteomics*, 3(8): 1620–1632.

[58] Amon L. M., Pitteri S. J., Li C. I., McIntosh M., Ladd J. J., Disis M., Porter P., Wong C. H., Zhang Q., Lampe P., Prentice R. L. and Hanash S. M., (2012). **"Concordant release of glycolysis proteins into the plasma preceding a diagnosis of ER^+ breast cancer".** *Cancer Research*, 72(8): 1935–1942.

[59] Ward P. S. and Thompson C. B., (2012). **"Metabolic reprogramming: a cancer hallmark even Warburg did not anticipate".** *Cancer Cell*, 21(3): 297–308.

[60] Mentis A. F. A. and Kararizou E., (2010). **"Metabolism and cancer: an up-to-date review of a mutual connection".** *Asian Pacific Journal of Cancer Prevention*, 11(6): 1437–1444.

[61] Gatenby R. A., Gawlinski E. T., Gmitro A. F., Kaylor B. and Gillies R. J., (2006). **"Acid-mediated tumor invasion: a multidisciplinary study".** *Cancer Research*, 66(10): 5216–5223.

[62] Bittencourt Jr. P. I. H., Peres C. M., Yano M. M., Hirata M. H. and Curi R., (1993). **"Pyruvate is a lipid precursor for rat lymphocytes in culture: evidence for a lipid exporting capacity".** *Biochemistry and Molecular Biology International*, 30(4): 631–641.

[63] Kondoh H., Lleonart M. E., Bernard D., and Gil J., (2007). **"Protection from oxidative stress by enhanced glycolysis; a possible mechanism of cellular immortalization".** *Histology and Histopathology*, 22(1): 85–90.

[64] Biamonti G. and Caceres J. F., (2009). **"Cellular stress and RNA splicing".** *Trends in Biochemical Sciences*, 34(3): 46–153.

[65] Serkova N. and Boros L. G., (2005). **"Detection of resistance to imatinib by metabolic profiling: clinical and drug development implications".** *American Journal of Pharmaco. Genomics*, 5(5): 293–302.

[66] Hsu P. and Sabatini D., (2008). **"Cancer cell metabolism: Warburg and beyond".** *Cell*, 134(5): 703–707.

[67] Lunt S. Y. and Vander Heiden M. G., (2011). **"Aerobic glycolysis: meeting the metabolic requirements of cell proliferation".** *Annual Review of Cell and Developmental Biology*, 27: 441–464.

[68] Smith A., and Muscat G., (2006). **"Orphan nuclear receptors: therapeutic opportunities in skeletal muscle".** *Am. J. Physiol. Cell Physiol.*, 291: 203–217.

[69] John S., Weiss J. N. and Ribalet B., (2011). **"Subcellular localization of hexokinases I and II directs the metabolic fate of glucose".** *PLoS ONE*, 6(3): e17674.

[70] Mathupala S. P., Ko Y. H. and Pedersen P. L., (2009). **"Hexokinase-2 bound to mitochondria: cancer's stygian link to the "Warburg effect" and a**

pivotal target for effective therapy". *Seminars in Cancer Biology*, 19: 17–24,

[71] Mathupala S. P., Ko Y. H. and Pedersen P. L., (2006). **"Hexokinase II: cancer's double-edged sword acting as both facilitator and gatekeeper of malignancy when bound to mitochondria".** *Oncogene*, 25(34): 4777–4786.

[72] Mendoza E. E., Pocceschi M. G., Kong X., Leeper D. B., Caro J., Limesand K. H. and Burd R., (2012). **"Control of glycolytic flux by AMP-activated protein kinase in tumor cells adapted to low pH".** *Translational Oncology*, 5(3): 208–216.

[73] Ferguson E. C. and Rathmell J. C., (2008). **"New roles for pyruvate kinase M2: working out the Warburg effect".** *Trends in Biochemical Sciences*, 33(8): 359–362.

[74] David C. J., Chen M., Assanah M., Canoll P. and Manley J. L., (2010). **"HnRNP proteins controlled by c-Myc deregulate pyruvate kinase mRNA splicing in cancer".** *Nature*, 463(7279): 364–368.

[75] Issemann I. and Green S., (1990). **"Activation of a member of the steroid hormone receptor superfamily by peroxisome proliferators".** *Nature*, 347: 645–650.

[76] Dreyer C., Krey G., Keller H., Givel F., Helftenbein G. and Wahli W., (1992). **"Control of the peroxisomal β-oxidation pathway by a novel family of nuclear hormone receptors".** *Cell,* 68: 879–887.

[77] Kliewer S. A., Forman B. M., Blumberg B., Ong E. S., Borgmeyer U., Mangelsdorf D. J., Umesono K. and Evans R. M., (1994). **"Differential expression and activation of a family of murine peroxisome proliferator-activated receptors".** *Proc. Natl. Acad. Sci. USA*, 91: 7355–7359.

[78] Rosen E. D., Walkey C. J., Puigserver P. and Spiegelman B. M., (2000). **"Transcriptional regulation of adipogenesis".** *Genes Dev*., 14: 1293–1307.

[79] Zhu Y., Alvares K., Huang Q., Rao M. S. and Reddy J. K., (1993). **"Cloning of a new member of the peroxisome proliferator-activated receptor gene family from mouse liver".** *J. Biol. Chem.*, 268: 26817–26820.

[80] Reddy J. K., Mannaerts G. P., (1994). "**Peroxisomal lipid metabolism"**. *Annu. Rev. Nutr.,* 14: 343–370.

[81] Smith A. and Muscat G., (2006). **"Orphan nuclear receptors: therapeutic opportunities in skeletal muscle".** *Am. J. Physiol. Cell Physiol.*, 291: C203–C217.

[82] Houseknecht K. L., Cole B. M. and Steele P. J., (2002). **"PPAR and its ligands: a review".** *Domest. Anim. Endocrinol*, 22: 1–23.

[83] Lin M. S., Chen W. C., Bai X. and Wang Y. D., (2007). **"Activation of peroxisome proliferator-activated receptor gamma inhibits cell growth via apoptosis and arrest of the cell cycle in human colorectal cancer".** *J. Dig. Dis.,* 8: 82-88.

[84] Grommes C., Landreth G. E. and Heneka M. T., (2002). **"Antineoplastic effects of Peroxisome proliferator-activated receptor gamma agonists".**

Lancer Oncol., 5: 419-29.

[85] Rubin G., Zhao Y., Kalus A. and Simpson E., (2000). **"Peroxisome proliferator-activated receptor gamma ligands estrogen biosynthesis in human breast adipose tissue; possible implication for the breast cancer therapy".** *Cancer Res.,* 60: 1604-8.

[86] Chattopadhyay N., Singh D., Heese O., Godbole M. M., Sinohara T., Black P. M., and Brown E. M., (2000). **"Expression of peroxisome proliferator-activated receptors in human astrocytic cells: PPAR gamma agonists as inducers of apoptosis".** *J. Neurosci. Res.,* 61: 67-74.

[87] Elstner E., Williamson E. A., Zang C., Fritz J., Heber D., Fenner M., Possinger K. and Koeffler H. P., (2002). **"Novel therapeutic approach: ligands for PPARgamma and retinoid receptors induce apoptosis in bcl-2-positive human breast cancer cells".** *Breast Cancer Res. Treat*, 74: 155-165.

[88] Lapillonne H., Konopleva M., Tsao T., Gold D., McQueen T., Sutherland R. L., Madden T. and Andreeff M., (2003). **"Activation of peroxisome proliferator-activated receptor γ by a novel synthetic triterpenoid 2-cyano-3, 12-dioxooleana-1, 9 dien-28-oic acid induces growth arrest and apoptosis in breast cancer cells,"** *Cancer Res.,* 63: 5926-39.

[89] Venkatachalam G., Kumar A. P., Sakharkar K. R., Thangavel S., Clement M.V. and Sakharkar M. K., (2011). **"PPARγ disease gene network and identification of therapeutic targets for prostate cancer".** *J. Drug Target*, 19: 781–796.

[90] Carter J. C. and Frank Church C., (2011). **"Peroxisome Proliferator-Activated Receptor-γ Ligands Alter Breast Cancer Cell Motility through Modulation of the Plasminogen Activator System".** *Journal of Oncology*, 2011: 594258.

[91] Warburg O., (1956). **"On respiratory impairment in cancer cells".** *Science*, 124: 269–270.

[92] Altenberg B. and Greulich K. O., (2004). **"Genes of glycolysis are ubiquitously overexpressed in 24 cancer classes".** *Genomics*, 84: 1014-20.

[93] Chandra V., Huang P., Hamuro Y., Raghuram S., Wang Y., Burris T. and Rastinejad F., (2008). **"Structure of the intact PPAR-c–RXR-a nuclear receptor complex on DNA".** *Nature*, 256: 350-357.

[94] Gervois P., Chopin-Delanno S., Fadel A., Dubois G., Kosykh V., Fruchart J., Najïb J., and Laudetand V., (1999). **"Bart Staels Fibrates Increase Human REV-ERBα Expression in Liver via a Novel Peroxisome Proliferator-Activated Receptor Response Element".** *Molecular Endocrinology*, 13: 400.

[95] Mukhopadhyay S., Das S. K. and Mukherjee S., (2004). **"Expression of Mn-Superoxide Dismutase Gene in Nontumorigenic and Tumorigenic Human Mammary Epithelial Cells".** *J. Biomed. Biotechnol.,* 4: 195-202.

[96] Tennant D. A., Duran R. V. and Gottlieb E., (2011). **"Targeting metabolic transformation for cancer therapy".** *Nat. Rev. Cancer*, 10: 267–277.

[97] Dreszer T. R., Karolchik D., Zweig A. S., Hinrichs A. S., Raney B. J., Kuhn R. M., Meyer L. R., Wong M., Sloan C. A., Rosenbloom K. R., Roe G., Rhead B.,

Pohl., Malladi V. S., Li C. H., Learned K., Kirkup V., Hsu F., Harte R. A., Guruvadoo L., Goldman M., Giardine B. M., Fujita P. A., Diekhans M., Cline M. S., Clawson H., Barber G. P., Haussler D. and James Kent W., (2012). **"The UCSC Genome Browser database: extensions and updates 2011".** *Nucleic Acids Res*., 40: D918-23.

[98] Lemay DG and Hwang DH., (2006). **"Genome-wide identification of peroxisome proliferator response elements using integrated computational genomics".** *J. Lipid Res.,* 47: 1583-7.

[99] Jiao X., Sherman B. T., Huang da W., Stephens R., Baseler M. W., Lane H. C., Lempicki R. A., (2012). **"DAVID-WS: a stateful web service to facilitate gene/protein list analysis".** *Bioinformatics*, 28: 1805-6.

[100] Stelzer G., Dalah I., Stein T. I., Satanower Y., Rosen N., Nativ N., Oz-Levi D., Olender T.., Belinky F, Bahir I., Krug H., Perco P., Mayer B., Kolker E., Safran M. and Lancet D., (2011). **"In-silico human genomics with Gene Cards".** *Hum. Genomics*, 5: 709-17.

[101] Baasiri R. A., Glasser S. R., Steffen D. L. and Wheeler D. A., (1999). **"The breast cancer gene database: a collaborative information resource".** *Oncogene*, 18: 7958-65.

[102] Stark C., Breitkreutz B. J., Chatr-Aryamontri A., Boucher L., Oughtred R., Livstone M. S., Nixon J., Van Auken K., Wang X., Shi X., Reguly T., Rust J. M., Winter A., Dolinski K. and Tyers M. (2011). **"The BioGRID Interaction Database: 2011 update".** *Nucleic Acids Res.,* 39: D698-704.

[103] Mi H., Dong Q., Muruganujan A., Gaudet P., Lewis S. and Thomas P. D., (2010). **"PANTHER version 7: improved phylogenetic trees, orthologs and collaboration with the Gene Ontology Consortium".** *Nucleic Acids Res.,* 38: D204-10.

[104] Du P., Feng G., Flatow J., Song J., Holko M., Kibbe W. A. and Lin S.M., (2009). "**From disease ontology to disease-ontology lite: statistical methods to adapt a general-purpose ontology for the test of gene-ontology associations".** *Bioinformatics*. 25: i63-8.

[105] Yeung N., Cline M. S., Kuchinsky A., Smoot M. E. and Bader G. D., (2008). **"Exploring biological networks with Cytoscape software".** *Curr. Protoc. Bioinformatics,* 8: 8.13.

[106] Gaci O., (2010). **"A topological description of hubs in amino acid interaction networks".** *Adv. Bioinform*, 257512 (No other details in PubMed).

[107] Scardoni G., Petterlini M. and Laudanna C., (2009). **"Analyzing biological network parameters with CentiScaPe".** *Bioinformatics,* 25: 2857–2859.

[108] Cossarizza A., Ceccarelli D. and Masini A., (1996). **"Functional heterogeneity of an isolated mitochondrial population revealed by cytofluorometric analysis at the single organelle level".** *Exp. Cell Res.,* 222: 84–94.

[109] Mathur A., Hong Y., Kemp B. K., Barrientos A. A. and Erusalimsky J. D., (2000). **"Evaluation of fluorescent dyes for the detection of mitochondrial**

membrane potential changes in cultured cardiomyocytes". *Cardiovasc Res.,* 46: 126–138.

[110] Reers M., Smith T. W., and Chen L. B., (1991). **"J-aggregate formation of a carbocyanine as a quantitative fluorescent indicator of membrane potential".** *Biochemistry*, 30: 4480–4486.

[111] Mazzoccoli G., Pazienza V., Panza A., Valvano M. R., Benegiamo G., Vinciguerra M., Andriulli A. and Piepoli A., (2012). **"ARNTL2 and SERPINE1: potential biomarkers for tumor aggressiveness in colorectal cancer".** *J. Cancer Res. Clin. Oncol.,* 138: 501-11.

[112] Marx N., Bourcier T., Sukhova G. K., Libby P. and Plutzky J., (1999). **"PPAR gamma activation in human endothelial cells increases plasminogen activator inhibitor type-1 expression: PPARgamma as a potential mediator in vascular disease".** *Arterioscler Thromb. Vasc. Biol.,* 19: 546–551.

[113] Panasyuk G., Espeillac C., Chauvin C., Pradelli L. A., Horie Y., Suzuki A., Annicotte J. S., Fajas L., Foretz M., Verdeguer F., Pontoglio M., Ferré P., Scoazec J. Y., Birnbaum M. J., Ricci J. E. and Pende M., (2012). **"PPAR gamma contributes to PKM2 and HK2 expression in fatty liver".** *Nat. Commun*., 3: 672.

[114] Mazurek S., (2012). **"Pyruvate kinase M2: A key enzyme of the tumor metabolome and its medical relevance".** *Biomedical Research.,* 23: 133-142.

[115] Bi X., Lin Q., Foo T. W., Joshi S., You T., Shen H. M., Ong C. N., Cheah P. Y., Eu K. W. and Hew C. L., (2006). **"Proteomic analysis of colorectal cancer reveals alterations in metabolic pathways: mechanism of tumorigenesis".** *Mol. Cell Proteomics,* 5: 1119-30.

[116] Unwin R. D., Craven R. A., Harnden P., Hanrahan S., Totty N., Knowles M., Eardley I., Selby P. J. and Banks R. E., (2003). **"Proteomic changes in renal cancer and co-ordinate demonstration of both the glycolytic and mitochondrial aspects of the Warburg effect".** *Proteomics*, 3:1620–1632.

[117] Perroud B., Lee J., Valkova N., Dhirapong A., Lin P. Y., Fiehn O., Kültz D. and Weiss R. H., (2006). **"Pathway analysis of kidney cancer using proteomics and metabolic profiling".** *Mol. Cancer*, 5: 64.

[118] Isidoro A., Casado E., Redondo A., Acebo P., Espinosa E., Alonso A. M., Cejas P., Hardisson D., Fresno Vara J. A., Belda-Iniesta C., González-Barón M. and Cuezva J. M., (2005). **"Breast carcinomas fulfill the Warburg hypothesis and provide metabolic markers of cancer prognosis".** *Carcinogenesis*, 26: 2095-104.

[119] Amon L. M., Pitteri S. J., Li C. I., McIntosh M., Ladd J. J., Disis M., Porter P., Wong C. H., Zhang Q., Lampe P., Prentice R. L. and Hanash S. M., (2012). **"Concordant release of glycolysis proteins into the plasma preceding a diagnosis of ER+ breast cancer".** *Cancer Res.,* 72: 1935-42.

[120] Huang J. W., Shiau C. W., Yang Y. T., Kulp S. K., Chen K. F., Brueggemeier R. W., Shapiro C. L. and Chen C. S., (2005). **"Peroxisome proliferator-**

activated receptor gamma independent ablation of cyclin D1 by thiazolidinediones and their derivatives in breast cancer cells". *Mol. Pharmacol.,* 67:1342-8.

[121] Patel L., Pass I., Coxon P., Downes C. P., Smith S. A. and Macphee C. H., (2001). **"Tumor suppressor and anti-inflammatory actions of PPARgamma agonists are mediated via upregulation of PTEN".** *Curr. Biol.,* 11: 764–768.

[122] Jiang K., He B., Lai L., Chen Q., Liu Y., Guo Q. and Wang Q., (2012). **"Cyclosporine A inhibits breast cancer cell growth by downregulating the expression of pyruvate kinase subtype M2".** *Int. J. Mol. Med.,* 30: 302-8.

[123] Martin D. S., Bertino J. R. and Koutcher J. A., (2000). **"ATP depletion+pyrimidine depletion can markedly enhance cancer therapy: fresh insight for a new approach".** *Cancer Res.,* 60: 6776–6783.

[124] Crowe D. L. and Chandraratna R. A., (2004). **"A retinoid X receptor (RXR)-selective retinoid reveals that RXR-α is potentially a therapeutic target in breast cancer cell lines, and that it potentiates anti-proliferative and apoptotic responses to peroxisome proliferator-activated receptor ligands".** *Breast Cancer Research,* 6: R546–R555.

[125] Bonofiglio D., Aquila S., Catalano S., Gabriele S., Belmonte M., Middea E., Qi H., Morelli C., Gentile M., Maggiolini M. and Andò S., (2006). **"Peroxisome proliferator-activated receptor-γ activates p53 gene promoter binding to the nuclear factor-κB sequence in human MCF7 breast cancer cells".** *Mol. Endocrinol.* 20: 3083–92.

[126] Higdon J. V. and Frei B., (2006). **"Coffee and health: a review of recent human research".** *Crit. Rev. Food Sci. Nutr.,* 46(2): 101-23.

[127] Leung W. W., Ho S. C., Chan H. L., Wong V., Yeo W. and Mok T. S., (2011). **" Moderate coffee consumption reduces the risk of hepatocellular carcinoma in hepatitis B chronic carriers: a case-control study**". *J. Epidemiol. Community Health,* 65(6): 556-558.

[128] Chou T. M. and Benowitz N. L., (1994). **"Caffeine and coffee: effects on health and cardiovascular disease".** *Comp. Biochem. Physiol. C. Pharmacl. Toxicol. Endocrinol.,* 109(2):173-89.

[129] Scalbert A. and Williamson G., (2000). **"Dietary intake and bioavailability of polyphenols".** *J. Nutr.,* 130: 2073–2085.

[130] Allred K. F., Yackley K. M., Vanamala J. and Allred C.D., (2009). **"Trigonelline is a novel phytoestrogen in coffee beans".** *J Nutr.,* 139: 1833–1838.

[131] Welsch C. W., Scieszka K. M., Senn E. R. and Dehoog J. V., (1983). **"Caffeine (1, 3, 7 trimethylxanthine), a temperate promoter of DMBA-induced rat mammary gland carcinogenesis".** *Int. J. Cancer,* 32(4): 479–484.

[132] Larsson S. C. and Wolk A., (2007). **"Coffee consumption and risk of liver cancer: a meta-analysis".** *Gastroenterology,* 132(5): 1740–1745.

[133] Bravi F., Bosetti C., Tavani A., Bagnardi V., Gallus S., Negri E., Franceschi S. and La Vecchia C., (2007). **"Coffee drinking and hepatocellular carcinoma risk: a meta-analysis.** *Hepatology*, 46(2): 430–435.

[134] Je Y., Liu W. and Giovannucci E., (2009). **"Coffee consumption and risk of colorectal cancer: a systematic review and meta-analysis of prospective cohort studies".** *International Journal of Cancer*, 124(7): 1662–1668.

[135] Tang N., Zhou B., Wang B. and Yu R., (2009). **"Coffee consumption and risk of breast cancer: a meta analysis".** *American Journal of Obstetrics and Gynecology,* 200(3): 290.e1–290.e9.

[136] Li J., Seibold P., Chang-Claude J., Flesch-Janys D., Liu J., Czene K., Humphreys K. and Hall P., (2011). **"Coffee consumption modifies risk of estrogen-receptor negative breast cancer".** *Breast Cancer Res.,*13(3): R49.

[137] Harris H. R., Bergkvist L. and Wolk A., (2012). **"Coffee and black tea consumption and breast cancer mortality in a cohort of Swedish women".** *Br. J. Cancer,* 107(5): 874-8.

[138] Lowcock E. C., Cotterchio M., Anderson L. N., Boucher B. A. and El-Sohemy A., (2013). **"High coffee intake, but not caffeine, is associated with reduced estrogen receptor negative and postmenopausal breast cancer risk with no effect modification by CYP1A2 genotype".** *Nutr. Cancer,* 65(3): 398-409.

[139] Simonsson M., Soderlind V., Henningson M., Hjertberg M., Rose C., Ingvar C. and Jernstrom H., (2013). **"Coffee prevents early events in tamoxifen-treated breast cancer patients and modulates hormone receptor status".** *Cancer Causes Control,* 24(5): 929-40.

[140] Guan Y. F., Zhang Y. H., Breyer R. M., Davis L. and Breyer M. D., (1999). **"Expression of peroxisome proliferator-activated receptor gamma (PPAR gamma) in human transitional bladder cancer and its role in inducing cell death".** *Neoplasia,* 1: 330–339.

[141] Suzuki T., Nakagawa T., Endo H., Mitsudomi T., Masuda A., Yatabe Y., Sugiura T., Takahashi T. and Hida T., (2003). **"The sensitivity of lung cancer cell lines to the EGFR-selective tyrosine kinase inhibitor ZD1839 ('Iressa') is not related to the expression of EGFR or HER-2 or to K-ras gene status".** *Lung Cancer,* 2003, 42: 35–41.

[142] Burgermeister E., Tencer L. and Liscovitch M., (2003). **"Peroxisome proliferator-activated receptor-gamma upregulates caveolin-1 and caveolin-2 expression in human carcinoma cells".** *Oncogene,* 22: 3888–3900.

[143] Smith A. G. and Muscat G. E., (2006). **"Orphan nuclear receptors: therapeutic opportunities in skeletal muscle".** *American Journal of Physiology,* 291(2): C203–C217.

[144] Amon L. M., Pitteri S. J., Li C. I., McIntosh M., Ladd J. J., Disis M., Porter P., Wong C. H., Zhang Q., Lampe P., Prentice R. L. and Hanash S. M., (2012). **"Concordant release of glycolysis proteins into the plasma preceding a diagnosis of ER^+ breast cancer".** *Cancer Research*, 72(8): 1935–1942.

[145] Nolte R.T., Wisely G. B., Westin S., Cobb J. E., Lambert M. H., Kurokawa R.,

Rosenfeld M. G., Willson T. M., Glass C. K. and Milburn M.V., (1998). **"Ligand binding and co-activator assembly of the peroxisome proliferator-activated receptor-γ".** *Nature,* 395(6698): 137–143.

[146] Bruning J. B., Chalmers M. J., Prasad S., Busby S. A., Kamenecka T. M., He Y., Nettles K. W. and Griffin P. R., (2007). **"Partial agonists activate PPARγ using a helix 12 independent mechanism",** *Structure,* 15(10):1258–1271.

[147] Tsukahara T., Tsukahara R., Yasuda S., Makarova N., Valentine W. J., Allison P., Yuan H., Baker D. L., Li Z., Bittman R., Parrill A. and Tigyi G., (2006). **"Different residues mediate recognition of 1-O-oleyl-lysophosphatidic acid and rosiglitazone in the ligand binding domain of PPAR1".** *J. Biol. Chem.,* 281(6): 3398-407.

[148] Haddad J. J., (2004). **"Redox and oxidant mediated regulation of apoptosis signaling pathways: immuno-pharmaco-redox conception of oxidative siege versus cell death commitment".** *Int. Immunopharmacol.,* 4(4): 475-93.

[149] Barrera G., (2012). **"Oxidative stress and lipid peroxidation products in cancer progression and therapy".** *ISRN Oncol.*, 2012: 137-289.

[150] Nishikawa T., Miyahara E., Horiuchi M., Izumo K., Okamoto Y., Kawai Y., Kawano Y. and Takeuchi T., (2012). **"Benzene metabolite 1,2,4 benzenetriol induces halogenated DNA and Tyrosines representing halogenative stress in HL-60 human myeloid cell line".** *Environ Health Perspect*, 120(1): 62-7.

[151] Pelicano H., Carney D. and Huang P., (2004). **"ROS stress in cancer cells and therapeutic implications".** *Drug Resist. Updat.,* 7(2): 97-110.

[152] Qanungo S., Das M., Haldar S. and Basu A., (2005). **"Epigallocatechin-3-gallate induces mitochondrial membrane depolarization and caspase-dependent apoptosis in pancreatic cancer cells".** *Carcinogenesis*, 26: 958–967.

[153] Cao X. H., Wang A. H., Wang C. L., Mao D. Z., Lu M. F., Cui Y. Q., and Jiao R. Z., (2010). **"Surfactin induces apoptosis in human breast cancer MCF-7 cells through a ROS/JNK-mediated mitochondrial/caspase pathway".** *Chem. Biol. Interact.,* 183: 357–362.

[154] Warburg O., (1956). **"On respiratory impairment in cancer cells".** *Science,* 124: 269–270.

[155] Carew J. S., Zhou Y., Albitar M., Carew J. D., Keating M. J. and Huang P., (2003). **"Mitochondrial DNA mutations in primary leukemia cells after chemotherapy: clinical significance and therapeutic implications".** *Leukemia,* 17: 1437-1447.

[156] Mammucari C. and Rizzuto R., (2010). **"Signaling pathways in mitochondrial dysfunction and aging".** *Mech. Ageing Dev.*, 131(7-8): 536-43.

[157] Galluzzi L., Kepp O., Trojel-Hansen C. and Kroemer G., (2012). **"Mitochondrial control of cellular life, stress, and death".** *Circ. Res.,* 111(9): 1198-207.

[158] Sakharkar M. K., Shashni B., Sharma K., Kaur S., Ranjekar P. and Sakharkar

K. R., (2013). **"Therapeutic Implications of Targeting Energy Metabolism in Breast Cancer".** *PPAR Res.,* 2013:109285.

[159] Kroemer G., Galluzzi L. and Brenner C., (2007). **"Mitochondrial membrane permeabilization in cell death".** *Physiol Rev.,* 2007, 87(1): 99-163.

[160] Bonofiglio D., Cione E., Qi H., Pingitore A., Perri M., Catalano S., Vizza D., Panno M. L., Genchi G., Fuqua S. A. and Andò S., (2009). **"Combined low doses of PPAR gamma and RXR ligands trigger an intrinsic apoptotic pathway in human breast cancer cells".** *Am. J. Pathol.*, 175(3): 1270-80.

[161] Li S., Zhou Q., He H., Zhao Y. and Liu Z., (2004). **"Peroxisome proliferator-activated receptor γ agonists induce cell cycle arrest through transcriptional regulation of Kruppel-like factor 4 (KLF4)".** *J. Biol Chem.,* 288(6): 4076-84.

[162] Altenberg B. and Greulich K. O., (2004). **"Genes of glycolysis are ubiquitously overexpressed in 24 cancer classes".** *Genomics*, 84: 1014-20.

[163] Jiang K., He B., Lai L., Chen Q., Liu Y., Guo Q. and Wang Q., (2012). **"Cyclosporine A inhibits breast cancer cell growth by downregulating the expression of pyruvate kinase subtype M2".** *Int. J. Mol. Med.,* 30: 302-8.

[164] Martin D. S., Bertino J. R. and Koutcher J. A., (2000). **"ATP depletion + pyrimidine depletion can markedly enhance cancer therapy: fresh insight for a new approach".** *Cancer Res.*, 60: 6776–6783.

[165] Mukhopadhyay S., Das S. K. and Mukherjee S., (2004). **"Expression of Mn-superoxide dismutase gene in non-tumorigenic and tumorigenic human mammary epithelial cells".** *Journal of Biomedicine and Biotechnology*, 4: 195–202.

[166] Fedele P., Calvani N., Marino A., Orlando L., Schiavone P., Quaranta A. and Cinieri S., (2012). **"Targeted agents to reverse resistance to endocrine therapy in metastatic breast cancer: where are we now and where are we going?"** *Critical Reviews in Oncology/Haematology*, 51(2): 85–94.

[167] Pelicano H., Martin D. S. and Huan P., (2006). **"Glycolysis inhibition for anticancer treatment",** *Oncogene*, 25: 4633–4646.

[168] Zhao Y., Butlerand E. and Tan M., (2013). **"Targeting cellular metabolism to improve cancer therapeutics".** *Cancer Metabolism Citation: Cell Death and Disease,* 4: 2012-33.

[169] Seyfried T. N. and Shelton L. M., (2010). **"Cancer as a metabolic disease".** *Nutrition & Metabolis*m, 7:7.

[170] Warburg O., (1956). **"On the origin of cancer cells".** *Science*, 123: 309–314.

[171] Altenberg B. and Greulich K.O., (2004). **"Genes of glycolysis are ubiquitously overexpressed in 24 cancer classes".** *Genomics*, 84: 1014–1020.

[172] Ros S. and Schulze A., (2013). **"Balancing glycolytic flux: the role of 6-phosphofructo-2-kinase/fructose 2,6-bisphosphatases in cancer metabolism".** *Cancer & Metabolism*, 1: 8.

[173] Hockel M. and Vaupel P., (2001). **"Biological consequences of tumor hypoxia".** *Semin Oncol.,* 28: 36-41.

[174] Liu H., Liu Y. and Zhang J. T., (2010). **"A new mechanism of drug resistance in breast cancer cells: fatty acid synthase overexpression-mediated palmitate overproduction".** *Mol. Cancer. Therapeutics*, 7: 263–270.

[175] Zhao Y., Liu H., Liu Z., Ding Y., Ledoux S. P., Wilson G. L., Voellmy R., Lin Y., Lin W., Nahta R., Liu B., Fodstad O., Chen J., Wu Y., Price J. E. and Tan M., (2011). **"Overcoming trastuzumab resistance in breast cancer by targeting dysregulated glucose metabolism".** *Cancer Res.*, 71: 4585–4597.

[176] Enns L. and Ladiges W., (2011). **"Mitochondrial redox signaling and cancer invasiveness".** *J. Bioenerg. Biomembr.,* 44(6): 635–63.

[177] Tous M., Ferré N., Rull A., Marsillach J., Coll B., Alonso-Villaverde C., Camps J. and Joven J., (2006). **"Dietary cholesterol and differential monocyte chemoattractant protein-1 gene expression in aorta and liver of apo E-deficient mice".** *Biochemical and Biophysical Research Communications*, 340(4): 1078–1084.

[178] Kota B. P., Huang T. H. and Roufogalis B. D., (2006). **"An overview on biological mechanisms of PPARs".** *Pharmacological Research*, 51(2): 85–94.

[179] Shashni B., Sakharkar K., Nagasaki Y and Sakharkar M. K., (2012). **"The glycolytic enzymes PGK1 and PKM2 as novel transcriptional targets of PPAR gamma in breast cancer pathophysiology".** *Journal of Drug Targeting*, 21(2): 161-74.

[180] Castelein H., Gulick T., Declercq P. E., Mannaerts G. P., Moore D. D. and Baes M. I., (1994). **"The peroxisome proliferator activated receptor regulates malic enzyme gene expression".** *The Journal of Biological Chemistry*, 269(43): 26754–26758.

[181] Lemay D. G. and Hwang D. H., (2006). "**Genome-wide identification of peroxisome proliferator response elements using integrated computational genomics".** *J. Lipid Res.*, 47: 1583–1587.

[182] Bilsen M. V., Vusse G. J. V. D., Gilde A. J., Lindhout M. and Lee K. A. J. M. V. D., (2002). **"Peroxisome proliferator-activated receptors: lipid binding proteins controlling gene expression".** *Molecular and Cellular Biochemistry,* 239(1-2): 131–138.

[183] Mansure J. J., Nassim R. and Kassouf W., (2011). **"Peroxisome proliferator-activated receptor gamma in bladder cancer: a promising therapeutic target in cancer".** *Cellular and Genetic Practices for Translational Medicine,* 8(7): 169–195.

[184] Woo C. C., Loo S. Y., Gee V., Yap C. W., Sethi G., Kumar A. P., Tan K. H., (2011). **"Anticancer activity of thymoquinone in breast cancer cells: possible involvement of PPAR-γ pathway".** *Biochemical Pharmacology,* 82(5): 464–475.

[185] Lu Y. L., Li G. L., Huang H. L., Zhong J. and Dai L. C., (2010).**"Peroxisome proliferator-activated receptor-γ 34C > G polymorphism and colorectal**

cancer risk: a meta-analysis". *World Journal of Gastroenterology*, 16(17): 2170–2175.

[186] Venkatachalam G., Kumar A. P., Yue L. S., Pervaiz S., Clement M. V. and Sakharkar M. K., (2009). **"Computational identification and experimental validation of PPRE motifs in NHE1 and MnSOD genes of human".** *BMC Genomics*, 10(Suppl 3): S5

[187] Jeong Y., Xie Y., Lee W., Bookout A. L., Girard L., Raso G., Behrens C., Wistuba II., Gadzar A. F., Minna J. D., Mangelsdorf D. J., (2012). **"Research resource: diagnostic and therapeutic potential of nuclear receptor expression in lung cancer".** *Molecular Endocrinology*, 26(8): 1443–1454.

[188] Forman B.M., Tontonoz P., Chen J., Brun R.P., Spiegelman B.M. and Evans R.M., (1997). **"15-Deoxy-delta 12,14 prostaglandin J2 is a ligand for the adipocyte determination factor PPAR".** *Cell*, 83: 803-812.

[189] Kliewer S.A., Lenhard J.M., Wilson T.M., Patel I., Morris D.C. and J.M. Lehmann., (1995). **"A prostaglandin J2 metabolite binds peroxisome proliferator-activated receptor gamma and promotes adipocyte differentiation".** *Cell*, 83: 813-819.

[190] Liu Y., Meng Y., Liu H., Li J., Fu J. and Chen X., (2006). **"Growth inhibition and differentiation induced by peroxisome proliferator activated receptor gamma ligand rosiglitazone in human melanoma cell line".** *Med Oncol.,* 23: 393–402.

[191] Shashni B., Sharma K., Singh R., Sakharkar K. R., Kaur S., Nagasaki Y. and Sakharkar M. K., (2013). **"Coffee component Hydroxyl Hydroquinone (HHQ) as a putative ligand for PPAR gamma and implications in breast cancer".** *BMC Genomics*, 14(Suppl 5): S6.

[192] Jiang K., He B., Lai L., Chen Q., Liu Y., Guo Q. and Wang Q., (2012), **"Cyclosporine A inhibits breast cancer cell growth by downregulating the expression of pyruvate kinase subtype M2".** *Int. J. Mol. Med.*, 30: 302–308.

[193] Maddocks K.I. and Blum K.A., (2014). **"Ibrutinib in B-cell Lymphoma".** *Curr. Treat. Options Oncol.,* 2014: Feb 1.

[194] Herman S. E. M., Gordon A. L., Hertlein E., Ramanunni A., Zhang X., Jaglowski S., Flynn J., Jones J., Blum K. A., Buggy J.J., Hamdy A., Johnson A. J. and Byrd J. C., (2011). **"Bruton tyrosine kinase represents a promising therapeutic target for treatment of chronic lymphocytic leukemia and is effectively targeted by PCI-32765".** *Blood*, 117(23): 6287–6296.

[195] Li S., Zhou Q., He H., Zhao Y. and Liu Z., (2013). **"Peroxisome proliferator-activated receptor γ agonists induce cell cycle arrest through transcriptional regulation of Kruppel-like factor 4 (KLF4)".** *J Biol Chem.,* 288(6): 4076-84.

[196] Mazurek S., (2012).**"Pyruvate kinase type M2: a key regulator of the metabolic budget system in tumor cells".** *Int. J. Biochem. Cell Biol*., 43(7): 969-80.

[197] Luo W., and Semenza G. L., (2012). **"Emerging roles of PKM2 in cell metabolism and cancer progression".** *Trends Endocrinol Metab*., 23(11): 560-6.

[198] Wu S. and Le H., (2013). **"Dual roles of PKM2 in cancer metabolism".** *Acta Biochim. Biophys. Sin. (Shanghai)*, 45(1): 27-35.

[199] Wallace D. C., (2012). **"Mitochondria and cancer".** *Nature Reviews Cancer* 12: 685-698.

[200] Kang J. and Pervaiz S., (2012). **"Mitochondria: Redox Metabolism and Dysfunction".** *Biochemistry Research International,* 2012(896751): 14.

[201] Gillies R. J., Robey I. and Gatenby R. A., (2008). "**Causes and Consequences of Increased Glucose Metabolism of Cancers".** *J. Nucl. Med.*, 49(2): 24S-42S.

[202] Ozawa S., Miyaoto C., Maehata Y., Suzuki A., Maeda T. and Baba Y., (2013). **"Acidic extracellular microenvironment and cancer".** *Cancer Cell Int.,* 2013(13): 89.

[203] Kroemer G., (2006). **"Mitochondria in cancer".** *Oncogene*, 25: 4630–4632.

[204] Taylor R. C., Cullen S. P. and Martin S. J., (2008). **"Apoptosis: Controlled demolition at the cellular level".** *Nature Reviews Molecular Cell Biology*, 9: 231–241.

[205] Ghobrial I. M., Witzig T. E. and Adjei A. A., (2005). **"Targeting Apoptosis Pathways in Cancer Therapy".** *Cancer J Clin.,* 55:178–194.

[206] Lowe S. W. and Lin A. W., (2000). "**Apoptosis in cancer".** *Carcinogenesis,* 21(3): 485-495.

[207] Saraste A. and Pulkki K., (2000). **"Morphologic and biochemical hallmarks of apoptosis".** Cardiovasc. Res., 45(3): 528-537.

[208] Oberhammer F. A., Hochegger K., Fröschl G., Tiefenbacher R. and Pavelka M., (1994), **"Chromatin condensation during apoptosis is accompanied by degradation of lamin A+B, without enhanced activation of cdc2 kinase".** *J. Cell Biol.,* 126(4): 827-37.

[209] Chang H. Y. and Yang X., (2000). **"Proteases for Cell Suicide: Functions and Regulation of Caspases".** *Microbiol. Mol. Biol. Rev*., 64(4): 821–846.

[210] Degterev A., Boyce M. and Yuan J., (2003). **"A decade of caspases".** *Oncogene*, 22: 8543–8567.

[211] Fulda S., (2009). **"Caspase-8 in cancer biology and therapy".** *Cancer Letters*, 281: 128–133.

[212] Kroemer G., Galluzzi L. and Brenner C., (2007). **"Mitochondrial membrane permeabilization in cell death".** *Physiol Rev.,* 87(1): 99-163.

[213] Bonofiglio D., Cione E., Qi H., Pingitore A., Perri M., Catalano S., Vizza D., Panno M. L., Genchi G., Fuqua S. A. and Andò S., (2009). **"Combined low doses of PPAR gamma and RXR ligands trigger an intrinsic apoptotic pathway in human breast cancer cells".** *Am. J. Pathol.*, 175(3): 1270-80.

[214] Gross A., McDonnell M. J. and Korsmeyer S., (1999). **"BCL-2 family members and the mitochondria in apoptosis".** *Genes & Dev*. 13: 1899-191.

[215] Pawlowski J. and Kraft A., (2000). **" Bax-induced apoptotic cell death".** *PNAS.*, 97: 2.

[216] Lalier L., Cartron P. F., Juin P., Nedelkina S., Manon S., Bechinger B. and Vallette F. M., (2007). **"Bax activation and mitochondrial insertion during apoptosis".** *Apoptosis,* 12(5): 887-96.

[217] Finucane D. M., Bossy-Wetzel E., Waterhouse N., Cotter T. and Green D. R., (1999). **"Bax-induced caspase activation and apoptosis via cytochromec release from mitochondria is inhibitable by Bcl-xl".** *The Journal of Biological Chemistry*, 274: 2225-2233.

[218] Gómez-Crisóstomo N. P., López-Marure R., Zapata E., Zazueta C. and Martínez-Abundis E., (2013). **"Bax induces cytochrome c release by multiple mechanisms in mitochondria from MCF7 cells".** *J. Bioenerg. Biomembr.,* 45: 441–448.

[219] Giovannucci E., Harlan D. M. and Archeretal M. C., (2010). **"Diabetes and cancer: a consensus report".** *CA Cancer Journal for Clinicians,* 60(4): 207–221.

[220] Liao S., Li J., Wang L., Zhang Y. and Wang C., (2010). **"Type 2 diabetes mellitus and characteristics of breast cancer in China".** *The Asian Pacific Journal of Cancer Prevention*, 11: 933–937.

[221] Boyle P., Boniol M. and Koechlinetal A., (2012). **"Diabetes and breast cancer risk: a meta-analysis".** *British Journal of Cancer*, 51(2): 85–94.

[222] Carpenter D. O., (2008). **"Environmental contaminants as risk factors for developing diabetes".** *Reviews on Environmental Health*, 23(1): 59–74.

[223] Tyagi S., Gupta P., Saini A. S, Kaushal C. and Sharma S., (2011). **"The peroxisome proliferator-activated receptor: a family of nuclear receptors role in various diseases".** *Journal of Advanced Pharmaceutical Technology & Research,* 2(4): 236–240.

[224] Sakharkar M. K., Shashni B., Sharma K., Kaur S., Ranjekar P. and Sakharkar K. R., (2013). **"Therapeutic Implications of Targeting Energy Metabolism in Breast Cancer".** *PPAR Res.*, 2013(109285): 11

ACKNOWLEGEMENTS

The path of success is not straight, but riddled with temptations, impediments and pitfalls all along. All these difficulties make us realize the importance of success humbly.

This thesis report could not have been prepared, if not for the help and encouragement from various people.

I am highly indebted to Prof. Yukio Nagasaki, who has been my sole reason to continue my research in Japan. I deeply appreciate his efforts for providing me a splendorous opportunity to work under his guidance, which has further helped me grow both personally and professionally. His persistent encouragement, constructive criticism, incomparable guidance and support from the preliminary to the concluding level enabled me to develop an understanding of the subject. I am thankful to him heart fully.

My PhD journey would be incomplete unless I thank my current supervisor, Prof. Motoo Utsumi. I owe my deepest gratitude to Prof. Utsumi for showing faith in me and encouraging me constantly during my rough time. His support and motivation has made this day possible.

It is my honour to acknowledge and extend my heartfelt gratitude to the to Prof. Kazuo Watanabe for trusting me and allowing me to wrap up my PhD work.

I thank my supervisor for 2 years Dr. Meena Sakharkar. She was the sole reason I came to Japan for my PhD research. During these 2 years I have learnt a lot from her.

It is my prerogative to thank Prof. Yutaka Ikeda, Dr. Toru Yoshitomi and Dr. Yukichi Horiguchi for their valuable guidance and timely support. The labors put forward and cooperation given by the Nagalabo staff members Mrs. Asuka Tsuji, Mrs. Junko Saeki and Mrs. Umeko Horiuchi is highly appreciated.

Moreover, efforts put forward by the thesis committee members; their valuable and insightful comments are sincerely appreciable.

I would further like to extend my thanks to my Nagasaki laboratory members, G- 30 staff and Graduate school of Life and Sciences (University of Tsukuba) for providing the excellent resources and best cordial environments for the study.

No words are measurable enough to appreciate and express my gratitude to my loving family, my father Dr. S.S Pujara, my mother Shanti, my sister Dr. Rubeena Kapoor and my brother Kartik. Their continuous encouragement and support has always contributed to my success.

I would further like to thank my lab member Karun Sharma for always being there since the day I came. I deeply appreciate his efforts to encourage me whenever I was let down.

I acknowledge with thanks the help, inspiration and cheerful company of my friends, Syuu and Annusara.

I offer my regards and blessings to all of those who supported me in any respect during the completion of the project.

Lastly, I thank almighty Lord to bestow his divine blessing on me through out the life. With all my love, thank you LORD.

Thank You All!

(Babita Shashni)

PUBLICATIONS

1. **Babita Shashni**, Karun Sharma, Rumani Singh, Kishore R Sakharkar, Sarinder K. Dhillon, Yukio Nagasaki and Meena K. Sakharkar (2013). **Coffee component Hydroxyl Hydroquinone (HHQ) as a putative ligand for PPAR gamma and implications in breast cancer**. *BMC Genomics*: 14 (Suppl 5): S6 **(*ISI-Cited Publication*)**.

2. Meena K. Sakharkar* and **Babita Shashni***, Karun Sharma, Sarinder K. Dhillon, Prabhakar R. Ranjekar, Kishore Sakharkar (2013). **Therapeutic implications of targeting energy metabolism in breast cancer.** *PPAR Research*: 2013:109285, **(PMID: 23431283).**

3. **Babita Shashni,** Kishore Sakharkar, Yukio Nagaskai, Sakharkar MK (2012). **The glycolytic enzymes PGK1 and PKM2 as novel transcriptional targets of PPAR gamma in breast cancer pathophysiology**. *Journal of Drug Targeting:* Vol. 21(2): 161-174, **(PMID: 23130662).**

   " * " Authors contributed equally.